EXPLORING ASYMMETRIES FROM GENES, TO BRAINS, TO MINDS: A MULTIMODAL NEUROIMAGING APPROACH TO THE PUTATIVE ROLE OF THE NODAL SIGNALLING PATHWAY IN NEUROCOGNITIVE DISORDERS VIA ATYPICAL CEREBRAL LATERALISATION

GLORIA ROMAGNOLI

Doctor of Philosophy

ASTON UNIVERSITY

September 2019

Aston University

Exploring asymmetries from genes, to brains, to minds: a multimodal neuroimaging approach to the putative role of the NODAL signalling pathway in neurocognitive disorders via atypical cerebral lateralisation

Gloria Romagnoli

Doctor of Philosophy

2019

This thesis investigates the relationship between functional and structural hemispheric asymmetries, by analysing brain anatomy, neurophysiology, neurocognitive and behavioural quantitative laterality measures, in a dyslexia family-based study. The main hypothesis developed and tested in the thesis is that atypical functional and structural hemispheric asymmetries might be the extended endophenotype of a disruption of the NODAL signalling pathway, at the level of the *PCSK6* gene, becoming clinically visible during brain development as neurocognitive disorders. In this context, the putative association of *PCSK6* rs11855415 genetic variant with developmental dyslexia is used as genotype-phenotype association model, according to which the *PCSK6* rs11855415-related structural and functional hemispheric asymmetries are studied as its extended endophenotype, and investigated via a multimodal integrated neuroimaging approach. Within this multidimensional study, different levels of data were acquired from each participant, including: DNA sampling for genotyping, magnetic resonance imaging scans of the brain, magnetoencephalography assessment of receptive language, neurocognitive and handedness testing. By deriving and integrating quantitative measures of grey matter asymmetries, hemispheric language lateralisation and handedness dominance in children with developmental dyslexia and their siblings or twins, this thesis builds a prototypical model of the postulated extended endophenotype of functional and structural hemispheric asymmetries related to *PCSK6* rs11855415 genetic variant.

Keywords: Magnetoencephalography; Magnetic Resonance Imaging; imaging genetics; neuroimaging endophenotype; *PCSK6* gene; functional and structural hemispheric asymmetries; grey matter asymmetries; language laterality; handedness laterality; developmental dyslexia; neurodevelopmental disorders.

To my other Half, Filippo,

to our perfect hemispheric asymmetries that make us One.

“La dissymétrie, je la vois partout dans l’univers.

L’univers est dissymétrique.”

Louis Pasteur, 1883

Acknowledgements

Firstly, I would like to thank my supervisors, Prof Joel B. Talcott and Dr Caroline Witton, for their guidance during the PhD, from my first step into ChildBrain project until the writing of this thesis; and my examiners, Prof Maaike Vandermosten and Prof Paul Furlong, for the very productive and thoughtful discussion during the PhD Viva Voce examination.

The PhD was fully funded by the EU-Childbrain Innovative Training Network (ITN), therefore my deepest gratitude is for the Marie Skłodowska-Curie Actions (MSCA) of the European Commission, for supporting my doctoral postgraduate education, promoting research mobility and providing me with the best research training opportunities as Marie Curie Early Stage Research Fellow.

I am indebted to the entire ChildBrain group, from the Project Coordinator Prof Paavo Leppänen and the Project Administrator Manager Dr Kaisa Lohvansuu, to all the Principal Investigators and Partners of the ITN, for their teaching and guidance during the Marie Curie workshops and secondments. In particular, I would like to thank Prof Robert Oostenveld and the Donders Institute, Dr Tiina Parviainen and the Jyväskylä Centre for Interdisciplinary Brain Research, Dr Dirk Smeets and Icometrix, Prof Mark A. Eckert and the Medical University of South Carolina, for warmly welcoming me in their labs, supervising my work, and having been a constant source of feedback on various iterations of this thesis. A special thanks also to Dr Silvia Paracchini and Angela Martinelli from the University of St Andrews, for the productive and stimulating interdisciplinary collaboration, at the core of this imaging genetics project.

The ChildBrain Early-Stage Researchers were a fantastic crew and source of encouragement, cooperation, help, fun and laughs during the last 4 years! We share unforgettable memories of our incredible workshops and secondments around the world, and I have really made some life-long friends. Special thanks to each one of them, Dr Maria Carla Piastra, Phan Vân Tan, Cecilia Mezzetti, Praghajith Rajhen, Weiyong Xu, Raul Granados, Amit Jaiswal, Caroline Beelen, Sam Van Bijnen, Abinash Pant, Marios Antonakakis, Simon Homölle, Anna Samsel, Diandra Brkic, and to all the reseachers I met in Jyväskylä, Nijmegen, Leuven and Charleston.

At the Aston Neuroscience Institute, I would like to thank the Director Prof Amanda Wood and every past and present researcher and member. In particular, a warm thanks goes to: the Aston Epilepsy team led by Prof Stefano Seri, including Andrea Scott, Dr Elaine Foley, Dr Ana Checa Ros, Dr Giacomo Minicuci, Peter Bill and the entire Neurophysiology team of the Birmingham Children's Hospital, for making my clinical attachment in Epilepsy so special and incredibly formative; to Dr Frank Pearson and Dr Shu Yau for their supportive collaboration while working at the Developmental Dyslexia Assessment Unit; to Prof Klaus Kessler, Dr Sukhvir Wright, Dr Valia Rodriguez, Dr Laura Shapiro, Dr Luc Boutsen, Dr Hongfang Wang,

Dr SÎan Worthen, to the invaluable radiographers Patti Price, Liz Squire, Kate Garas, and to the Clinics Administrators Liz Byrne and Sarah Paris, for their crucial and constant support. A special thanks goes to the best research administrator and student support, Caroline Brocklebank, for the invaluable PhD monitoring and guidance towards the thesis submission.

There are a number of “Aston-ishing” colleagues and friends who have made this PhD journey much more enjoyable and special than it would have been otherwise. I would like to specially thank Dr Lucia Quitadamo, Ewelina Rosiecka, Alison Gwilliams, Ainara Jauregi, Robert Seymour, Dr Ellie Huizeling, Dr Doro Smith, Dr Kelly Murphy, Dr Paras Joshee, Daniel King, Nicola-Jayne Tuck, Dr Sam Westwood and Andrew Ssemata, to name but a few. A special thanks also to the Aston Biomedical Engineering friends, Dr Antonio Fratini, Alberto Recchioni, Dr Tecla Bonci, Dr Francesco Menduni, and the rest of the “Brummie crew”, Dr Sasan Amirhassankhani, Silvia Gallo, Paolo Tonti, Sonia Trave Huarte, and all friends in Birmingham.

A special thanks goes to Prof Urlich Stephani, Dr Gert Wiegand, Prof Paolo Curatolo and Prof Cinzia Galasso, who encouraged me to pursue research ever since I was a medical student at the University of Rome Tor Vergata and at the Christian-Albrechts University of Kiel.
It has been a long pathway since then, passing through the Marie Curie ITN, and continuing now at the UCL Queen Square Institute of Neurology, in London. A heartfelt thanks goes therefore to my present supervisor and mentor Prof John S. Duncan, for supporting my post-doctoral growth since 2018, to Dr Fergus Rugg-Gunn, Dr Sofia Eriksson, Dr Beate Diehl, Mr Andrew McEvoy, to the amazing EpiNav and WADD teams, to the entire Video-Telemetry Unit of the National Hospital for Neurology and Neurosurgery led by Dr Fahmida Chowdhury, and to the all Department of Clinical and Experimental Epilepsy led by Prof Ley Sander. I especially thank the Registrars Dr Alexandre Mathy and Dr Kushan Karunaratne, the Clinical Fellows Dr Michael Kinney and Dr Benjamin Whatley, the DCEE PA Jane de Tisi, the MDT coordinator Samuela Columbano, and all the Epilepsy Researchers, Dr Ali Alim-Marvasti, Fernando Perez Garcia, Dr Vejay Vakharia, Dr Katri Silvennoinen, Dr Sara Zagaglia, Dr Rita Demurtas, Dr Luigi Agrò, Dr Marco Perulli, Luke Allen, Hassan Hawsawi, to name but a few, for sharing joys and challenges of the last 12 months at Queen Square towards my PhD submission.

Above all, I would like to thank my fantastic family, my parents Marina and Mario, and my sister Giorgia: wherever I go, whatever is my goal, you are my infinite source of strength and love! A heartfelt thanks also to Laura, Maurizio and Alessandra for the constant nurturance, encouragement and presence at each step of this important journey.

My deepest gratitude goes to my better half, Filippo, for being my rock with your unconditional love and patience, for constantly believing in me and always standing by my side!

Last, but certainly not least, THANKS are due to my amazing patients, and their families, who took part in ChildBrain research experiments, making this thesis possible and extremely fun!

Table of Contents

List of Figures

List of Tables

Chapter 1: Introduction

This doctoral research was part of the ChildBrain project, an Innovative Training Network (ITN) and European Training Network (ETN) of the Marie Skłodowska-Curie Actions (MSCA), funded by the Framework Programme for Research and Innovation 'Horizon 2020' of the European Commission (H2020-EU.1.3.1.; grant agreement ID 641652), to support excellence and worldwide mobility in research (ChildBrain project websites: http://childbrain.eu/; https://cordis.europa.eu/project/id/641652).

The purpose of the ChildBrain ITN was to train 15 Early Stage Researchers (ESRs) in the field of neurosciences, with the aim of developing innovative brain imaging-based tools to improve diagnosis and treatment of developmental neurocognitive disorders. To accomplish such goal, a cross-disciplinary and trans-sectorial European training network of experts from academia (University of Jyväskylä, University of Leuven, Aston University, University of Münster, Radboud University) and industry (IcoMetrix NV, BESA GmbH, MEGIN Oy) was established for hosting and training the ESRs. Each ESR was assigned to one of the following work packages (WPs): 1) the 'Childhood neurodevelopmental disorders WP', to research on the neural underpinnings of dyslexia, attention deficit hyperactivity disorder, epilepsy and hearing loss; 2) the 'Brain development WP', to look at the neural correlates of typical brain development; 3) the 'Brain research methods WP', to develop new multimodal data analysis and child-adjusted methodologies.

In quality of ESR number 4 of the ChildBrain project, my research fell within the scope of the first WP, with focus on multimodal neuroimaging clinical applications in neurocognitive disorders in collaboration with the ITN and partner institutions. The core topic of my investigations was the cerebral lateralisation in atypical neurodevelopment, in particular the structural and functional hemispheric asymmetries potentially related to a genetic variant of *PCSK6*, that was found to be associated with greater right-hand skills in developmental dyslexia (Scerri et al., 2011; Brandler et al., 2013; Brandler and Paracchini, 2014).

Asymmetries between the two halves of the body as well as between the two hemispheres of the brain are a core principle and a fundamental organisational property of all vertebrates (Ocklenburg et al., 2013; Ströckens et al., 2013; Güntürkün and Ocklenburg, 2017). Despite the importance of the asymmetric nature of the human brain, its neurobiological meaning has not been fully understood yet, in particular with regard to the ontological relationships 'body-brain asymmetries' and 'functional-structural hemispheric asymmetries'.

This introduction will, firstly, present the most recent insights from the literature (Brandler et al., 2013; Brandler and Paracchini, 2014; Schmitz et al., 2017, 2019) on the potential shared ontogenesis between structural and functional hemispheric asymmetries, and between brain and visceral asymmetries via the NODAL signalling pathway, in order to provide the conceptual

background for the hypothesis of the thesis. Against such backdrop, it will be then introduced the research question, regarding the *PCSK6* gene's putative role in the embryological neurodevelopment of atypical functional and structural brain asymmetries; and, ultimately, it will be outlined how we are going to explore this hypothesis, by analysing the extended endophenotype of a genotype-phenotype model applied to developmental dyslexia.

1.1 The Embryology of Brain Asymmetries

1.1.1 Structural Asymmetries

The very first asymmetry is detected in humans at the end of 5 gestational weeks, with the heart starting to loop towards the left side (Steding, 2009). This is followed by a rostrocaudal embryonic twist, that initiates asymmetries at the level of other organs (Kathiriya and Srivastava, 2000), such as the liver (Hutchins and Moore, 1988), the stomach and the lungs, respectively at 6, 7 and 8 gestational weeks (Steding, 2009), for a complete establishment of visceral asymmetries at the end of the embryonic period.

In a similar way to the visceral organs that develop from an initial condition of symmetry, the brain differentiates from the neural tube, an unpaired structure starting to grow ventrally into prosencephalon, mesencephalon and rhombencephalon at 6 gestational weeks, and forming the cerebral hemispheres approximately 2 weeks later (Chi et al., 1977a; Steding, 2009). The first cerebral structure to appear asymmetrical is the choroid plexus (enlarged on the left), at the beginning of the foetal period (Abu-Rustum et al., 2013), in line with the 'left-faster-than-right' maturation rates of the diencephalon, temporal lobe, basal ganglia and choroid plexus at 9–16 gestational weeks (De Kovel et al., 2018). This early hemispheric asymmetry was suggested to potentially be at the origin of a leftward shift in the balance of neurophysiology of peptides, cytokines and growth factors synthesised by cerebrospinal fluid (Corballis, 2013). This shift of chemical activity towards the left might also contribute to progressively determine the typical leftward asymmetry of the brain (Hering-Hanit et al., 2001; Kivilevitch et al., 2010; Andescavage et al., 2017), in particular at the level of the occipital (Weinberger et al., 1982) and temporal lobes, with the planum temporale becoming importantly asymmetrical at the 31st gestational week (Chi et al., 1977b; Kasprian et al., 2011).

1.1.2 Functional Asymmetries

Within the same epoch in which structural hemispheric asymmetry emerges, signs of motor asymmetry have been detected by a number of ultrasound studies. Three foetuses out of four show a strong preference of right arm movements from the 10th gestational week (Hepper et al., 1998; McCartney and Hepper, 1999), as well as a strong preference for head-turning toward the right side that persists after birth (Hepper et al., 1990, 1991; Dunsirn et al., 2016).

The preferred head turning direction has been shown to predict hand use in reaching tasks in infancy (Coryell and Michel, 1978; Michel, 1981; Konishi et al., 1986), and it correlates with handedness laterality quotient (Ocklenburg and Güntürkün, 2009) and handedness in childhood (Hepper et al., 1990, 1991, 1998, 2005). Kinematic analyses of foetal arm movements also confirmed the consistency of prenatal hand preference until school age (Parma et al., 2017).

Perceptional asymmetries, such as the right ear advantage for dichotically presented syllables (Entus, 1980; Bertoncini et al., 1989), can be detected already in newborns and infants, suggesting an early lateralisation of receptive language processing. A more sustained left posterior temporal and left frontal activations have been observed in preterm infants at 28-30 gestational weeks, tested with linguistic discrimination tasks (Mahmoudzadeh et al., 2013), and in the first postnatal week in response to language stimuli (Peña et al., 2003; Gervain et al., 2008). Differently, productive language lateralisation (e.g. coordination of the speech articulators) develops later with language acquisition, throughout infancy and childhood (Minagawa-Kawai et al., 2011; Bishop, 2013; Haag et al., 2010).

1.1.3 Asymmetrical Gene Expression

Investigating gene expression differences between the left and right frontal and temporal cortices, a consistent asymmetrical expression of *LMO4* was observed in the foetal perisylvian cortex (Sun et al., 2005). Similarly, functional gene groups involved in the nervous signal transmission (Karlebach and Francks, 2015) and in brain asymmetry foetal development, such as *AR*, *LEFTY1* and *PCSK6,* were also found lateralised at the early foetal stage (Muntané et al., 2017). Interestingly, in line with the foetal preference of right arm movements, pronounced foetal gene expression asymmetries were seen in the spinal cord (Ocklenburg et al., 2017), suggesting that asymmetrical gene expression at this level might contribute to induce the early motor asymmetries observed after the 10th gestational week.

1.2 A Possible Shared Ontogenesis with Visceral Asymmetries

Previous genetic models postulated the existence of one single gene encoding for the two major functional hemispheric asymmetries of handedness and language (Annett, 1964; McManus, 1985). Nowadays, the sequencing of the human genome is revealing a far more complex scenario behind the causative mechanisms of functional hemispheric asymmetries, but there is new room to reconsider the Annett's theory of a common embryological development between handedness and language lateralisation, within the context of a potential shared ontogenesis between brain and visceral asymmetries, via the NODAL signalling pathway (Brandler et al., 2013; Brandler and Paracchini, 2014; Schmitz et al., 2017, 2019). Such mechanisms would take place at the level of primary cilia, that are

hair-like structures, 3-15 µm long, projecting from the eukaryotic cell surface and particularly represented in the brain, with multiple functions in the development and functioning of the central nervous system (Trulioff et al., 2017).

1.2.1 The NODAL Signalling Pathway

Structural visceral asymmetries in vertebrate embryos are preceded by a cascade of molecular events, that lead to the development of specific and typical asymmetries along the left-right axis, thus breaking the antecedent symmetric condition. In this process, the NODAL signalling pathway plays a key role at the level of the primitive pit, called node, that is transiently present at the midline during gastrulation. The node contains two types of primary cilia: posteriorly angled clockwise rotating cilia, that create a leftward flow, and mechanosensory immotile cilia at the edge of the node, detecting the asymmetric nodal flow (Tabin and Vogan, 2003; Babu and Roy, 2013), that is then transduced to an increase of intracellular calcium ions on the left side (Figure 1.1a). This mechanism is able to trigger leftward asymmetrical expression within the node of genes like *LEFTY2, PITX2* and *NODAL* (Takao et al., 2013). *NODAL* gene encodes for the homonymous intercellular signalling protein, NODAL, of the transforming growth factor beta (TGF-beta) family (Zhou et al., 1993), that is cleaved into its active form by the PCSK6 endoprotease (Figure 1.1b). To specify whether a cell is meant to develop or not on the left side of the embryo, the left-sided expression of *NODAL* is then transmitted from the node anteriorly to the lateral plate mesoderm (LPM), by another TGF-beta protein called growth/differentiation factor 1 (GDF1) (Rankin et al., 2000). The activation of the NODAL signalling pathway in the left LPM is only possible with the simultaneous asymmetric expression of *NODAL, LEFTY2*, and *PITX2* genes, since *LEFTY2* encodes for a protein inhibiting the NODAL pathway in the right LPM (Meno et al., 2001; Sakuma et al., 2002), while *PITX2* encodes for a transcription factor that is asymmetrically expressed from the 5th gestational week (Piedra et al., 1998).

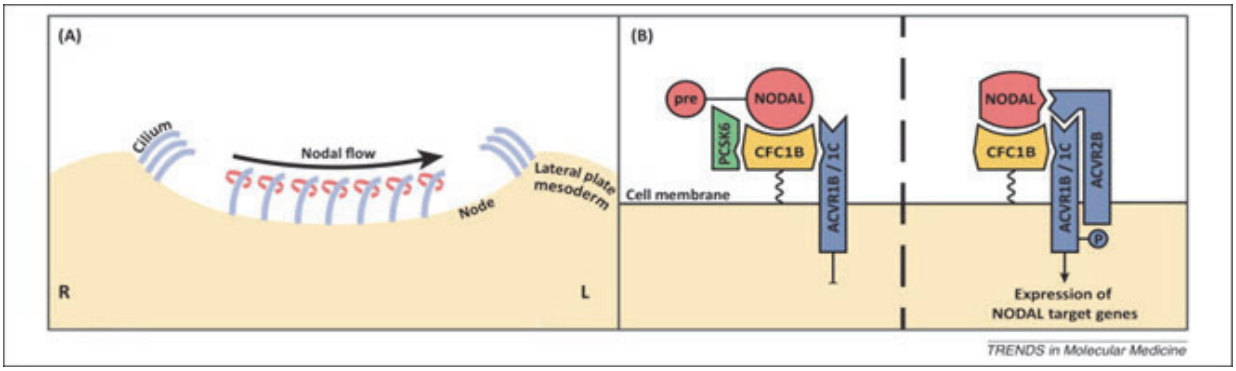

Figure 1.1: Establishment of left/right (LR) asymmetry during development: a) cross-section of the developing embryo during gastrulation; b) zoomed in representation of NODAL signalling at the surface of a cell on the left side of the node. Figure and caption from Brandler and Paracchini 2014.

The first insights on the possible NODAL involvement not only in visceral but also in brain asymmetries came from the knock-out of *Pcsk6* gene in mice, leading to left/right phenotypes (Constam and Robertson, 2000; Barth et al., 2005), such as heterotaxia (or *situs inversus*, consisting in the reversal of visceral asymmetries), and midline disorders, like agenesis of the corpus callosum, where *PCSK6* is highly expressed in the human brain (Johnson et al., 2003). Along the same lines, findings from studies using frequent *situs inversus* (fsi) line of zebrafish (Concha et al., 2000) as well as human neuroimaging (Berretz et al., 2019) have supported the hypothesis that hemispheric asymmetries might be influenced by the same genes underlying visceral asymmetries (Concha et al., 2000). Zebrafish of the mutant line fsi showed concordance of visceral-brain asymmetry, including alteration of some functional lateralisation (Barth et al., 2005); furthermore, the condition of *situs inversus* was found in association with atypical right-hemispheric language dominance at the magnetoencephalography, and with a reversed brain petalia asymmetry at the magnetic resonance imaging (Ihara et al., 2010).

Interestingly, grey matter asymmetries in both temporal and frontal lobes have been recently shown to be associated with the same intronic 33bp variable-number tandem repeat (VNTR) polymorphism in *PCSK6* (rs10523972) (Berretz et al., 2019) that was previously found to be associated with degree of handedness, in a cohort of 1113 healthy adults (Arning et al., 2013). These results provided further support to the putative role of *PCSK6* in the biological mechanisms underlying the establishment of brain lateralisation and thus handedness (Arning et al., 2013), also supporting the assumption that degree of handedness, instead of direction, might be a more appropriate indicator of hemispheric dominance. Further insights on the possible role of *PCSK6* in brain asymmetries, with reference to both handedness and language, came from a genome-wide association study for a quantitative measure of relative hand skill (Scerri et al., 2011), that revealed a significant association of the *PCSK6* rs11855415 variant with increased relative right-hand skills in dyslexic individuals. This finding was later replicated by Brandler et al. (2013) in three independent dyslexia cohorts, with the most strongly associated *PSCK6* variant being rs7182874; in the same study, no association was found in a sample from the general population.

1.3 Ciliopathies, Asymmetries and Dyslexia

Ciliogenesis is of particular importance for the neurodevelopment, as primary cilia are a core actor in cortical morphogenesis (Marshall and Nonaka, 2006). More than 1000 ciliary proteins are involved in cilium assembly and functioning (Davis and Katsanis, 2012), and mutations in their genes can lead to a broad spectrum of genetic syndromes, known as ciliopathies. Such disorders display a wide array of clinical phenotypes, where *situs inversus*, abnormal corpus callosum and neurocognitive impairment are common features. Primary ciliary dyskinesia, hydrocephalus, Joubert syndrome, Meckel-Gruber syndrome, acrocallosal

syndrome are just few examples within the broad clinical spectrum of ciliopathies. Because of its highly heritable nature and the implication of its candidate genes in ciliogenesis, also developmental dyslexia has been proposed as disorder to be included under the umbrella of 'ciliopathies', at the mild end of the spectrum (Kere, 2014). In line with this, defects at the level of primary cilia have been recently hypothesised to comprise the missing link between atypical left/right asymmetry and impaired neurodevelopment in neurocognitve disorders, such as dyslexia, autism and schizophrenia, where abnormal functional and structural brain asymmetries are often displayed (Trulioff et al., 2017).

1.3.1 Dyslexia as Neurological Model for Asymmetries

Reading disability, known as developmental dyslexia, is a neurodevelopmental specific learning disorder, exhibited in 5 - 15% of school-age children (Habib and Giraud, 2013; Schulte-Körne, 2014). This is characterised by a specific difficulty in achieving reading fluency, resulting from underlying impairments in word decoding and recognition and/or spelling and reading comprehension (Lyon, 2003; Fletcher et al., 2007; International Dyslexia Association, 2002; American Psychiatric Association, 2013).

Developmental dyslexia is known to be neurobiological in origin and highly heritable (40–84%) (Astrom et al., 2007; DeFries et al., 1987; Eicher and Gruen, 2013). Linkage studies (Démonet et al., 2004; Fisher and DeFries, 2002; McGrath et al., 2006) have so far found nine loci (*DYX1-DYX9*) and six candidate genes in association with dyslexia: *DCDC2* and *KIAA0319* within the *DYX2* locus on chromosome 6p21; *DYX1C1* on chromosome 15q21 within *DYX1* locus; *C2ORF3* and *MRPL19* in the *DYX3* locus on chromosome 2p16-p15; and *ROBO1* on chromosome 3p12-q12 within the *DYX5* locus (Carrion-Castillo et al., 2013; Cope et al., 2005; Eicher et al., 2014; Massinen et al., 2009; Meng et al., 2005; Schumacher et al., 2006; Taipale et al., 2003). Three out of nine dyslexia candidate genes, *DYX1C1, DCDC2* and *KIAA0319*, have been found implicated in ciliary growth in the developing neocortex (Chandrasekar et al., 2013; Massinen et al., 2011; Brandler and Paracchini, 2014). In line with this, the emerging evidence from genome-wide association studies (GWASs) (Scerri et al., 2011; Brandler et al., 2013; Brandler and Paracchini, 2014) that the genetic variant rs11855415 of *PCSK6* is highly associated with increased relative right-hand skills in dyslexia, on the one hand, supports the hypothesis that dyslexia might be a mild ciliopathy (Kere, 2014), and, on the other hand, offers a putative genetic substrate to the primary ciliary mechanisms possibly involved in abnormal neurodevelopment and atypical left/right asymmetry (Trulioff et al., 2017).

The causative role of atypical asymmetries in dyslexia had been largely debated over the last century, with Orton (1925) being the first to claim a poorly lateralised brain as a possible cause for reading disability; a hypothesis on which Annett (1985) later built up her genetic theory of a postulated 'right shift' factor' underlying atypical language and handedness

lateralisation in dyslexia. Because of the lack of appropriate noninvasive technique to assess language dominance, in alternative to the presurgical procedure of Wada test (requiring the injection of anaesthetic into one carotid artery, to cause the transient inactivation of the corresponding hemisphere) (Abou-Khalil, 2007), most studies at that time used handedness like a proxy measure for language (Bishop, 2013), and showed that dyslexic children were more likely to be non-right-handed compared to controls (Eglinton and Annett, 1994). Nevertheless, handedness is an indirect indicator of hemispheric dominance, and the actual relationship with language laterality is significant but not precise, with 96% of right-handers versus 73% of left-handers showing left hemisphere language dominance (Rasmussen and Milner, 1975; Knecht et al., 2000). The first reliable evidence of a weaker language lateralisation in children and adults with developmental dyslexia in comparison to typically developing individuals, was established at a later date, based on functional neuroimaging techniques, like functional transcranial Doppler ultrasound (Knecht et al., 1998; Illingworth and Bishop, 2009), functional magnetic resonance imaging (Badcock et al., 2012; Park et al., 2012; Sun et al., 2010), and magnetoencephalography (Papanicolaou et al., 2003; Simos et al., 2000; Breier et al., 2003; Sarkari et al., 2002).

As far as dyslexia-associated structural hemispheric asymmetries are concerned, evidence of atypical lateralisation (rightward asymmetry or symmetry) has been mainly shown at the level of language-related regions, in the temporal (planum temporale and superior temporal gyrus), frontal (prefrontal regions) and parietal (planum parietale and angular gyrus) lobes, by a plethora of magnetic resonance imaging studies over the last 40 years (Hier et al., 1978; Galaburda and Kemper, 1979; Galaburda, 1989; Galaburda et al., 1985, 1990; Haslam et al., 1981; Rumsey et al., 1986, 1997; Larsen et al., 1990; Hynd et al., 1990; Duara et al., 1991; Kushch et al., 1993; Dalby et al., 1998; Leonard et al., 1993; Schultz et al., 1994; Jernigan et al., 1991; Plante et al., 1991; Gauger et al., 1997; Beaton, 1997; Shapleske et al., 1999; Eckert and Leonard, 2000; Habib, 2000; Chiarello et al., 2006; Leonard and Eckert, 2008).

The evidence that dyslexia is associated with both atypical structural and functional hemispheric asymmetries, and with genes implicated in both ciliogenesis and left/right asymmetries, makes it a good neurological model to study *in vivo* the still unclear links between: 1) handedness and language; 2) functional and structural brain asymmetries; 3) atypical hemispheric asymmetries and neurodevelopmental disorders; 4) NODAL signalling pathway and hemispheric asymmetries; 5) primary cilia and neurodevelopmental disorders. Each of these links can be either seen as an independent, compartimentalised and stand-alone relationship, similarly to what has been done over the last century, or differently, it can be looked at with a holistic eye, and considered as a small part of a big puzzle, impossible to see without putting together all the single pieces and looking at them as a whole. The latter is the kind of approach through which this thesis dives into the big puzzle of hemispheric

asymmetries, from genes to brains to minds, by using developmental dyslexia and *PCSK6* as, respectively, putative neurological and genetic terms of a genotype-phenotype model, of which we want to investigate the endophenotype.

1.4 Hypothesis and Study Design

The main hypothesis of the thesis is that atypical structural and functional hemispheric asymmetries might be the extended endophenotype of a disrupted NODAL signalling pathway, that might become clinically visible as developmental neurocognitive disorders. To test this, the putative association of the *PCSK6* rs11855415 genetic variant with developmental dyslexia will be used as genotype - clinical phenotype association model, while the related structural and functional hemispheric asymmetries will be studied as its postulated extended endophenotype, and investigated via a multimodal integrated neuroimaging approach.

1.4.1 Hemispheric Asymmetries as Extended Endophenotype

The concept of endophenotype (term derived from the ancient Greek *endo*- that means “internal”, and therefore invisible) was first used in insect biology, as opposite to the concept of exophenotype (term derived from the ancient Greek *exo*- that means “external”, and therefore visible) (John and Lewis, 1966). Over time, the terminology has been better defined according to stringent and precise criteria, to help the identification of endophenotypes, in particular in the field of neuropsychiatry (Glahn et al., 2014). Definition criteria of an endophenotype are: (1) heritability; (2) association with the disorder in the relevant population; (3) state-independence (presence in an individual regardless the presence of the disorder); (4) co-segregation with the disorder within the family; (5) presence in non-affected family members at a higher rate than in the general population; 6) reproducibility of measurement (Gershon and Goldin, 1986; Gottesman and Gould, 2003; Leboyer et al., 1998; Lenox et al., 2002). Therefore, the use of the term has been clearly confined to the concept of a measurable trait unobservable by the unaided eye, positioned along the pathway that runs between the genotype and phenotype level, closer to the underlying genetic mechanisms than the clinical phenotype, with a presumed effect size of genetic variations larger than on clinical phenotype (Gottesman and Gould, 2003; Prasad and Keshavan, 2008). Critically, co-segregation and heritability criteria distinguish an endophenotype from the more general definitions of biomarker or intermediate phenotype, which are, respectively, any biological associated measure, and a mild, incomplete expression of parent phenotypes (Lenzenweger, 2013; Glahn et al., 2014; Gould and Gottesman, 2006), despite some authors used the term intermediate phenotype as synonymous to endophenotype (Meyer-Lindenberg and Weinberger, 2006).

The combination of functionally related endophenotypes into a network-dimension, where the included traits are linked to each other by established or putative functional mechanisms,

has been proposed by Prasad and Keshavan (2008), and introduced with the concept of "extended endophenotype". Definition criteria of an extended endophenotype are: (1) each trait of the extended endophenotype should meet the criteria of the endophenotype; (2) the extended endophenotype should involve different levels of investigation and analysis (e.g. structural and physiological, cognitive and physiological, neurochemical and physiological); (3) the included endophenotypes should co-occur within the families of affected individuals, and should be correlated within the same individual; (4) the included endophenotypes should be mechanistically related (e.g. deficit of declarative memory, abnormal hippocampal functioning, gamma band oscillatory changes, abnormal prefrontal BOLD response) (Prasad and Keshavan, 2008).

In line with what suggested by Prasad and Keshavan (2008), the combined study of functional and structural hemispheric asymmetries as extended endophenotype may help towards: 1) the delineation of the pathway from NODAL to clinical phenotype; 2) the delineation of subpathways connecting structural asymmetries to functional laterality, as well as language to handedness; 2) the deconstruction of the diagnostic phenotype of dyslexia into biologically more meaningful phenotypes and endophenotypes; 3) the development of more rational and targeted interventions; 4) the identification of potential "branch points" for other related neurodevelopmental disorders.

This thesis will analyse the extended endophenotype of neuroimaging-derived functional and structural hemispheric asymmetries (Figure 1.2), by examining co-segregation between brain anatomy and neurophysiology quantitative measures. The empirical chapters will investigate two of the three putative *PCSK6*-related endophenotypes: Chapter 3 will focus on structural asymmetries of cortical and subcortical grey matter, through two magnetic resonance imaging (MRI) studies; Chapter 4 will look at receptive language lateralisation, through two studies using magnetoencephalography (MEG); across both experimental chapters, *PCSK6* genotype and dyslexia affection status will be used as independent variables, whose asymmetry effect on language lateralisation and grey matter asymmetries will be tested (e.g *PCSK6*) or controlled for (e.g. affection status).

1.4.2 A Multimodal Neuroimaging Approach

An integrated multimodal neuroimaging approach has been applied to characterise the postulated extended endophenotype, by using a range of research tools, from behavioural and neuropsychological batteries, to MRI and MEG.

Different dimensions of data have been acquired from each participant, according to a multilevel data acquisition. This started with DNA sampling for genotyping, along with the administration of neuropsychologal batteries, to define neurocognitive and handedness profiles; these tests were then followed by MRI scans of brain anatomy and connectivity, and

at last by MEG recording of resting state and receptive language paradigms, for a total of 6 dimensions of data, and 6 levels of acquisition (as shown in Figure 1.3).

Such multidimensional strategy entailed that subjects tested in a certain level of the acquisition pipeline had also been tested in the previous levels, but not necessarily would have been tested in the following ones. Due to the multi-stage, prospective and potentially narrowing data collection, sample size decreased by progressing of levels, until the last level of acquisition including only those subjects who completed each level of the study.

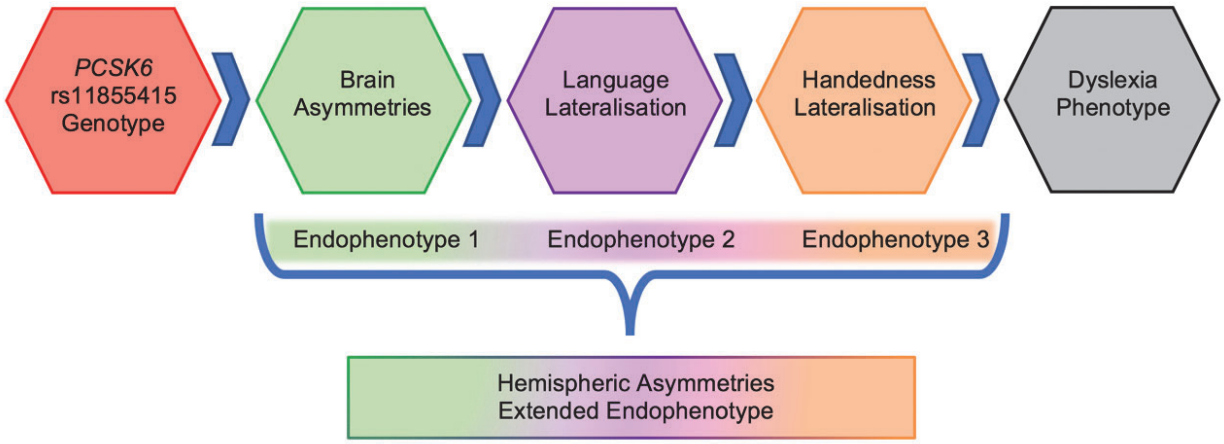

Figure 1.2: DImensions of the PCSK6 rs11855415*-related extended endophenotype: Endophenotype 1 is represented by brain structural asymmetries (studied in Chapters 3 and 5), Endophenotype 2 by language lateralisation (studied in Chapters 4 and 5), and Endophenotype 3 by handedness dominance (studied as secondary focus across Chapters 3, 4 and 5).*

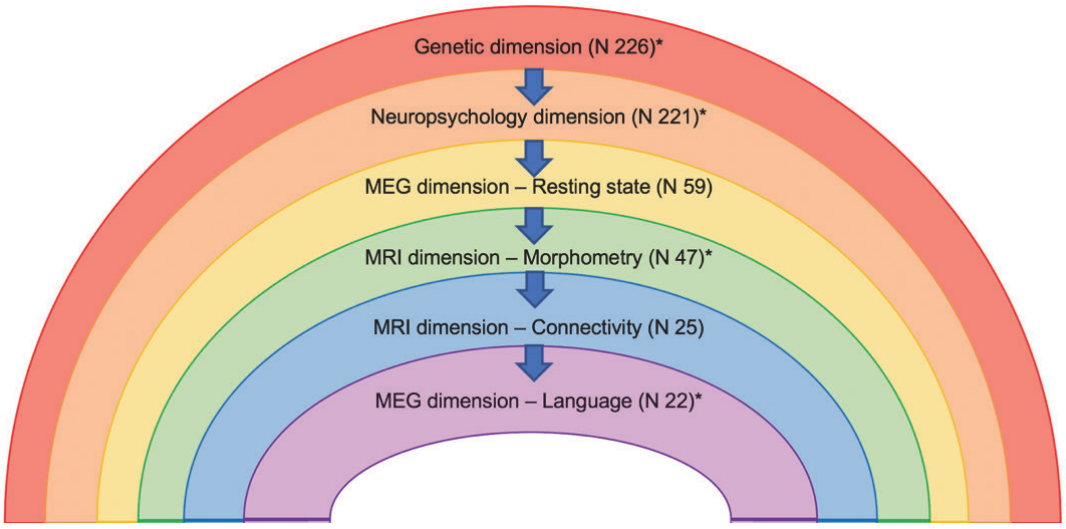

*Figure 1.3: Structure of the multidimensional-multilevel-multimodal data acquisition, where each dimension of data is acquired in progressive levels, by using different modalities: from DNA sampling to neuropsychology and behavioural tests, magnetic resonance imaging (MRI) and magnetoencephalography (MEG). *Dimensions on which the empirical chapters focus.*

The endophenotype criteria of Gottesman and Gould (2003) will be tested using a family-based study design (Glahn and Blangero, 2011), through which the hypotheses of pleiotropy, heritability, association with the disorder, co-segregation within families, and the presence of common genetic factors between candidate endophenotypes and phenotype can be confirmed at once, or inferred using genetic correlations (Glahn et al., 2014). However, the criterion of state-independence (Gottesman and Gould, 2003) cannot explicitly be tested with this kind of studies, since it would require repeated measurements, but it can be assumed if the trait is present in unaffected family members (Glahn et al., 2014).

The postulated extended endophenotype of quantitative structural (MRI-derived) and functional (MEG-derived) hemispheric asymmetries will be studied in a *PCSK6*-genotyped paediatric population, through a dyslexia case-sibling association study, including twins when present. According to this study design, each dyslexic child is associated to one or more unaffected siblings or twins: eligible cases were considered children who underwent a complete dyslexia assessment and received a positive diagnosis at our Developmental Dyslexia Assessment Unit (DDAU), as well as those siblings whose diagnostic condition of dyslexia was already noted; eligible controls were considered the unaffected siblings/twins who reached the age of diagnosis without showing signs of reading disability, as well as children who underwent the DDAU assessment resulting not to be affected by a specific learning disability.

To investigate the hypothesised *PCSK6*-related asymmetry effects, this case-sibling population was then grouped by *PCSK6* genotype into carriers vs non-carriers, and matched by dyslexia affection status, to ensure the state-independence of significant *PCSK6*-related asymmetries. To control for asymmetry confounding factors, participants were also matched by age and gender, since structural and functional cerebral lateralisation processes continue after birth throughout the lifespan and are also modulated by gender (Zhong et al., 2017). For example, a putative disproportional age representation towards adolescence, or a male over-representation in the group of carriers, may potentially lead to a significantly high level of asymmetries, likely to be misinterpreted as related to *PCSK6*, should age and gender be not adequately controlled as asymmetry confounders.

The choice of a family-based study to investigate endophenotypes helps, on the one hand, to address the population stratification bias, thus avoiding possible spurious associations that may be detected with cases and controls coming from different source populations with varying allele frequencies (Cardon and Palmer, 2003); and, on the other hand, it increases the chance of including individuals who carry the genetic variant of interest. However, the advantage of this study design can result in subjects being potentially overmatched on many variables, with a potential loss of power up to 50% than if using unrelated individuals (Witte et al., 1999).

This issue has been partially circumvented by the fact that our study follows up on genome-wide association studies' findings, according to which the *PCSK6* rs11855415 genetic variant was found to be highly associated with increased relative right-hand skills in dyslexic individuals (Scerri et al., 2011; Brandler et al., 2013), with average effect size of the minor allele being 0.35 standard deviations (Scerri et al., 2011).

Furthermore, the choice of sampling individuals from a dyslexia case-sibling population improves the study's power of identifying meaningful genotype-endophenotype correlations, if compared either to a population-based design or to a family-based study preceding a GWAS. The strategy of using previous GWAS' findings as hypothesis to be tested via a family-based study increases the power of the observed biological endophenotype effects, and also helps to sidestep phenotype integrity (Pal and Strug, 2014; Alhusaini et al., 2016).

Chapter 2: General Materials and Methods

2.1 Ethics Statement

Written informed consent was given by the parents/caregivers and by every child participating in one or more parts of the ChildBrain multimodal study. The consent was obtained according to the Declaration of Helsinki and it was approved by the Aston University Ethics Committee (ethics n. 372, n. 408, n. 488, n.1220).

2.2 Participants and Data Acquisition

The Dyslexia and Development Assessment Unit (DDAU) of the Aston Brain Centre (ABC) assesses for dyslexia approximately 60 children per annum and maintains a database of families that are in principle interested in participating in the ABC neurodevelopmental research studies.

For the ChildBrain multimodal study, a total of 221 children, between 6 and 17 years of age (mean age of 12.6 years) have been recruited between May 2013 and November 2018.

Following the psychological assessment at the DDAU of the child who was affected or likely to be affected by dyslexia, probands as well as his/her siblings/twins were invited to participate in the genetic-cognitive subset of our research study, that took place on the same day of the assessment, when possible.

A follow-up was then conducted with families via email, in order to: 1) provide all the relevant information concerning neuroimaging research investigations; 2) establish willingness to participate into one or more parts of our three-fold study, including genetics, magnetoencephalography and magnetic resonance imaging investigations; 3) book an appointment at the ABC to complete the study with probands and, when available, their siblings/twins. Further informed consents, specific for neuroimaging investigations, were signed by participants and their carers in person on the second meeting day.

During each part of the multimodal study, participants were allowed to have breaks at any time, and, at the end of their tasks, they received a personal award certificate for having done science at the ABC and contributing to advance brain research.

They were also debriefed with contact information, in case they wished to enquire further about the developments of ChildBrain project at any stage; this included information about the Marie Curie ITN project and its specific websites, through which outputs and findings of the study are disseminated as they become available.

Each participant was paid with £10 Amazon voucher for each part of the multimodal study (minimum £10, maximum £30), as reimbursement of their time and efforts; travel costs for the family were paid at standard University rates. In addition to the Amazon vouchers, each

participant received via email screen-shots of the 3 orthogonal projections (axial, sagittal, coronal views) for each of the MRI sequences performed at the Aston MRI Unit, so for the T1-weighted imaging (T1) and, when available, the diffusion tensor imaging (DTI).

Cognitive, behavioural, genetic and neuroimaging data were acquired as described in the following sections.

2.2.1 Psychological Assessment

According to the Diagnostic and Statistical Manual of Mental Disorders (DSM-5) of the American Psychiatric Association (APA, 2013), four criteria need to be met to make diagnosis of specific learning disorder: a) persistency of the symptoms for at least 6 months, despite specific intervention; b) academic skills that are substantially below what is expected for the child's age, with negative effect on school achievement; c) school-age onset of the difficulties, even if the disorder could fully manifest later; d) learning difficulties unrelated to other conditions, such as intellectual disability, sensory problems, neurological pathologies, economic/environmental disadvantage, lack of instruction, or difficulties in speaking/understanding the language. Furthermore, the severity of the learning disorder (mild, moderate, high severity) is expressed based on the level of support needed by the patient to fulfil the required tasks at school/ home/ workplace (mild/ moderate/ high level of support) (Petretto and Masala, 2017).

Differently from the DSM-5 approach, previous international diagnostic guidelines from both the DSM-4 (APA, 1994) and the 10th revision of the International Statistical Classification of Diseases and Related Health Problems (World Health Organization, 1992) agreed on considering the "principle of discrepancy" as the core diagnostic criterion for dyslexia, with regard to the discrepancy between the level of general cognitive ability and the specific learning abilities, as well as between the level of achievement in specific academic skills and the level of schooling (Petretto and Masala, 2017). The main consequence of eliminating the discrepancy criterion between general cognitive and specific learning abilities is indeed the high heterogeneity of intellectual abilities displayed by dyslexic individuals, ranging from high, average to below average (excluding only intellectual disability). Therefore, although the psychometric assessment of intelligence is not central to make diagnosis anymore, an accurate neuropsychological and psychometric evaluation is still crucial for a deeper understanding of the heterogeneity of the functional profiles of dyslexic patients, in order to support their potentials and define interventions (Petretto and Masala, 2017).

At the Aston Brain Centre's DDAU, children with specific learning disorders underwent a careful phenotypic assessment conducted by the Educational Psychologist (EP), using a standard battery of reading-related psychometric tests: British Ability Scales (BAS), Wechsler Intelligence Scales for Children (WISC), Wechsler Abbreviated Scale of Intelligence (WASI),

Wechsler Individual Achievement Test (WIAT), Wide Range Achievement Test (WRAT3) of single word reading and spelling. The assessment took place in English, therefore the first language of participants had to be English, as inclusion criterion.

On the same day, whether possible, those children who consented for being enrolled in the ChildBrain multimodal study were also administered the Test of Word Reading Efficiency (TOWRE), contextually with handedness tasks and saliva collection, as described in the next paragraphs (2.2.2 and 2.2.3).

Furthermore, parents/ carers of each child enrolled in the ChildBrain study completed some questionnaires: the Child Communication Checklist (CCC), to evaluate child expressive language ability; the Child Behaviour Checklist (CBCL) and the ASEBA Brief Problem Monitor (BPM)'s Internalizing, Externalizing, Attention Problems and Total Problems scales, to assess comorbid attention-deficit hyperactivity disorder (ADHD) symptoms (Achenbach et al., 2011), that are estimated to be present in one-third of people with learning disabilities (APA, 2013).

In addition, neuropsychological differences in hemispheric functioning were evaluated by analysing verbal intelligence quotient (VIQ) and performance intelligence quotient (PIQ) subtests. Subtracting the PIQ from VIQ, we derived the VIQ-PIQ discrepancy as measure of hemispheric asymmetries. The expected population mean of both VIQ and PIQ is 100, hence their expected discrepancy in a normal population is zero (Wechsler, 1981; Kaufman, 1990).

2.2.2 Handedness Assessment

Hand preference of each participant was assessed with the Annett Handedness Questionnaire (Annett, 1970). From the Annett's 12-item questionnaire, we derived the so-called Laterality Quotient (LQ), using the Oldfield's formula (Oldfield, 1971):

$$LQ = [(Right-Left) / (Right+Left)] \times 100$$

The LQ ranges from −100 to +100, where positive values indicate right-handedness, negative values left-handedness, higher absolute values indicate more consistent handedness and lower absolute values more ambidexterity or inconsistent handedness.

In order to investigate different aspects of handedness, three further measures were calculated based on each individual LQ, following the protocol of Arning et al. (2013): a) handedness direction, grouping participants into right-handers (RH, with LQ between 1 and 100) and left-handers (LH, with LQ between -100 and 0); b) categories of handedness consistency, classifying participants into six groups: consistent left-handers (LQ = -100), inconsistent left-handers (LQ = -99 to -50), ambidexter with a tendency towards left-handedness (LQ = -49 to 0), ambidexter with a tendency towards right-handedness (LQ = 1 to

49), inconsistent right-handers (LQ = 50 to 99) and consistent right-handers (LQ = 100); c) a dichotomous measure of degree of handedness (handedness consistency), independent from individual hand preference, grouping participants according to consistent (LQ either 100 or -100) or inconsistent (all other LQs) handedness.

To also gain a quantitative measure of hand skill, the classic pegboard task was used. In this simple motor task, participants had to move ten pegs from holes on the lower side of the pegboard to its upper side. This was repeated three times with the left hand and three times with the right hand, and the time needed to perform the task with each hand was recorded. As quantitative measure of hand skill asymmetries, we calculated the so-called Peg Quotient (PegQ), using the following formula:

$$PegQ = 2 \times (Left-Right)/ (Left + Right)$$

In the PegQ formula, Left is the average time in seconds needed to perform the task with the left hand, and Right is the average time in seconds needed to perform the task with the right hand (Ocklenburg et al., 2016). A positive PegQ indicates a superior relative right-hand skill, while negative PegQ indicates a better relative left-hand ability (Scerri et al., 2011).

2.2.3 DNA Collection and Genotyping

Saliva samples were collected from participants, by using the non-invasive Oragene kit. This procedure simply required the child to 'spit' into a plastic container, which was anonymised with a unique participant code, and sent for DNA extraction, storage and genotyping to Dr Silvia Paracchini's laboratory, at the School of Medicine, University of St Andrews, United Kingdom. Genotypes were generated on the Illumina OmniExpress SNP array (730,525 markers), that is a 24-sample BeadChip belonging to the Next-Gen genome-wide association study (GWAS).

Following the manufacturer’s protocol, samples were analysed using the Illumina HumanOmniExpress BeadChip process and genome build GRCh37/hg19. All data collected was evaluated using Illumina’s GenomeStudio v2011.1 software. It was followed the quality control protocol set out by Anderson et al. (2010), excluding individuals with: discordant sex information, a low genotyping success rate (≤98%), duplicate identity or assigned to the wrong individuals (identity by state IBS metric ≥0.1875).

After DNA analysis, participants were stratified by genotype in two groups: (1) the ‘non-carriers’, being the subjects without the minor rs11855415 allele (T/T); and (2) the ‘carriers’, being the subjects showing the minor rs11855415 allele, in either homozygosity (A/A) or heterozygosity (A/T).

2.2.4 MRI Data Acquisition

This step required participants to have an MRI scan at the Aston MRI centre, which took approximately 15 minutes. Before undertaking the scan, children were screened for any contra-indicators, by using the Aston Brain Centre standard primary and secondary screening forms.

The MRI brain scanning was performed with the 3 Tesla Trio Magnetom MRI scanner from Siemens Medical Systems. During the examination, each child laid supine in the scanner, keeping the eyes closed or, upon request, watching videos on a little mirror (provided by the manufacturer) placed in front of the eyes and reflecting the images projected on an MRI-safe screen located at the opposite end of the scanner, by a projector placed outside the MRI room. Scanner noise was attenuated with earplugs, and headphones were used for audio and communication. Head motion was limited with foam padding (provided by the manufacturer) placed around the head; the necessity of head immobility was emphasized and encouraged with each subject. MRI image datasets were acquired with a standard T1-weighted high-resolution anatomic scan of magnetization-prepared rapid gradient echo (MPRAGE) sequence: Repetition Time (TR)=1900ms, Echo Time (TE)=3.37ms, Inversion Time (TI)=1100ms, Flip Angle=15°, Field of View (FoV)=256mm, Averages=1, matrix=256×256, slice thickness of 1 mm. Structural MRI acquisition of each subject was conducted with the same slice orientation, paralleled to the anterior commissure and commissural posterior line. Before proceeding with saving the images acquired, we confirmed whether they were uncontaminated with major head motion.

The MRI data were copied from the MRI scanner, and imported to a personal computer running a Linux operating system. Proper MRI images input format for off-line MRI analyses were obtained by using DCM2NII in MRIcron (Rorden et al., 2007), which converted DICOM (Digital Imaging and COmmunications in Medicine) files to NIfTI (Neuroimaging Informatics Technology Initiative) format. Images were then analysed by using FMRIB Software Library (FSL v6.0, https://fsl.fmrib.ox.ac.uk), Childmetrix (Icometrix https://icometrix.com/), and Statistical Parametric Mapping Software (SPM12, https://fil.ion.ucl.ac.uk/spm/) in the MATLAB R2017a environment (The MathWorks® Inc., Natick, MA.), as detailed in Chapter 3 (Paragraphs 3.2.2 and 3.3.2).

2.2.5 MEG Data Acquisition

Magnetoencephalography (MEG) data were recorded at the Wellcome Trust Laboratory for MEG studies at the ABC, in a magnetically shielded room, by using an Elekta Neuromag TRIUX whole-head system (Helsinki, Finland), with 204 planar dc-SQUID gradiometers and 102 magnetometers, at sampling rate of 2000 Hz and band-pass filter of 0.1–660 Hz. Participants seated comfortably inside the scanner in an upright position, with five coils placed

on the head, three on the forehead and one on each mastoid, for continuous head position monitoring. The translation between the MEG coordinate system and the individual structural MRI space was made by digitising three head position fiducials with a Polhemus Fastrack device, at the nasion, left and right pre-auricular points. Polhemus was also used to define and measure the individual surface head shape, and to localise the electromagnetic head coils with respect to the surface. Visual and auditory stimuli were presented using Presentation® software (Neurobehavioral Systems, Inc.) and projected (by a projector placed outside the shielded room) on a translucent screen, positioned at a distance of 85 cm from the child, subtending a 3-degree visual angle.

The high-resolution anatomical MRI scans acquired at the Aston MRI Unit were used for co-registration with MEG data. MaxFilter software (Elekta Neuromag Oy, version 2.2.10) with transformation to default head position and temporal extension of signal space separation (tSSS) (Taulu and Hari, 2009) was used respectively to: decrease variance between-subjects, due to the head positions inside the helmet being variable; and remove signal artefacts, due to movements during the recording. MaxFiltered data were visually inspected to make a comparison between default and original head position, and to identify “bad channels” to be removed if present. MEG data were then analysed in the MATLAB R2017a environment (The MathWorks® Inc., Natick, MA.), by using FieldTrip toolbox (Oostenveld et al., 2011; http://fieldtriptoolbox.org/) and Statistical Parametric Mapping (SPM12) (http://fil.ion.ucl.ac.uk/spm/), as described in Chapter 4 (Paragraphs 4.3.2, 4.3.3, 4.4.2, 4.4.3, 4.4.4, 4.4.5, 4.4.6).

Chapter 3: Magnetic Resonance Imaging Studies

3.1 Introduction

Quantitative neuroanatomical imaging-derived traits show moderate-to-high heritability in affected and healthy populations (Peper et al., 2007; Glahn et al., 2007; Goldman et al., 2008; Den Braber et al., 2013), and are often used in imaging genomics, as quantitative endophenotypes for genome-wide mapping studies (Thompson et al., 2014; Alhusaini et al. 2016). In particular, neuroimaging measures fit particularly well in the concept of atypical hemispheric asymmetries as extended endophenotype, being able to provide quantitative information (e.g. volume, shape, cortical thickness and surface) about brain structures that are believed by some authors to underpin functional hemispheric asymmetries (Ocklenburg et al., 2016; Hervé et al., 2013; Amunts, 2010).

3.1.1 Brain Asymmetries and Quantitative MRI Traits

According to the Ocklenburg's triadic model, there are three independent structural determinants of functional asymmetries: the corpus callosum, white matter intrahemispheric networks and grey matter asymmetries (Figure 3.1) (Ocklenburg et al., 2016). This paradigm assumes that stronger grey matter asymmetries lead to stronger functional asymmetries, where increase of grey matter would correlate to the increase of the function, and viceversa a decreased grey matter would yield a reduction of functional efficacy (Ocklenburg et al., 2016).

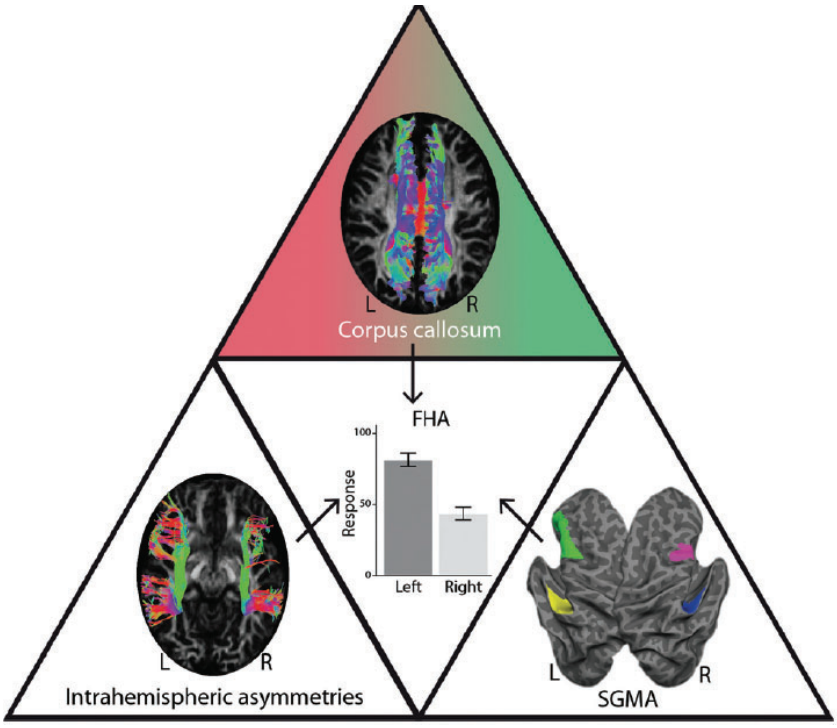

Figure 3.1: The Ocklenburg's triadic model. The structural determinants of functional asymmetries according to this model are: structural grey matter asymmetries (SGMA) (bottom right), corpus callosum (top) and asymmetries of intrahemispheric white matter pathways (bottom left). Figure and caption from Ocklenburg et al. 2016.

The most prominent of the human grey matter asymmetries is within the planum temporale, a leftward asymmetric intrasylvian region in the superior temporal sulcus, involved in language perception (Galaburda et al., 1990; Steinmetz et al., 1991; Chance, 2014). However, the extent to which its asymmetry correlates to functional language lateralisation is still unclear (Ocklenburg et al., 2016). A positive correlation between planum temporale and lateralisation induced by dichotic listening has been observed in right-handed males, but not in left-handed males and females (Dos Santos Sequeira et al., 2006).

Moreover, the transverse temporal gyrus, the pars opercularis of the inferior frontal gyrus and the insula, in addition to the planum temporale, showed significant leftward volumetric lateralisation in both left- and right-hemispheric language dominant individuals (Greve et al., 2013), but only the insular volume has been found to be significantly larger in the left, rather than in the right, hemispheric dominants (Greve et al., 2013), and also correlated with functional lateralisation in the dichotic listening as well as in a word generation fMRI task (Greve et al., 2013; Chiarello et al., 2013).

Interestingly, grey matter asymmetries in temporal and frontal lobes have been recently found to be associated with an intronic 33bp VNTR polymorphism in *PCSK6* (rs10523972) (Berretz et al., 2019), also shown to be associated with handedness direction in a cohort of healthy adults (Arning et al., 2013). These recent findings corroborate the hypothesis of a role of *PCSK6* in hemispheric asymmetries, and complement previous observations from genome wide association studies on the association between *PCSK6* rs11855415 and increased relative right-hand skills in dyslexic individuals (Scerri et al., 2011; Brandler et al., 2013).

Against such backdrop, quantitative MRI-derived endophenotypes will be examined in this chapter, with the ultimate goal of investigating whether NODAL signalling pathway may influence atypical structural hemispheric asymmetries. Based on previous GWAS' findings about dyslexia, *PCSK6* and functional hemispheric asymmetries, such as handedness (Scerri et al., 2011; Brandler et al., 2013), the first MRI study will explore the hypothesis of a putative correlation between brain structural measures, such as voxel-based grey matter morphometry and asymmetry, and the minor allele of *PCSK6* rs11855415 variant, in a small population of dyslexic children and matched siblings/twins. The second study will follow up on the preliminary results of the first exploratory study, by applying an innovative paediatric MRI analysis tool in a larger cohort of dyslexic children and matched siblings/twins, and exploring structural brain asymmetry dimensions in relation to the *PCSK6* rs11855415 minor allele.

Different softwares and analysis pipelines are used in the two studies, contextually with ChildBrain secondments and different phases of training during the PhD. MRI data analyses will be described in detail in the specific sections of each MRI study (paragraphs 3.2.2 and 3.3.2).

3.2 A Voxel-Based Morphometry Exploratory Study

This MRI study preliminarily investigates whether atypical grey matter asymmetries might be associated to *PCSK6* rs11855415 variant in dyslexic children and matched-siblings. As described in the Introduction Chapter 1, the hypothesis of *PCSK6*-associated atypical cortical asymmetries has been driven by the findings of previous genome-wide association studies, showing a significant association between greater functional hemispheric asymmetries and the minor allele of *PCSK6* rs11855415 variant, in cohorts of dyslexic individuals (Scerri et al., 2011; Brandler et al., 2013).

The related SPM analysis training was conducted at the University College London Wellcome Trust Centre for Neuroimaging. Prof Mark A. Eckert provided guidance about image processing, during my secondment in his laboratory at the Medical University of South Carolina. The entire training was funded by the ChildBrain MSCA-ITN research programme.

3.2.1 Participants

In this early exploratory study, brain MR images from 7 children, carrying the *PCSK6* rs11855415 minor allele in homozygosity (A/A) or heterozygosity (A/T), were compared to the scans of 7 non-carriers (T/T). The two groups were matched by age, gender and affection status, in order to investigate the state-independent *PCSK6*-related endophenotype.

Participants were sampled from the Aston Brain Centre multimodal database, containing all the *PCSK6*-genotyped dyslexic children and their affected/unaffected relatives who underwent an MRI scan at the Aston MRI Centre. A total of 14 MR images from *PCSK6*-genotyped children were initially identified, including 4 dyslexic and 10 typical readers, 4 females and 10 males, between 7.5 and 17.8 years of age (mean 12.6 years ± 2.9). Among the carriers, only one child showed an homozygotic genotype, so it was not possible to look for a potential additive effect of the minor allele (A) in homozygosis, or for a possible linear effect from T/T to A/T to A/A on structural asymmetries, in line to what was previously shown in relation to functional asymmetry by Scerri et al. (2011) and Brandler et al. (2013).

3.2.2 MRI Data Analysis

3.2.2.1 Tissue-type Segmentation and Volume Quantification

To examine the total volumes of grey matter (GM) and white matter (WM) in both groups, the following FSL v6.0 (FMRIB Software Library, https://fsl.fmrib.ox.ac.uk) analysis pipeline was applied: 1) T1-weighted MRI images were brain-extracted using BET (Smith, 2002) to remove skull and skin tissues; 2) tissue-type segmentation was performed by using FAST (FMRIB's Automated Segmentation Tool) (Zhang et al., 2001) package, that segments a 3D image of the brain into different tissue types, whilst also correcting for spatial intensity

variations (also known as bias field); 3) the tissue volume quantification was conducted with 'fslstats', that estimates the total tissue volume for a given class of the Partial Volume Estimate (PVE) components, namely, GM, WM, and cerebrospinal fluid (CSF).

3.2.2.2 Voxel-based Grey Matter Morphometry Analysis

To investigate voxel-based differences of GM morphometry between carriers and non-carriers, structural data were analysed with FSL-VBM8 (Douaud et al., 2007; http://fsl.fmrib.ox.ac.uk/fsl/fslwiki/FSLVBM), an optimised VBM protocol (Good et al., 2001) using FSL tools (Smith et al., 2004). The resulting images were averaged and flipped along the x-axis to create a left-right symmetric study-specific GM template, to reduce the effect of inter-subject brain variability during the registration procedure. As second step, all native GM images were non-linearly registered to this study-specific template, and modulated by using the Jacobian of the warp field, in order to correct for local expansion or contraction, due to the non-linear component of the spatial transformation from native space to registration template.

The modulated GM images were then smoothed with an isotropic Gaussian kernel of 8mm, for the Threshold Free Cluster Enhancement (TFCE)-based analysis (Smith and Nichols, 2009). Finally, differences in cerebral GM density (or voxel intensity, that is the GM concentration per unit of intracranial volume, and accounts for brain size differences and volume changes from spatial transformation) between carriers and non-carriers were assessed by voxel-wise General Linear Model (GLM); the hypothesis of the two-sample *t*-test was 'group 1 (non-carriers) > group 2 (carriers)'. We then run permutation-based non-parametric testing (5000 permutations) (Nichols and Holmes, 2002), correcting for multiple comparisons across space, by cluster-size shareholding at p-values<0.05.

3.2.2.3 Voxel-wise Grey Matter Asymmetry Analysis

To investigate volumetric hemispheric asymmetries of the GM in each subject, and then test the potential effect of *PCSK6* (comparing carriers with non-carriers), we followed the SPM 12-step asymmetry analysis pipeline by Kurth et al. (2015). The processing steps are briefly explained below: 1) the first step (estimate and write) involved bias-correcting the raw T1-weighted images for inhomogeneities, extracting the brain, and segmenting it into GM, WM and CSF volume probability maps; 2) then, the SPM's image calculator 'ImCalc' was used to flip the images at midline; 3) a symmetric DARTEL study-specific template was created from the original and flipped GM and WM segments; 4) the module 'Create Warped' was used to warp the original and flipped tissue segments (created in Step 2) to the symmetric DARTEL template (created in Step 3); 5) a right-hemispheric mask in symmetric template space was created in MRIcron, to limit the analysis to the right hemisphere; 6) to calculate the Asymmetry Index (AI), we used the MATLAB script 'calculate', which generated the masked AI images from the original warped GM images and the right hemispheric mask; 7) the module 'Smooth'

was used to smooth all the AI images created in Step 6, with '8 8 8' as size of the smoothing kernel; 8) to generate the study-specific 'mean template' in symmetric space, the PVE label images were created, flipped and warped, to finally create the mean of all warped PVE label images, further adjusted to restrict the template to the right hemisphere, for projecting the resulting significance clusters; 9) we created and explicit binary mask using 'ImCalc', to restrict the statistical analysis to brain regions expected to contain true signal ; 10) we then proceeded with the statistical analysis of the smoothed AI images, by using the module 'Factorial design specification', specifying one-sample *t*-test (to look at the interhemispheric differences in the whole sample) and two-sample *t*-test (to look at the interhemispheric difference between carriers and non-carriers) as statistical models, and applying the mask created in Step 9; the hypothesis for the two-sample *t*-test was 'group 1 (non-carriers) > group 2 (carriers)'; 11) for better interpretation of the resulting significance maps, we correct them for multiple comparisons at the cluster level, enabling SPM's nonstationary correction; to save only the significant clusters, we run the function 'Threshold and transform spmT-maps'; 12) to calculate the mean AI and hemispheric grey matter volumes (in mm^3) of the significance asymmetric cluster on the right and left hemisphere, we run the MATLAB script 'extract' for each subject. Positive high AI values indicate a rightward asymmetry, while negative AI values indicate a leftward asymmetry (Figure 3.2).

According to this protocol, voxel-wise asymmetry is quantified before conducting statistical analysis, in order not to affect the results by side effects of smoothing. In symmetric space, asymmetry can be quantified also by calculating the simple left-right difference; however, this difference would reflect symmetric changes in brain size, while AI safeguards against symmetric scaling effects, being a normalised asymmetry measure.

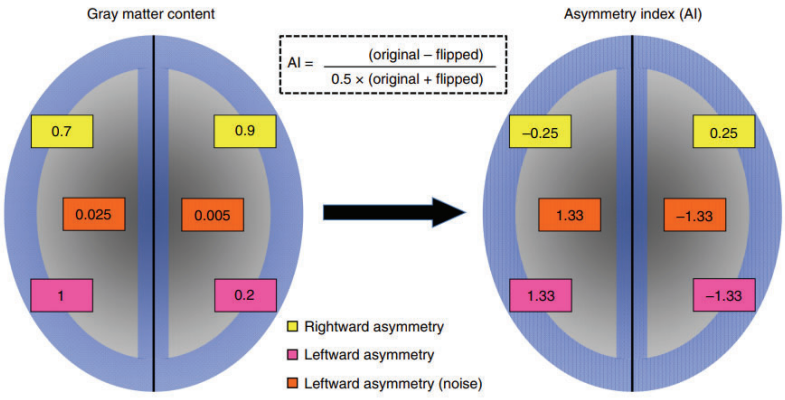

Figure 3.2: The Asymmetry Index (AI) Model. On the left, model of voxel-wise GM content with 1 = 100% GM and 0 = no GM. More GM in the right hemisphere (rightward asymmetry) will lead to positive AI values on the right and negative values on the left (yellow AI values). More GM in the left hemisphere (leftward asymmetry) will lead to negative AI values on the right and positive values on the left (pink AI values). Small hemispheric differences in regions with low GM content (e.g., due to noise) can produce the same results (orange AI values) as extreme hemispheric differences (pink AI values). To solve this ambiguity, it is important to do a cluster-specific extraction of volume and AI value. Figure and caption from Kurt et al., 2015.

3.2.3 Statistics

Statistical analyses were conducted by using different methods. In the FSL-VBM analysis, the GLM was used to compare voxel-wise differences in GM density between carriers and non-carriers; non-parametric statistics were also performed using 'randomise' with 5000 permutations and using the TFCE option. In the SPM voxel-wise asymmetry analysis, differences between carriers and non-carriers were examined via the GLM in SPM8; all findings resulting from the group comparisons were corrected for multiple comparisons on cluster level. The rest of the statistical analysis was performed in SPSS® version 23 statistical software (IBM, Armonk, NY, USA), where group comparisons were done by two-sample *t*-tests, and correlations were revealed by bivariate Pearson's correlation (including continuous and dichotomous categorical variables). Given the exploratory nature of this statistical analysis, further correction for multiple comparisons was not applied.

3.2.4 Results

3.2.4.1 Handedness

The analysis of handedness measures (LQ and PegQ), comparing carriers to non-carriers, did not reveal significant differences between the groups.

3.2.4.2 White Matter and Grey Matter Volumes

Both GM and WM total volumes, as well as the GM/ WM ratio, were found increased in the carriers compared to the non-carriers, but only the GM volumetric difference between the groups reached the uncorrected significance threshold of 0.05 (p=0.024).

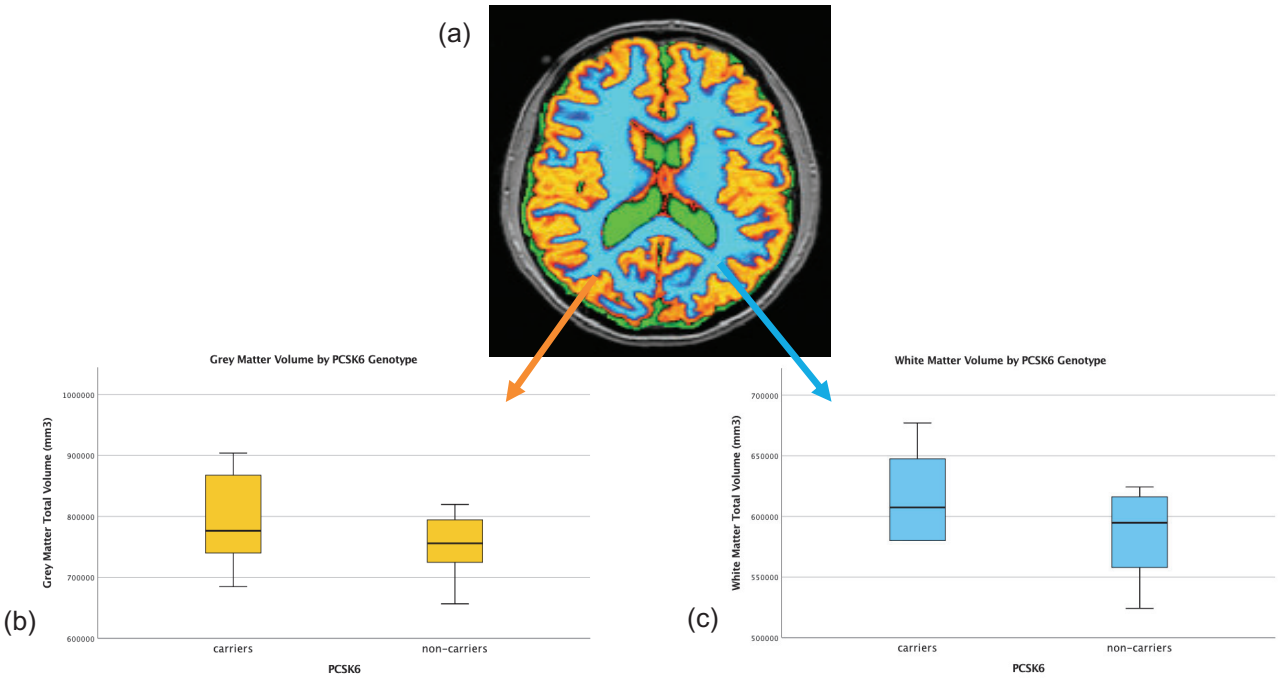

Figure 3.3: Partial Volume Quantification Results: a) FSL internal brain tissues segmented, white matter (WM) in blue, liquor in green and grey matter (GM) in yellow; b) box-plot of GM total volume in carriers and non-carriers; c) box-plot of WM total volumes in carriers and non-carriers.

3.2.4.3 Voxel-based Grey Matter Morphometry

The VBM analysis comparing carriers to non-carriers showed a significantly different cluster of GM density in the pars opercularis of the right inferior frontal gyrus (IFG) (red area in Figure 3.4a,b,c). In this brain region, carriers exhibited a lower density of GM compared to the non-carriers (p<0.05).

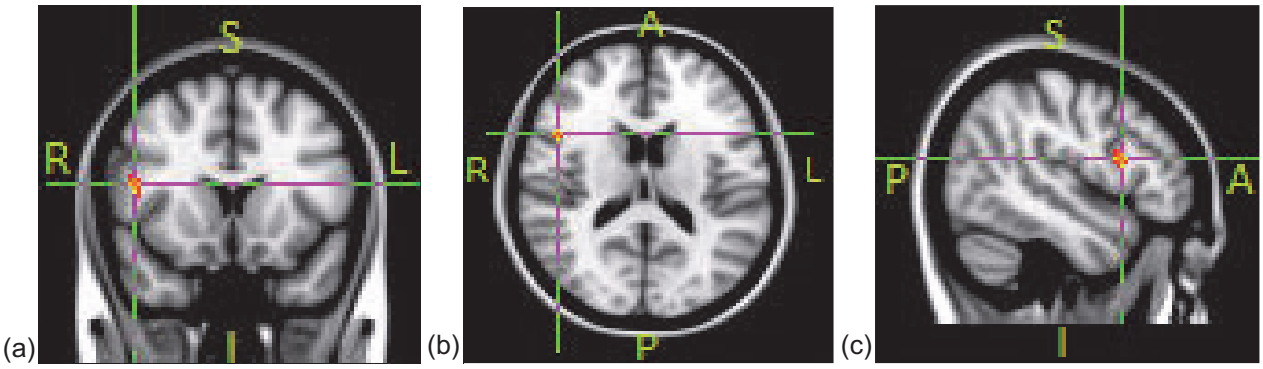

Figure 3.4: FSL-VBM output of the GM density cluster in coronal (a), axial (b), sagittal (c) views.

3.2.4.4 Voxel-wise Grey Matter Asymmetry

The voxel-wise GM asymmetry analysis between the right and the left hemisphere showed a significant rightward asymmetric cluster (AC) at the level of the Inferior Frontal Sulcus (IFS) (yellow area in Figure 3.5a,b,c) (p<0.05) in the entire group. The analysis of the hemispheric asymmetries comparing carriers to non-carriers did not evidence any significant difference; neither the AI nor the volume of the AC differed significantly between carriers and non-carriers.

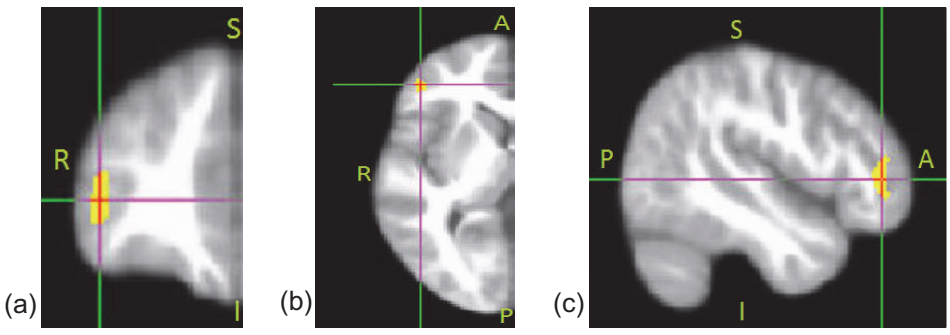

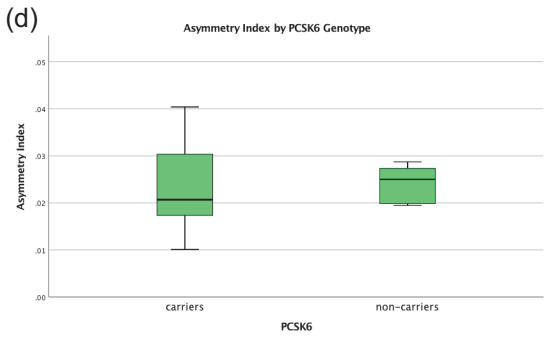

Figure 3.5: Asymmetry analysis results

At the top, SPM output showing the asymmetric cluster (in yellow) in coronal (a), axial (b), and sagittal (c) views.

At the bottom, boxplot (d) of the asymmetry index in carriers and non-carriers.

3.2.4.5 Interphenotypic Correlations

In each group, we looked for possible interphenotypic associations between behavioural, cognitive, handedness and neuroimaging measures.

As far as carriers were concerned, they exhibited three statistically significant positive correlations: 1) between WM and GM total volumes (r = 0.773, p = 0.042); 2) between the AC's GM volume of the right hemisphere and the LQ (r = 0.903, p = 0.036); 3) between the AC's GM volume of the left hemisphere and the ASEBA Brief Problem Monitor (BPM) Attention problems score (r = 0.811, p = 0.050). Furthermore, they showed two statistically significant negative correlations: 1) between the AC's GM volume of the right hemisphere and the BPM Internalising problems score (r = -0.821, p = 0.045); 2) between the AI and the BPM Total problems score (r = -0.814, p = 0.049).

As far as the non-carriers were concerned, they presented three statistically significant positive correlations: 1) between WM and GM total volumes (r = 0.839, p = 0.018); 2) between GM total volume and the BPM Internalising problems score (r = 0.819, p = 0.024); 3) between the AC's GM volume of the left hemisphere and gender (r = 0.773, p = 0.041). Furthermore, non-carriers showed a highly significant positive correlation between WM total volume and the BPM Internalising problems score (r = 0.886, p = 0.008), and a statistically significant negative correlation between WM total volume and GM/WM ratio (r = -0.795, p = 0.032).

All significant correlations are outlined in Table 3.1. A scatterplot matrix (SPLOM) of significant correlations is provided for each group (Figures 3.6 and 3.7); separate scatterplots of asymmetry-related correlations exhibited by carriers are also displayed (Figure 3.8a,b,c).

Table 3.1: Significant interphenotypic correlations observed in carriers and non-carriers, with respective r coefficient, p-value and sample size.

Significant Correlations	*r* coefficient	*p*-value	Sample Size
Carriers			
WM – GM	0.773	0.042*	7
AC RH - LQ	0.903	0.036*	5
AC RH – BPM I	-0.821	0.045*	6
AC LH – BPM A	0.811	0.050*	6
AI – BPM T	-0.814	0.049*	6
Non-carriers			
WM – GM	0.839	0.018*	7
WM – GM/WM	-0.795	0.032*	7
WM – BPM I	0.886	0.008**	7
GM – BPM I	0.819	0.024*	7
AC LH - Gender	0.773	0.041*	7

*WM = white matter volume in mm^3; GM = grey matter volume in mm^3; AC = asymmetric cluster's grey matter volume in mm^3; RH = right hemisphere; LH = left hemisphere; LQ = laterality quotient; AI = asymmetry index; BPM I, A, T = Brief Problem Monitor Internalising, Attention, Total problems scores. *Correlation significant at 0.05 (2-tailed, uncorrected). **Correlation significant at 0.01 (2-tailed, uncorrected).*

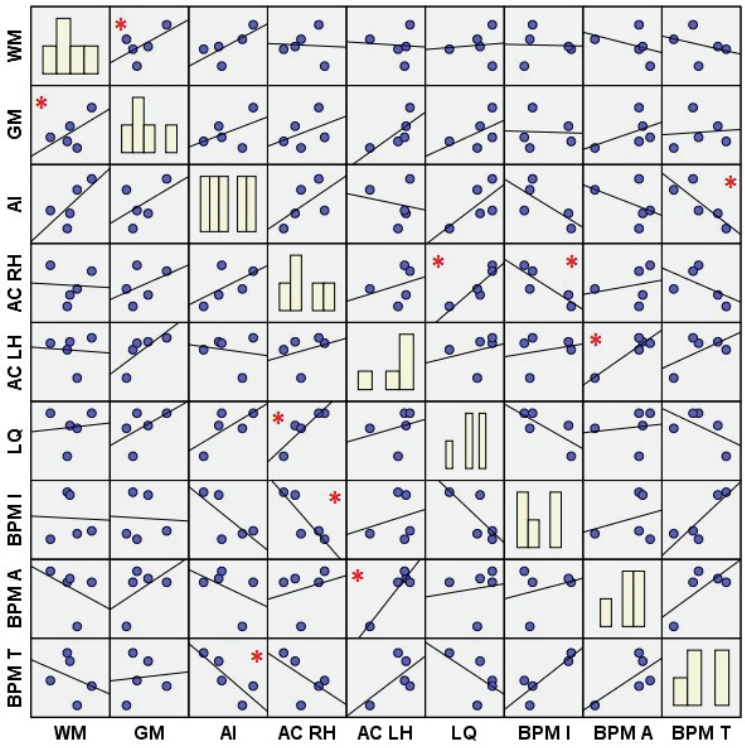

*Figure 3.6: Scatterplot matrix (SPLOM) of significant interphenotypic correlations observed in carriers. Histograms of the variables are shown in the diagonal. WM = white matter volume in mm^3; GM = grey matter volume in mm^3; AC = asymmetric cluster; RH= right hemisphere; LH = left hemisphere; LQ = laterality quotient; AI = asymmetry index; BPM I, A, T = Brief Problem Monitor Internalising, Attention, Total problems scores. *Correlation is significant at the 0.05 level (2-tailed, uncorrected). **Correlation is significant at the 0.01 level (2-tailed, uncorrected).*

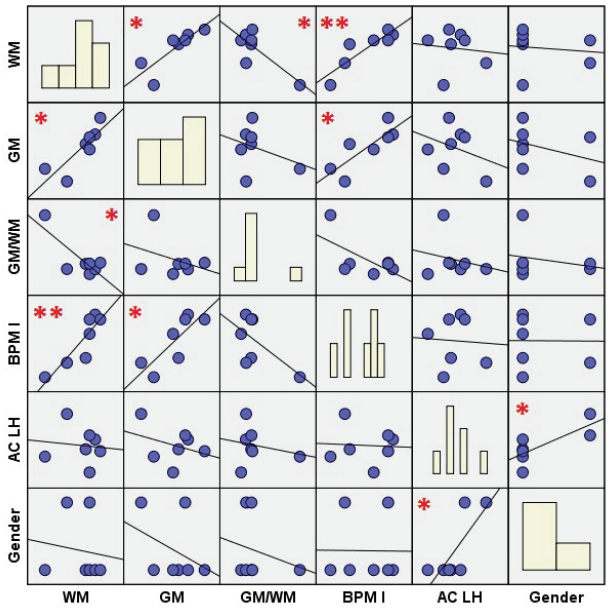

*Figure 3.7: Scatterplot matrix (SPLOM) of significant interphenotypic correlations observed in non-carriers. Histograms of the variables are shown in the diagonal. WM = white matter volume in mm^3; GM = grey matter volume in mm^3; AC = asymmetric cluster; LH = left hemisphere; BPM I = Brief Problem Monitor Internalising problems score. *Correlation is significant at the 0.05 level (2-tailed, uncorrected). **Correlation is significant at the 0.01 level (2-tailed, uncorrected).*

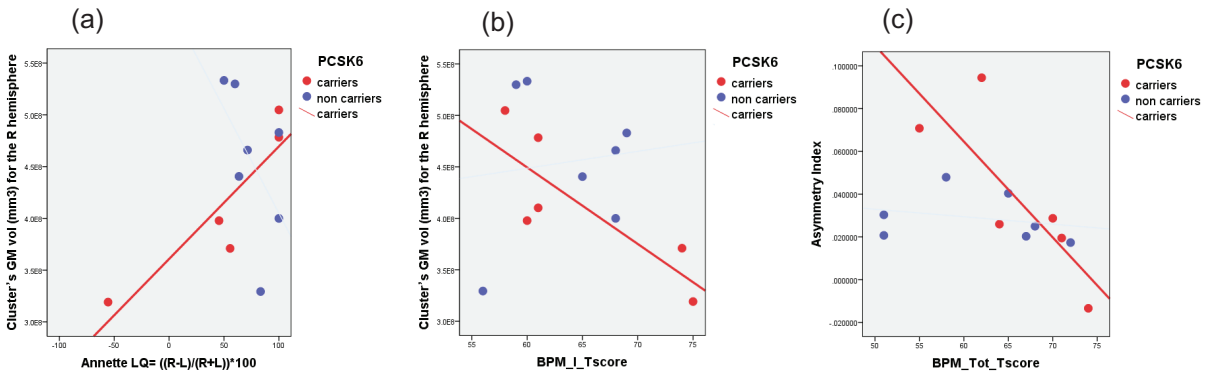

Figure 3.8: Scatterplots of the significant correlations observed in carriers, between asymmetry and behavioural measures: a) positive correlation between handedness laterality quotient (LQ) and the volume of the asymmetric grey matter (GM) cluster on the right (R) hemisphere; b) negative correlation between the latter and Brief Problem Monitor (BPM) Internalising (I) problems score; c) negative correlation between the asymmetry index and BPM Total (T) problems score.

3.2.5 Discussion

Conscious of the main caveat of this exploratory study, represented by its limited power due to the small sample of subjects examined, we must interpret any preliminary finding cautiously. At the same time, these insights can be used to drive future steps and expand research questions, in particular with regard to the *PCSK6*-related grey matter asymmetries (see the next MRI study, presented in paragraph 3.4).

On the basis of previous GWASs (Scerri et al., 2011; Brandler et al., 2013) that showed a significant association between the minor allele of *PCSK6* rs11855415 and increased relative right-handedness in dyslexia, we wanted to test whether atypical structural hemispheric asymmetries might be a state-independent endophenotype of *PCSK6* rs11855415, and therefore present also in those unaffected siblings carrying the minor allele.

In terms of handedness, we did not confirm the endophenotype hypothesis, as there was no difference in PegQ and LQ between carriers and non-carriers.

To some extent, even their neuroimaging-derived profiles, in terms of voxel-wise GM hemispheric asymmetries, were similar in both groups. In fact, the whole population exhibited a significant rightward asymmetric GM cluster in the IFS, with comparable asymmetric cluster's hemispheric volumes as well as asymmetry indices, between carriers and non-carriers. However, the right volume of the asymmetric cluster in the IFS was positively correlated with handedness LQ in carriers; therefore, the higher is the right volume, the higher will be the handedness LQ and the degree of right-handedness. Such correlation might therefore represent a feature of the postulated extended endophenotype, potentially linking *PCSK6* genotype to dyslexia phenotype via handedness, in line with previous findings on *PCSK6*-associated increased relative right-hand skills in dyslexia (Scerri at al., 2011; Brandler et al., 2013). Nevertheless, the handedness aspect of the *PCSK6*-related extended endophenotype

has not been fully addressed in the thesis, since the main research focus is on the neuroimaging-derived endophenotypes.

Although we did not observe a significant difference in terms of voxel-wise GM asymmetries between carriers and non-carriers, we found a significantly higher total volume of GM as well as a significantly lower density of GM in the pars opercularis of the right IFG, in carriers compared to non-carriers. Previous VBM studies explored GM volume in dyslexic subjects carrying a deletion within other dyslexia candidate genes implicated in ciliogenesis, such as *DCDC2* (Meda et al., 2008), and also found an increased GM total volume in carriers compared to non-carriers, as well as regional volumetric differences at the level of many structures, such as the inferior, middle and superior frontal gyrus (Meda et al., 2008).

In our study, the IFG volumetric difference associated to the minor allele was interestingly very close to where both carriers and non-carriers displayed the IFS righward asymmetric cluster. Therefore, both morphometry and asymmetry analyses pointed towards the inferior frontal lobe (inferior frontal gyrus and sulcus) as a key region for *PCSK6*, although showing significant similarities between the groups in terms of asymmetry (both groups presented a rightward GM asymmetric cluster in the IFS), and significant differences in terms of morphometry (carriers presented a lower GM density in the IFG compared to non-carriers). Thus, these preliminary findings may be suggestive of a crucial involvement of the inferior frontal lobe in the postulated *PCSK6*-associated structural endophenotype.

Interestingly, the right opercular portion of the IFG is the right homologous of what the Broca's area is on the left hemisphere. Broca's region includes pars opercularis and pars triangularis of the left IFG, both of which contribute to verbal fluency, respectively from the production and semantic processing standpoint (Fauci et al., 1998). The right pars opercularis has been instead implicated in impulse control in the go/no go tasks (Aron, Robbins and Poldrack, 2004), as well as in risk aversion (Christopoulos et al., 2009). Abnormalities at this level may therefore lead to behavioural problems, due to an increase of impulsivity and risk attitudes (Knoch et al., 2006; Fecteau et al., 2007). This seems to be concordant with our asymmetry findings, according to which carriers showed significant negative correlations between the volume of the asymmetric cluster on the right hemisphere and the BPM Internalising problems score, as well as between the asymmetry index and the score of BPM Total problems. In contrast, a positive correlation was found between the asymmetric cluster's volume on the left hemisphere and the BPM Attention problems score. It seems therefore that *PCSK6*-related hemispheric asymmetries at this level may not only have effects on functional asymmetries, such as handedness and language, but also on behavioural problems. As such, it would be of great interest to explore further these hemispheric asymmetries in relation to the comorbidity between dyslexia and attention deficit hyperactivity disorder (ADHD), to understand whether *PCSK6* might influence also behavioural traits like inattention, impulsivity and hyperactivity, via atypical structural asymmetries.

3.3 Structural Asymmetries in the Aston Brain Centre *PCSK6* Cohort

This second MRI study builds on the preliminary findings of the exploratory VBM study presented in the previous section, with the aim of investigating further the postulated asymmetry endophenotype, by examining the entire Aston Brain Centre MRI cohort of *PCSK6*-genotyped children.

This was a collaborative research with Icometrix (Leuven, Belgium), an industrial company expert in brain imaging artificial intelligence solutions, and member of the ChildBrain Network. My ChildBrain secondment at Icometrix was supervised by Dr Dirk Smeets, and conducted in collaboration with Thanh Vân Phan, ChildBrain Early Stage Researcher number 11 and PhD candidate at the Katholieke Universiteit Leuven, who developed Childmetrix tool to optimise paediatric MRI analyses.

3.3.1 Participants

Participants were selected from the Aston Brain Centre multimodal database, containing all the *PCSK6*-genotyped dyslexic children and their affected/unaffected siblings/twins who underwent an MRI scan at the Aston MRI Centre, as well as handedness and reading assessment at the Aston DDAU. A total number of 47 children between 6 and 17.8 years of age (mean 11.9 years ± 1.3) were included: 19 females and 28 males; 27 dyslexic and 13 typical readers; 3 left-handed and 41 right-handed; 19 with consistent handedness and 25 with inconsistent handedness; 29 non-carriers (T/T) and 17 carriers (A/T, A/A) of the minor allele (A) of *PCSK6* rs11855415 variant. Among the carriers, only two children showed homozygotic genotypes (A/A), so it was not possible to look for a potential additive effect of the minor allele in homozygosis; neither to investigate whether there was a linear effect from T/T to A/T to A/A, with the latter genotype potentially corresponding to a stronger structural asymmetry, in line with what was previously shown in terms of functional asymmetry by Scerri et al. (2011) and Brandler et al. (2013).

Cases with missing values (e.g. undefined handedness scores, or undetermined genotypes for contaminated saliva samples) were excluded on an analysis-by-analysis basis (pairwise deletion).

3.3.2 MRI Data Analysis

3.3.2.1 Volumetric Analysis in Childmetrix

Childmetrix is an MRI analysis tool, suitable for paediatric brain imaging data (Phan et al., 2018), based on the age-specific independent paediatric population-based atlases of the NeuroImaging & Surgical Technologies Lab of the Montreal Neurological Institute (MNI) (Evans and Group, 2006; Almli et al., 2007; Fonov et al., 2009); these atlases were created by

averaging 324 brain scans of healthy children enrolled in the National Institutes of Health-funded MRI study of normal brain development (http://nist.mni.mcgill.ca/?p=974).

In such multi-atlas system, five age groups between 4.5 and 18.5 years are represented: pre-puberty (4.5-8.5 years), pre- to early puberty (7-11 years), pre- to mid-puberty (7.5-13.5 years), early to advanced puberty (10-14 years) and post-puberty (13-18.5 years). Each atlas consists of a brain template, a brain mask and probability maps for the three main tissues (GM, WM and CSF). Label maps of cortical regions from Mindboggle adult atlas (Klein et al., 2012; https://mindboggle.info/) and of subcortical regions from the Child and Adolescent Neurodevelopment Initiative (CANDI) Share atlas (Kennedy et al., 2012), were also added to Childmetrix, and adjusted to each age-specific brain template, with affine and non-rigid registration and manual corrections.

Childmetrix cross-sectional pipeline works by processing T1-weighted brain images acquired at one time point, to provide volumetric measures of the whole brain, cortical grey matter (CGM) regions, white matter (WM) regions, cerebrospinal fluid (CSF) and subcortical structures.

For the current study, each T1-weighted image entered in Childmetrix was matched to a specific atlas, using normalised mutual information, on the basis of the age of the subject and the similarity between individual brain and atlas. After the pre-processing steps of skull-stripping, bias-correction and atlas-to-image registration, probability maps of GM, WM and CSF were obtained with an optimised Gaussian Mixture Model, considering image intensities, spatial prior knowledge of the tissues, intensity non-uniformities, and spatial consistency based on Markov Random Field (Phan et al. 2018). The CGM was then extracted from the GM probability maps, and parcellated into 62 regions, according to the parcellation map of the age-specific atlas. To obtain a first propagation of cortical labels from the atlas space to the subject T1-weighted image space, an initial non-rigid registration between the individual T1-weighted image and the atlas template was performed. This was further refined via a second non-rigid registration between the skeleton of the individual binarised CGM segmentation and the skeleton of the binarised propagated atlas cortical labels. CGM voxels were then individually assigned to the cortical labels, and regional GM volumes were computed by multiplying the voxel size by the sum of the probability of each voxel assigned to the cortical region of interest to be GM tissue.

The subcortical regions were segmented using the dataset from CANDIShare as reference. After affine and non-rigid registration of the age-specific atlas to the subject image, the subcortical labels were propagated to the subject with the corresponding transformations. Only for thalamus and hippocampus, for which manual segmentations were available in reference atlases, multi-atlas segmentation was done by using the Simultaneous Truth And Performance Level Estimation (STAPLE) label fusion method (Warfield et al., 2004).

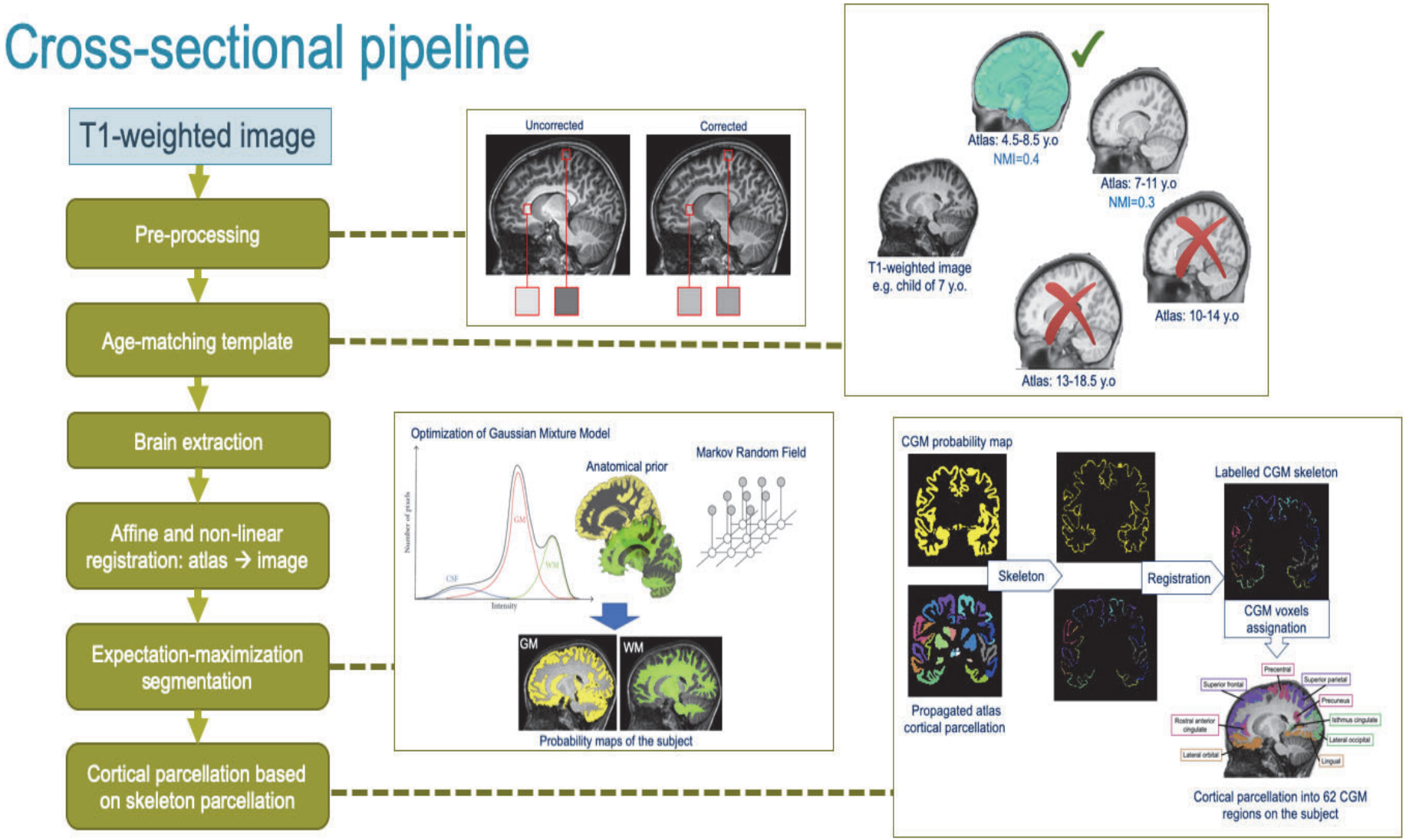

Figure 3.9: Childmetrix pipeline. Courtesy of Thanh Vân Phan (Icometrix).

3.3.2.2 Computation of Asymmetry Indeces

To perform the asymmetry analysis, Childmetrix unpaired regions were excluded, for a total of 38 cortical and subcortical paired regions included. For each pair of regions, a lateralisation quotient (LQ) was computed by using the following the formula:

LQ= [(Volume Right Hemisphere) - (Volume Left Hemisphere)/
(Volume Right Hemisphere + Volume Left Hemisphere)] x 100

The LQ has a range between −100 and 100, with negative values indicating leftward asymmetries, positive values rightward asymmetries, and higher values a stronger asymmetry in the respective direction. Additionally, we determined the absolute value of the LQ, as a measure of degree of asymmetry independent of its direction. The absolute LQ has a range between 0 and 100, with higher values indicating stronger asymmetries, irrespective of direction. Furthermore, based on the individual LQ, we determined the direction of asymmetry for each participant as dichotomous variable, by categorising a negative LQ (leftward asymmetry) as 0, and a positive LQ (rightward asymmetry) as 1.

These calculations resulted in three asymmetry measures as dependent variables (DV): LQ, degree of asymmetry, direction of asymmetry.

The procedure was directly informed by the work of Berretz et al. (2019), who found for the first time in the published literature an association between a genetic variant within *PCSK6* (rs10523972, intronic 33bp VNTR polymorphism) and hemispheric asymmetries of the grey matter.

3.3.3 Statistics

Statistical analyses were performed in SPSS® version 25 statistical software (IBM, Armonk, NY, USA). For each analysis, subjects were grouped according to the independent variable of interest, and matched by age, gender and the other independent variables potentially affecting asymmetry.

To disentangle any cross-influence on brain structural asymmetries not directly related to *PCSK6*, three independent variables (IV) were considered: 1) *PCSK6* rs10523972 genotype (henceforth referred to as *PCSK6* genotype), grouping carriers vs non-carriers of the minor allele; 2) degree of handedness (determined as described in Chapter 2, paragraph 2.2.2), grouping consistent vs inconsistent; 3) affection status, grouping dyslexic vs unaffected. Therefore, to investigate *PCSK6*-related endophenotype, carriers and non-carriers were matched by age, gender, affection status and degree of handedness; to look at the effect of degree of handedness, subjects with consistent and inconsistent handedness were matched

by age, gender, affection status and genotype; to explore the effect of dyslexia status, dyslexic and unaffected siblings were matched by age, gender, degree of handedness and genotype. Cases with missing values were excluded on an analysis-by-analysis basis (pairwise deletion).

The three DV (LQ, degree of asymmetry, direction of asymmetry) were analysed with different tests: the two interval-scaled variables, LQ and degree of asymmetry, were tested parametrically, using two-sample *t*-test; the nominal variable represented by direction of asymmetry was instead tested with the non-parametric Mann-Whitney test. As 38 different brain areas were analysed, Bonferroni correction resulted in a corrected significance threshold of $p = 0.05/38 = 0.00131579$.

3.3.4 Results

3.3.4.1 Lateralisation Quotient

None of the comparisons reached significance for the Bonferroni-corrected threshold (0.001). However, the uncorrected significance threshold of 0.05 was reached by the following effects: 1) *PCSK6* genotype's effect on the pars opercularis of the inferior frontal gyrus (IFG), precuneus and insula (Table 3.2, Figure 3.10); 2) degree of handedness' effect on the caudate nucleus, IFG pars opercularis, precentral gyrus, supramarginal gyrus and amygdala (Table 3.3); 3) affection status' effect on the medial orbitofrontal area and isthmus of the cingulate (Table 3.4).

Table 3.2: *Brain areas with significant p-values (<0.05), derived from the t-test with LQ as DV and PCSK6 genotype as IV.*

Region	Mean Carriers	Mean Non-Carriers	t	df	*p*
IFG Pars Opercularis	11.41±10.46	1.92±11.22	2.835	44	0.007
Precuneus	2.73±7.14	1.66±6.57	2.120	44	0.040
Insula	0.56±4.21	4.47±5.87	-2.397	44	0.021

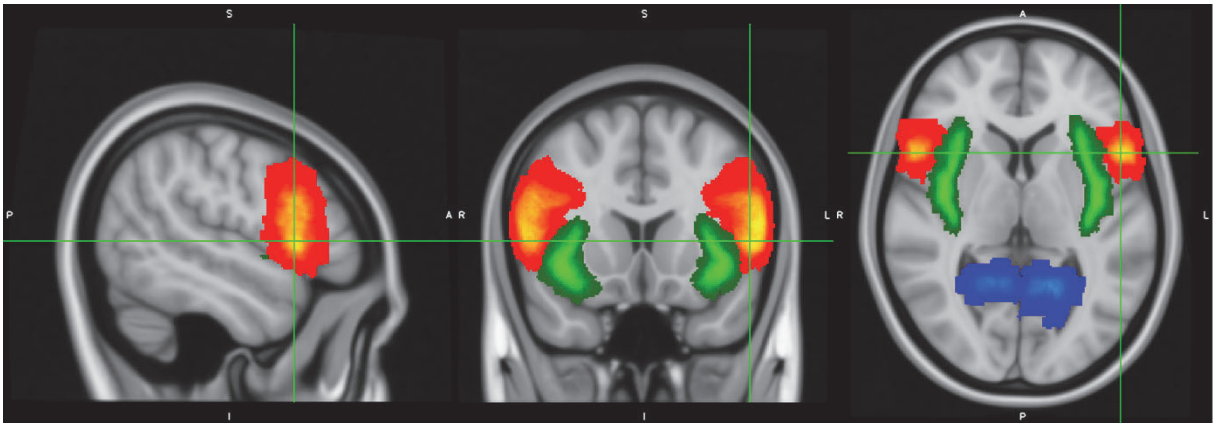

Figure 3.10: Sagittal, coronal and axial MNI template projections of the brain areas (IFG in red-orange, precuneus in blue, insula in green) with significant p-values (<0.05), derived from the t-test with LQ as DV and PCSK6 genotype as IV.

Table 3.3: Brain areas with significant p-values (<0.05), derived from the t-test with LQ as DV and degree of handedness as IV.

Region	Mean Consistent Handedness	Mean Inconsistent Handedness	t	df	*p*
Caudate Nucleus	1.33±1.66	4.47±5.87	-2.068	42	0.045
IFG Pars Opercularis	0.70±10.69	8.23±11.03	-2.270	42	0.028
Precentral Gyrus	-5.91±4.68	-2.74±4.78	-2.198	42	0.034
Supramarginal Gyrus	-0.69±8.48	-6.63±5.51	2.812	42	0.007
Amygdala	1.81±3.04	-0.422±3.95	2.048	42	0.047

Table 3.4: Brain areas with significant p-values (<0.05), derived from the t-test with LQ as DV and affection status as IV.

Region	Mean Dyslexic	Mean Unaffected	t	df	*p*
Medial Orbitofrontal	9.50±7.11	3.81±8.78	2.191	38	0.035
Isthmus Cingulate	1.22±6.71	-4.81±6	2.751	38	0.009

3.3.4.2 Degree of Asymmetry

None of the comparisons reached significance for the Bonferroni-corrected threshold (0.001). However, the uncorrected significance threshold of 0.05 was reached by: 1) *PCSK6* genotype's effect on lateral orbitofrontal area, superior frontal gyrus (SFG), precentral gyrus, amygdala and insula (Table 3.5, Figure 3.11); 2) degree of handedness' effect on precentral gyrus (Table 3.6); 3) affection status' effect on transverse temporal gyrus (Table 3.7).

Table 3.5: Brain areas with significant p-values (<0.05), derived from the t-test with degree of asymmetry as DV and PCSK6 genotype as IV.

Region	Mean Carriers	Mean Non-Carriers	t	df	*p*
Lateral Orbitofrontal	2.69±1.95	4.43±3.22	2.010	44	0.051
Superior Frontal Gyrus	3.44±2.19	5.37±3.48	2.298	43.7	0.026
Precentral Gyrus	3.55±2.88	5.87±3.49	2.310	44	0.026
Amygdala	3.84±1.82	2.63±2.02	-2.030	44	0.048
Insula	3.46±2.31	6.11±4.05	2.469	44	0.017

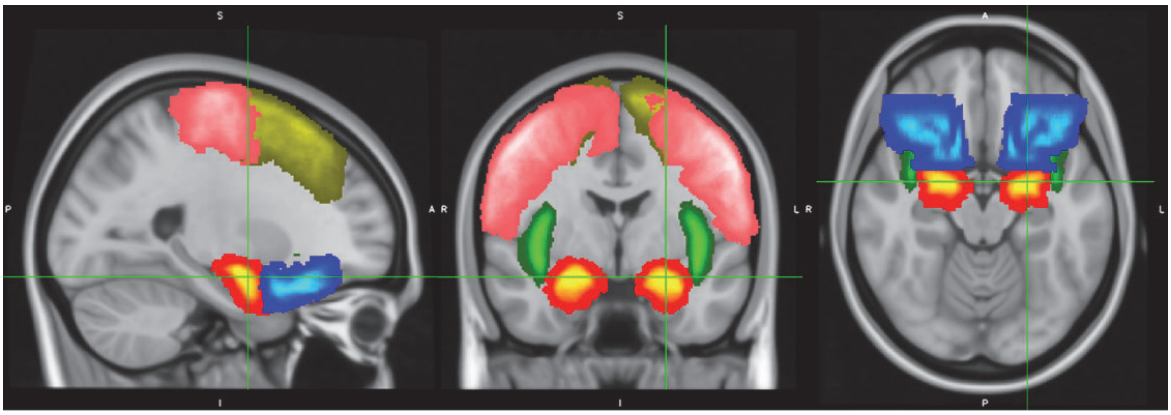

Figure 3.11: Sagittal, coronal and axial MNI template projections of the brain areas (orbitofrontal in blue, SFG in pink, precentral gyrus in yellow, amygdala in red-orange, insula in green) with significant p-values (<0.05), derived from the t-test with degree of asymmetry as DV and PCSK6 genotype as IV.

Table 3.6: Brain areas with significant p-values (<0.05), derived from the t-test with degree of asymmetry as DV and degree of handedness as IV.

Region	Mean Consistent Handedness	Mean Inconsistent Handedness	t	df	*p*
Precentral Gyrus	6.49±3.78	4.40±3.25	1.972	42	0.055

Table 3.7: Brain areas with significant p-values (<0.05), derived from the t-test with degree of asymmetry as DV and affection status as IV.

Region	Mean Dyslexic	Mean Unaffected	t	df	*p*
Transverse Temporal Gyrus	12.87±9.61	21.80±12.30	1.972	38	0.017

3.3.4.3 Direction of Asymmetry

None of the comparisons reached significance for the Bonferroni-corrected threshold (0.001). However, the uncorrected significance threshold of 0.05 was reached by the following effects: 1) *PCSK6* genotype's effect on globus pallidus, IFG pars opercularis and fusiform gyrus (Table 3.8, Figure 3.12); 2) degree of handedness' effect on the supramarginal gyrus (Table 3.9); 3) affection status' effect on the medial orbitofrontal area and isthmus of the cingulate (Table 3.10).

Table 3.8: Brain areas with significant p-values (<0.05), derived from the Mann-Whitney test with direction of asymmetry as DV and PCSK6 genotype as IV.

Region	Carriers	Non-Carriers	Mann-Whitney U	N	*p*
Globus Pallidus	Left	Right	167.000	46	0.026
IFG Pars Opercularis	+Right	Right	322.000	46	0.040
Fusiform Gyrus	Right	Left	321.000	46	0.049

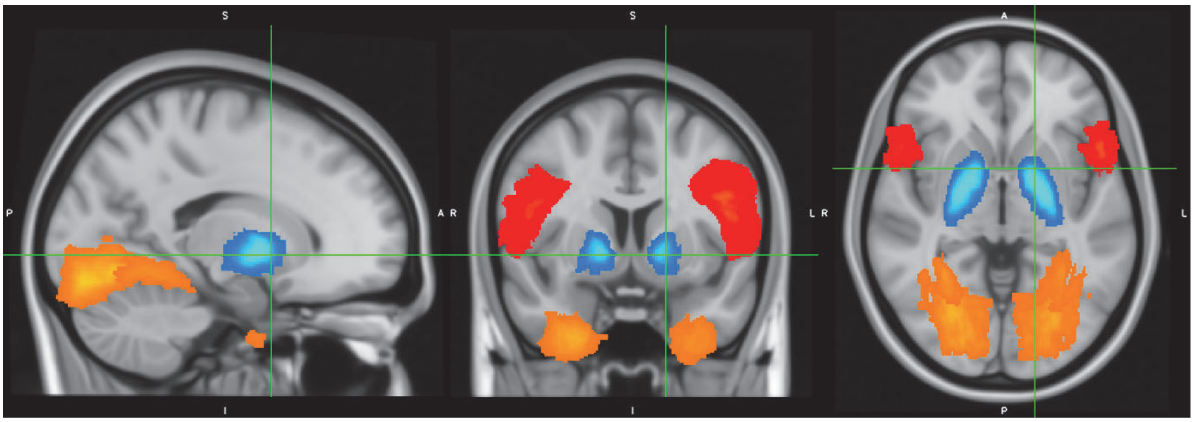

Figure 3.12: Sagittal, coronal and axial MNI template projections of the brain areas (globus pallidus in blue, IFG in red, fusiform gyrus in orange) with significant p-values (<0.05), derived from the Mann-Whitney test with degree of asymmetry as DV and PCSK6 genotype as IV.

Table 3.9: Brain area with significant p-value (<0.05), derived from the Mann-Whitney test with direction of asymmetry as DV and degree of handedness as IV.

Region	Consistent Handedness	Inconsistent Handedness	Mann-Whitney U	N	*p*
Supramarginal Gyrus	Left	+Left	141.000	44	0.004

Table 3.10: Brain areas with significant p-values (<0.05), derived from the Mann-Whitney test with direction of asymmetry as DV and affection status as IV.

Region	Dyslexic	Unaffected	Mann-Whitney U	N	*p*
Medial Orbitofrontal	+Right	Right	114.500	40	0.004
Isthmus Cingulate	Right	Left	112.000	40	0.034

3.3.4.4 Corpus Callosum and Total Volumes

Significant differences (p<0.05) were found by comparing volumes of the whole brain (p=0.012), corpus callosum (p=0.039) and total GM (p=0.008) between carriers and non-carriers, where the first ones showed higher volumes than the second ones (Table 3.11; Figures 3.13a, b, c, d). No significant difference between the two groups was observed instead when comparing their total WM volumes.

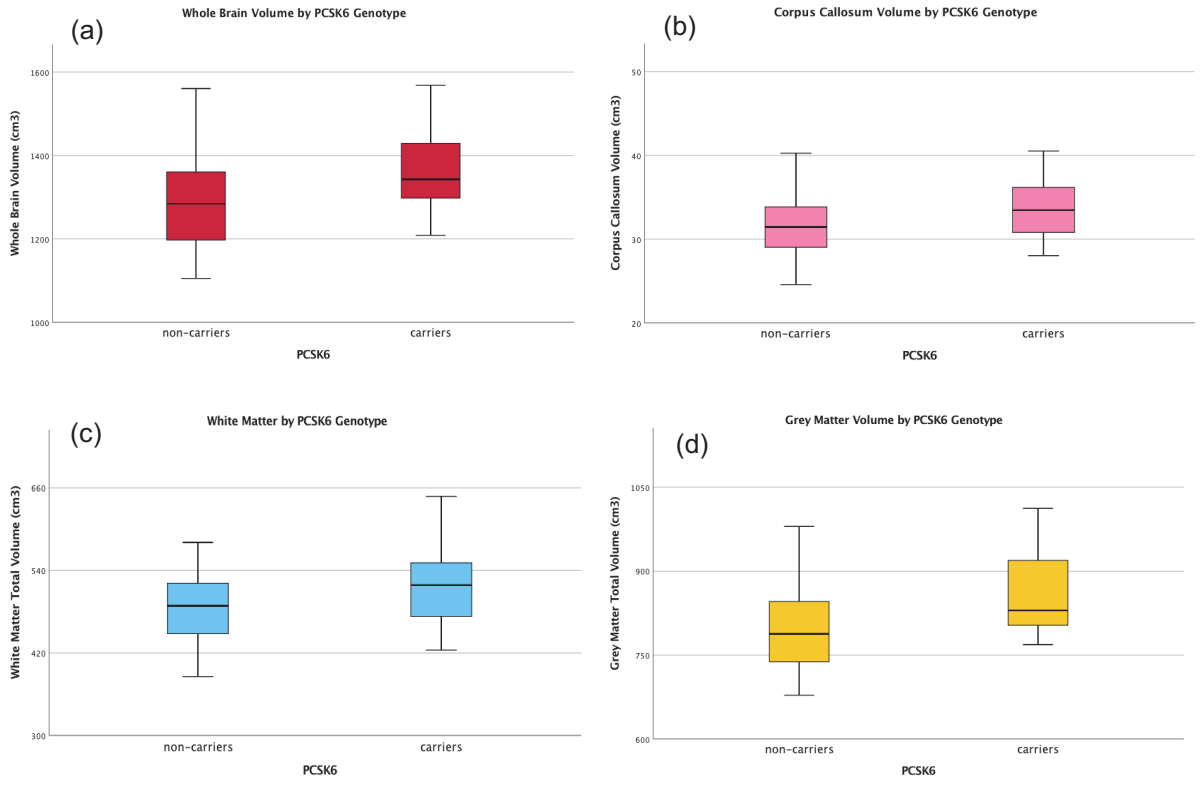

Figure 3.13: Boxplots of whole brain (a), corpus callosum (b), total grey matter (c) and total white matter (d) volumes in carriers and non-carriers.

*Table 3.11: Volumetric differences of whole brain, total grey matter, total white matter and corpus callosum, between non-carriers and carriers (Levene's test and t-test reported). *Significant p-values (<0.05), derived from the t-test with the hypothesis 'non-carriers > carriers'.*

Region	Levene's F	Sig.	t	df	*p*
Corpus Callosum	1.078	0.305	-2.129	44	0.039*
Whole Brain	0.045	0.832	-2.618	44	0.012*
Total Grey Matter	0.003	0.960	-2.762	44	0.008*
Total White Matter	0.564	0.457	-1.953	44	0.057

3.3.5 Discussion

3.3.5.1 Grey Matter Asymmetries

The asymmetry indeces (lateralisation quotient, degree of asymmetry and direction of asymmetry) of cortical and subcortical GM volumes were analysed as dependent variables of *PCSK6* rs11855415 genetic variant, to investigate the genotype's influence on hemispheric structural asymmetries.

Significant (p<0.05) associations were observed between *PCSK6* genotype and LQ of the pars opercularis of the IFG, precuneus and insula, indicating respectively: a more rightward lateralisation of the pars opercularis in carriers (LQ=11.41±10.46) than in non-carriers (LQ=1.92±11.22); a less rightward asymmetric insula (LQ=0.56±4.21) in carriers than in non-carriers (LQ=4.47±5.87); a more leftward precuneus in carriers (LQ=-2.73±7.14) than in non-carriers (LQ=1.66±6.57).

Furthermore, a significant association was found between *PCSK6* genotype and direction of asymmetry of the pars opercularis of the IFG (right), globus pallidus (left) and fusiform gyrus (right). These findings complement those from our exploratory VBM study (described in paragraph 3.2), where we observed a significant volumetric difference of the pars opercularis of the right IFG between carriers and non-carriers (Figure 3.4), but no significant difference in asymmetry (Figure 3.5). The current analysis revealed instead significant *PCSK6*-associated asymmetries at this very level.

In addition, a significant association was found between *PCSK6* genotype and degree of asymmetry of the lateral orbitofrontal region, superior frontal gyrus, precentral gyrus, insula and amygdala, where carriers (with mean respectively, 2.69±1.95, 3.44±2.19, 3.55±2.88, 3.46±2.31) showed a lower degree of asymmetry than non-carriers (with mean respectively, 4.43±3.22, 5.37±3.48, 5.87±3.49, 6.11±4.05), with the exception of the amygdala, that was more asymmetric in carriers (3.84±1.82) than in non-carriers (2.63±2.02). This may suggest a potential influence of the *PCSK6* rs11855415 genetic variant on the development of a less lateralised brain cortex, that potentially may yield a lower degree of lateralisation also on the functional side.

Interestingly, Berretz et al. (2019) recently found the intronic 33bp VNTR polymorphism in *PCSK6* (rs10523972) being associated with asymmetries of both temporal and frontal structures in a typical population, indicating a stronger rightward lateralisation (LQ=10.82±1.13) of the dorsolateral prefrontal cortex (BA46) in the homozygous carriers of the minor allele. Therefore, our results seem to corroborate the first *PCSK6*-related imaging findings to be published in literature (Berretz et al., 2019), supporting the hypothesis that *PCSK6* genetic variants may be not only relevant for functional asymmetries like degree of handedness (Scerri et al., 2011; Brandler et al., 2013; Arning et al., 2013), but also for structural GM asymmetries.

To disentangle the structural asymmetry effects of handedness lateralisation from the ones related to *PCSK6* rs11855415 genotype, degree of handedness was also analysed as independent variable. This was found to be significantly associated with degree of asymmetry of the precentral gyrus, where children with consistent handedness showed a higher degree of asymmetry (6.49±3.78) than those with inconsistent handedness (4.40±3.25). Such finding may be suggestive of a direct correspondence between a more asymmetric structural makeup of the motor hand cortex and a more lateralised handedness function.

Furthermore, a significant association was observed between degree of handedness and LQ of the caudate nucleus, pars opercularis of the IFG, precentral gyrus, supramarginal gyrus and amygdala. And, interestingly, a more rightward lateralisation of the IFG pars opercularis was displayed by children with inconsistent (LQ=8.23±11.03) than consistent handedness (LQ=0.70±10.69). To better understand this last finding, it is useful to look at it in a comparative manner to the significant positive correlation, observed in the VBM study (described in paragraph 3.2), between the right volume of the rightward IFS asymmetry and the handedness LQ, in the carriers of the minor allele (Figure 3.8a). Both observations bring in fact evidence to a potential association between handedness measures (LQ and degree) and the inferior frontal regions (IFG pars opercularis and IFS), where we observed: a *PCSK6*-related higher right volume of the IFS rightward asymmetric cluster, associated with a higher degree of right-handedness; and a more rightward IFG pars opercularis asymmetry, in association with inconsistent handedness (low degree of handedness), independently from *PCSK6* rs11855415 genetic variant. With regard to the latter association, it is important to notice that Arning et al. (2013) found a lower degree of handedness to be associated with a different *PCSK6* genetic variant, rs10523972, in a typical population; therefore, it would be crucial to understand whether our structural findings associated with inconsistent handedness and unrelated to *PCSK6* rs11855415, might be instead related to *PCSK6* rs10523972 genetic variant. On the other hand, the potential fil rouge of the *PCSK6* rs11855415-related endophenotype may seem to link the minor allele to rightward asymmetric frontal regions (IFG pars opercularis), whose increased right volume (IFS) in turn may correlate positively to a higher degree of right-handedness (high LQ).

To distinguish the asymmetry effects of dyslexia from the ones related to *PCSK6* rs11855415 genotype, affection status was also analysed as independent variable. Dyslexia was found to be significantly associated to brain asymmetry measures, such as LQ and direction of asymmetry of the medial orbitofrontal area and isthmus of cingulate. A more rightward lateralisation of both medial orbitofrontal region and isthmus of the cingulate was observed in dyslexic children (respectively, 9.50±7.11 and 1.22±6.71) than in unaffected siblings (respectively, 3.81±8.78 and -4.81±6).

Finally, unaffected children showed a significantly higher degree of asymmetry of the transverse temporal gyrus (21.80±12.30) than dyslexic patients (12.87±9.61). This asymmetric structure is placed rostrally to and may be indicative of the asymmetry of the planum temporale, that was instead not part of the asymmetry analysis, as it was unlisted in the paediatric atlas. The planum temporale is well noted to be more symmetric in dyslexic individuals than in the 78% of the typical population, that in contrast presents a leftward asymmetry of this region (Hier et al., 1978; Galaburda and Kemper, 1979; Haslam et al., 1981; Rumsey et al., 1986, 1997; Larsen et al., 1990; Hynd et al., 1990; Duara et al., 1991; Kushch et al., 1993; Dalby et al., 1998; Leonard et al., 1993; Schultz et al., 1994; Jernigan et al., 1991; Plante et al., 1991; Gauger et al., 1997; Chiarello et al., 2006). Therefore, assuming that the asymmetry observed at the level of the transverse temporal gyrus may reflect the abovementioned well-known asymmetry of the contiguous planum temporale, this was displayed, as expected, by the unaffected siblings compared with dyslexic children, independently from *PCSK6* rs11855415 genotype; the impact of which on brain asymmetries was also independent from the dyslexia status, and mainly observed in the frontal lobe.

3.3.5.2 Volumetries

As far as the volumetric analyses of unpaired stuctures and tissue volumes are concerned, similarly to Meda et al.'s (2008) and to our previous VBM results (described in paragraph 3.2), a significantly higher total grey matter volume was observed in carriers than in non-carriers, along with significant higher volumes of the whole brain and corpus callosum, but not of the total white matter.

We did not analyse further features (e.g. shape, single segments, fractional anisotropy, mean diffusivity) of the corpus callosum, but it would be crucial pursuing further these investigations, given that *PCSK6* is most strongly expressed in the midline of the nervous system, and mainly in the spinal cord and the corpus callosum (Johnson et al., 2003). According to the Ocklenburg's triadic model of the structural determinants of functional asymmetries (Figure 3.1; Ocklenburg et al., 2016), the top of the triangle is occupied by the corpus callosum, that is the major commisure of the human brain, and of crucial importance for the existence and the extent of functional hemispheric asymmetries (Witelson, 1985; Aboitiz et al., 1992; Hines et al., 1992; Clarke and Zaidel, 1994; Jäncke and Steinmetz, 1994; Moffat

et al., 1998; Westerhausen and Hugdahl, 2008; Nowicka and Tacikowski, 2011; Ocklenburg et al., 2016). There are contrasting functional models of the callosal commissure, assuming either an excitatory (Ringo et al., 1994; Yazgan et al., 1995) or inhibitory (Cook, 1984; Bloom and Hynd, 2005) or combined action on functional lateralisation (Bloom and Hynd, 2005; Van der Knaap and Van der Ham, 2011; Ocklenburg et al., 2016). Interestingly, significant shape difference has been found at the level of the posterior midbody of the corpus callosum (containing interhemispheric fibers from auditory corteces) of dyslexic children compared with controls, suggesting a potential divergent callosal growth pattern during late childhood (Von Plessen et al., 2002); this in turn may influence auditory phonological decoding function, as well as the atypical symmetry of the planum temporale displayed in dyslexia. Similarly, a shape analysis of the corpus callosum in our cohort might be of help to elucidate whether there is any significant callosal difference associated with *PCSK6* rs11855415 genetic variant; and whether this putative difference might be physiologically related to the specific cortical GM asymmetries that we observed in association with the minor allele, in particular to the rightward asymmetry of the pars opercularis of the IFG.

Chapter 4: Magnetoencephalography Studies

4.1 Introduction

Neuroimaging studies are providing increasing evidence that language functions are based on the interaction between the left and the right hemisphere, and characterised by large individual differences in hemispheric asymmetries and interhemispheric interactions (e.g. Federmeier and Kutas, 1999; Coulson and Williams, 2005; Coulson and Wu, 2005).

Determining individual profiles of language hemispheric organisation has not only theoretical value for a better understanding of the physiology of language in both typical and atypical development, but also practical importance for presurgical non-invasive mapping of language in the planning of brain surgery, in particular to treat refractory epilepsy. Nevertheless, there is no consensus yet on optimal non-invasive methodologies to map language hemispheric organisation and dominance.

4.1.1 Language Asymmetry and the N400m Event-Related Field

Neurophysiological markers of language processing, such as the event-related fields (ERFs), that are the magnetic counterparts of the electrical event-related potentials (ERPs), can provide uniquely disambiguating and innovative insights into language group and individual profile of hemispheric dominance.

ERPs are time-locked small voltage fluctuations recorded at the scalp level, produced by the summation of post-synaptic potentials synchronised with a certain stimulus presentation (Van Petten and Luka, 2006). Among the ERP components that are sensitive to language processes and psycholinguistic manipulations, the N400 has certainly been the most utilised since its discovery by Kutas and Hillyard in 1980 (Kutas and Hillyard, 1980; Van Petten and Rheinfelder, 1995; Van den Brink et al., 2001; Holcomb and Neville, 1990; Olichney et al., 2000; Hahne and Friederici, 2002; Coulson et al., 2005). This is a negative-going voltage fluctuation peaking around 400ms (350-500ms) post-stimulus onset, and typically considered an index of lexical and semantic processing (e.g. Lau et al., 2008; Kutas and Federmeier, 2011; Wang et al., 2012).

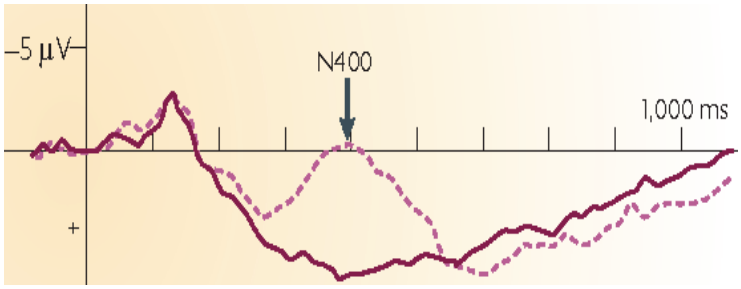

Figure 4.1: The N400 effect in sentential context. Figure from Lau et al., 2008.

The amplitude of the N400 has specific correlations with the following target word's features: word frequency (inverse correlation), neighbourhood size (direct correlation), priming (inverse correlation) and cloze probability (inverse correlation) (e.g. Kutas and Federmeier, 2011; Grey and Van Hell, 2017). The latter is defined as the probability of the target word to complete a certain sentence in a meaningful way, and it can be considered the most important determinant of the N400 amplitude, with the strongest inverse linear relationship. This means that as a word becomes less predictable (incongruent), given the sentential context, the N400 amplitude becomes stronger relatively to more predictable (congruent) words. The relative amplitude of the waveform time-locked to the incongruent word compared to the congruent word is called the "N400 effect" (Kutas and Hillyard, 1980).

The N400 semantic context effect has been shown to be equally valid for printed, spoken, and signed target words (Neville et al., 1992), but its spatial distribution is difficult to localise, because of the spatial blurring between the brain and the scalp, imposed by electrical insulation of the skull.

On the one hand, when the stimulus is auditorily presented, the scalp topography of the N400 effect is typically centro-parietal, bilateral and symmetric in both congruent and incongruent experimental conditions; only few works were able to show significant, but inconsistent, asymmetries (right>left: Van Petten and Rheinfelder, 1995; Van den Brink et al., 2001; left>right: Holcomb and Neville, 1990; Hahne and Friederici, 2002; for a more extensive review see Van Petten and Luka, 2006). On the other hand, when the stimulus is visually presented, the scalp distribution shows a typical slightly rightward asymmetry in both conditions (e.g. Kutas and Hillyard, 1982; Holcomb and Neville, 1990; Olichney et al., 2000; Coulson et al., 2005; for a more extensive review see Van Petten and Luka, 2006), and, interestingly, this rightward asymmetry becomes larger when modulated by rhyme judgments on visually presented words (Barrett and Rugg, 1989; Kramer and Donchin, 1987; Rugg, 1984). The surprising fact that rhyming written words elicit a larger rightward negative potential has been defined by Van Petten and Rheinfelder (1995) as a "paradoxical lateralisation", since the conversion of orthography to phonology is a well-known left-lateralised ability (Levy and Trevarthan, 1977; Rodel et al., 1983; Patterson and Besner, 1984), and therefore the rightward N400 scalp-asymmetry may be probably due to a slight tilt in the left hemisphere, causing a summed electrical dipole pointing slightly toward the right. Similarly, the lack of lateralisation of the N400 modulated by auditory stimulus can be explained by the presence of bilateral dipolar sources, that are probably strongest on the left but oriented towards the head vertex, producing therefore negative potentials over the midline, so that no lateralisation can be seen (Wang et al., 2012).

Differently, language lateralisation can be observed with the distribution of the N400m ERF, that has a better spatial resolution than its electrical counterpart, while preserving the same

good temporal resolution (Hämäläinen et al., 1993). This is thanks to the magnetic transparency property of the skull, as well as to the sensitivity of the scalp magnetic fields to the geometrical orientation of the intracranial current flow (particularly if co-registered with structural images, showing the individual gyral and sulcal patterns). However, this sensitivity is limited to the intracranial sources that are tangential (rather than perpendicular) to the skull; therefore, ERF can better detect the activity originating from cortex in sulci (rather than in gyri), that, nevertheless, represents the two-thirds of the cortical sheet (Zilles, 1990; Armstrong et al., 1995). As far as the N400m topography is concerned, MEG results showed a more disambiguating distribution over the temporal lobes and a typical leftward asymmetry, without surprising paradoxical lateralisation (e.g. Nobre et al., 1994; Salmelin et al., 1996; Simos et al., 1997; Helenius et al., 1998; Halgren et al., 2002; Kwon et al., 2005; Wang et al., 2012). Although the difference between language modalities (spoken, written, and signed) has not been fully explored yet, the N400m can be used as a reliable marker to map language activation and lateralisation in the assessment of hemispheric dominance, particularly in combination with individual MR images.

Against such backdrop, both MEG studies presented in this chapter will use the N400m ERF: first, to obtain reliable language maps in a paediatric typical population; then, to assess receptive language lateralisation in a larger cohort of dyslexic children and matched siblings/twins genotyped for *PCSK6* rs11855415, in order to explore whether this genetic variant, that seems to influence handedness in dyslexia (Scerri et al., 2011; Brandler et al., 2013), might influence also language lateralisation.

Different softwares and analysis pipelines are used in the two studies, contextually with ChildBrain secondments and different phases of the PhD training. MEG data analyses will be described in detail in the specific sections of each MEG study (paragraphs 4.3. and 4.4).

4.2 The N400m Auditory Paradigm

To lateralise language in a reliable and child-friendly way, we used a MEG auditory paradigm developed at the ABC in 2015 by Dr Shu Yau, to implement the epilepsy pre-surgical planning protocol of the Birmingham Children's Hospital, with the use of a high temporal resolution non-invasive tool like the MEG. Dr Yau's MSCA-funded project was led by Prof Joel B. Talcott, and run in collaboration with Dr Caroline Witton, Prof Stefano Seri and Dr Elaine Foley. Once the paradigm was validated in typically developing children, it was also used in children having refractory epilepsy, as part of their pre-surgical workup, as well as in children having dyslexia and their siblings/twins, as part of the ChildBrain multimodal research project. For the purpose of this study, only ChildBrain data will be reported.

According to the N400m paradigm, two types of spoken sentences were used as two main conditions, and presented to the participant auditorily. Such auditory stimuli were able to

modulate the N400m event-related field (ERF) without requiring the participant to use word recognition skills (phonological awareness, decoding and sight word recognition), that are known to be impaired in developmental dyslexia, as well as in other neurological disorders that can present dyslexia in comorbidity.

The condition called “congruent” (C) included sentences ending with a high-cloze probability word, e.g. *the child went outside to play*; while the condition called “incongruent” (IC) included sentences ending with a semantically anomalous word, unexpected given the sentential semantic context, e.g. *the child went outside to wall*. A third type of sentences, containing either the word *alien* or *aliens,* was used to orient the attention of the child onto the spoken sentences throughout the entire duration of the paradigm, with the task of catching aliens by pressing a button as soon as the word *alien/aliens* was heard. The *alien/aliens* sentences were then excluded from the N400m analysis, primarily to avoid signal contamination due to the button pressing, and, conceptually, because the attentional component of the paradigm did not fall within the scope of this specific language lateralisation study.

A set of 60 pairs of sentences were constructed for the two experimental conditions, C and IC, for a total of 120 sentence trials, divided in 10 blocks of 12 sentences each. Each couple of C-IC sentences was identical up to the final target words, that were matched on frequency and duration, e.g. *wall/play*. Each experiment started with a 3000ms fixation trial, followed first by a 200ms warning tone, and then a 800ms pause; after this, a 4000-5000ms sentence ending with a 200ms target word was auditorily presented.

Every next sentence trial began 4000ms after the offset of the previous sentence. To reduce eye blinks during sentence trials, subjects were instructed to fixate on a rectangular shape, presented visually 1000ms before the beginning of the sentence (Figure 4.2). As a sanity check, to ensure that the semantic level of the task was appropriate for the subject, 30 sentences randomly chosen from the list of 120 sentences were read aloud to the participant at the end of the experiment, asking whether the sentence did make sense or not. An adequate semantic level was confirmed if at least 95% (>27) of the sentences were interpreted correctly.

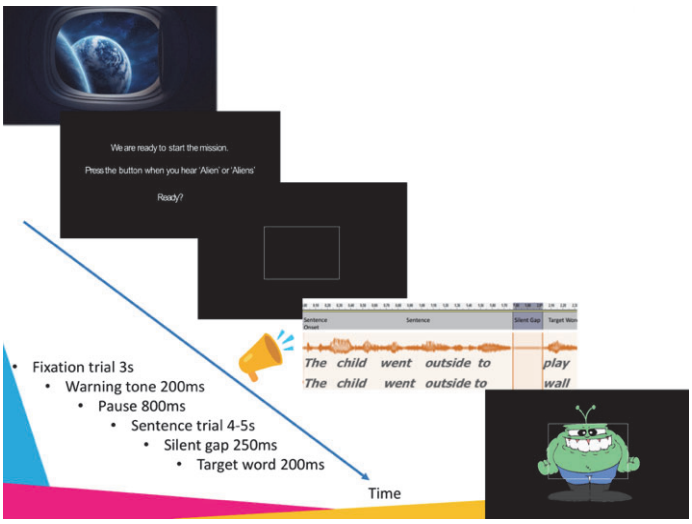

Figure 4.2: The structure of the child-friendly N400m paradigm, with times of trials and stimuli.

4.3 A Pilot Study to Lateralise Language

The first MEG study is a pilot experiment, addressing the challenge of obtaining reliable receptive language maps in a paediatric population, with the ultimate goal of providing a viable mean to be used in clinical settings, particularly in children under medication and/or having neurocognitive disorders affecting their ability to perform reading tasks.

The MEG analysis training for this study was conducted in the context of my secondment at the Donders Institute for Brain, Cognition and Behaviour (Radboud University, Nijmegen, The Netherlands), under the supervision of Prof Robert Oostenveld. Further training in the piloting stage was provided during my secondment at the Jyväskylä Centre for Interdisciplinary Brain Research (University of Jyväskylä, Finland), under the supervision of Prof Tiina Parviainen. Both secondments were part of the ChildBrain MSCA-ITN research programme.

4.3.1 Participants

Ten healthy children, English native speakers, right-handed, between 6 and 17 years of age (mean age, 9 years) took part in the experiment at the Wellcome Trust MEG Lab of the ABC. Subjects were asked to seat comfortably and still under the MEG helmet, and to listen attentively to spoken sentences. As specified more extensively in paragraph 4.2.2, they were given the task of catching aliens by pressing a button when either the word *alien* or *aliens* was heard; two types of sentences, congruent (C) and incongruent (IC) were auditorily presented, ending respectively with a high-cloze probability word and a semantically anomalous word, in order to modulate the N400m ERF.

4.3.2 MEG Data Pre-processing

MaxFilter software (Elekta Neuromag Oy, version 2.2.10) with transformation to default head position and temporal extension of signal space separation (tSSS) (Taulu and Hari, 2009) was used to, respectively, decrease variance between-subjects, due to asymmetric positions of the head inside the helmet, and to remove signal artefacts due to movements. MaxFiltered data were visually inspected, and channels with artefacts were removed if present. The difference between default and original head position's coordinates was carefully checked, to ensure it did not exceed the suggested maximum distance of 25mm (Elekta Oy, 2010).

MEG data were then analysed in the MATLAB R2017a environment (The MathWorks® Inc., Natick, MA.) using FieldTrip software package, an open-source MATLAB toolbox for neurophysiological data analysis (Oostenveld et al., 2011). Data were band-pass filtered from 6 to 40 Hz, and segmented into 1200ms long epochs, ranging from −200 to 1000ms relative to stimulus onset. Trials containing artefacts, due to eye blinks, head movements, muscle or SQUID jumps, were further detected using FieldTrip visual artefact rejection tool, and manually rejected if the trial-by-channel magnetometer variance was unusually high, for a final minimum

amount of 90% of trials kept, and an equal number of trials per condition. Jump artefacts refer to the brisk changes of the recorded signals, that can be due to trapped flux within sensors, or to electromagnetic interferences of the environment with the high sensitivity of the recording devices.

4.3.3 Event-Related Field Analysis

For each subject, the event-related field (ERF) of both IC and C conditions was obtained by averaging the trials separately for each condition, with a baseline correction between -200ms and 0 relative to stimulus onset. For sensor-level comparison, gradiometers were preferred to magnetometers, for the following reasons: 1) gradiometers are less sensitive than magnetometers to the noise of the sources originating far from the sensors; 2) neuronal sources of the signal are typically situated directly below the planar gradient (Hämäläinen et al., 1993); 3) it is possible to calculate the activation produced in a contiguous set of sensors, necessary for the cluster-randomisation algorithm used for the statistical analysis. To this end, the pairs of planar gradiometers in two orthogonal directions were combined, with the use of the vector sum method implemented in FieldTrip. Based on both visual inspection of the ERFs and the a priori knowledge that the N400m peaks around 400ms post-stimulus, a time window of 300–600ms was selected for quantifying the ERFs of the two conditions. The averaged values within this time interval entered the statistical analysis.

4.3.4 Statistics

To increase the sensitivity of the statistics and control for multiple comparisons, a cluster-based random permutation approach was used (Maris and Oostenveld, 2007), testing the significance of the difference between the two conditions, while controlling the type-1 error rate. The method can be briefly summarised in the following steps: 1) a simple dependent-samples *t*-test was performed for each sensor; 2) all contiguous sensors exceeding a pre-set significance level of 5% were clustered; for each cluster, the sum of the *t* statistics was used in the cluster-level test statistic; 3) a null distribution assuming no difference between conditions was created, by 1000 times randomly assigning the conditions in subjects, and calculating the largest cluster-level statistics for each randomisation; 4) the actually observed cluster-level test statistic was compared against the null distribution, and clusters falling in the highest or lowest 2.5th percentile were considered significant (Wang et al., 2012).

4.3.5 Results

A larger N400m was observed over the left hemisphere, as shown in the multiplot of the grand average ERFs for the C and IC conditions (Figure 4.3a). Comparing the ERFs of the two conditions, a larger N400m was elicited by the IC condition at both individual and group level, approximately between 300 and 550ms after the target word. These data are in line with

previously reported ERF equivalents of the N400 ERP (Salmelin et al., 1996; Helenius et al., 1998, 2002; Halgren et al., 2002; Wang et al., 2012).

Both C and IC conditions and their difference showed similar ERF topographies: 1) bilateral activity at both subject and group level; 2) strong dipolar pattern on the left hemisphere over temporal regions, more accentuated in the IC than in the C condition; 3) weak dipolar pattern over the right hemisphere (see individual ERF topoplots in Figure 4.3b).

By clustering simultaneously over neighbouring channels and neighbouring time points between 250 and 550ms, two significant (p<0.05) consecutive channel-time clusters were observed at the group level: 1) from 300 to 449ms in the occipital-parietal regions; 2) from 450 to 454ms in the left posterior parieto-occipito-temporal areas; 3) from 455 to 531ms in the left temporal lobe (see channel-time cluster topoplots in Figure 4.3c).

4.3.6 Discussion

The N400m topography showed occipito-temporal and temporo-parietal activations, with a clear left-hemispheric dominance (Figure 5c), consistently with the findings of a plethora of studies on the N400m modulation with respect to congruency of sentences (e.g. Nobre et al., 1994; Salmelin et al., 1996; Simos et al., 1997; Helenius et al., 1998; Halgren et al., 2002; Silva-Pereyra et al., 2003; Kwon et al., 2005; Wang et al., 2012; Jacob et al., 2019).

The strength of the activation of the right homologous regions was variable across subjects. Individual variability of the non-dominant hemisphere's contribution to the N400m has been observed in healthy population, confirming the unique nature of the individual interhemispheric relationship underlying hemispheric language dominance (Federmeier and Kutas, 1999; Coulson and Williams, 2005; Coulson and Wu, 2005; Hagoort et al., 2009). In particular, the activation has been shown to be more bilateral as the semantic complexity of the information being processed increases (Federmeier et al., 2008).

The contribution to the N400m from posterior regions, such as the left temporo-parietal junction (Simos et al., 1997; Helenius et al., 1998) and the posterior middle temporal gyrus (Dale et al., 2000; Halgren et al., 2002; Maess et al., 2006), has been consistently observed in MEG studies. According to the "functional neuroanatomic model for word semantic processing" (Lau et al., 2008), the inferior and middle temporal gyri would subtend to the storage and activation of lexical representations, while the anterior temporal cortex and the angular gyrus would integrate incoming information into contextual and syntactic representations. As far as the occipital cortex activation is concerned, what we observed might reflect the flexible recruitment of visual areas within conceptual network (Hoenig et al., 2008; Jacob et al., 2019); according to the semantic models of the "embodied abstraction", perceptual networks are recruited in language tasks during unexpected contexts (Binder and Desai, 2011; Jacob et al., 2019).

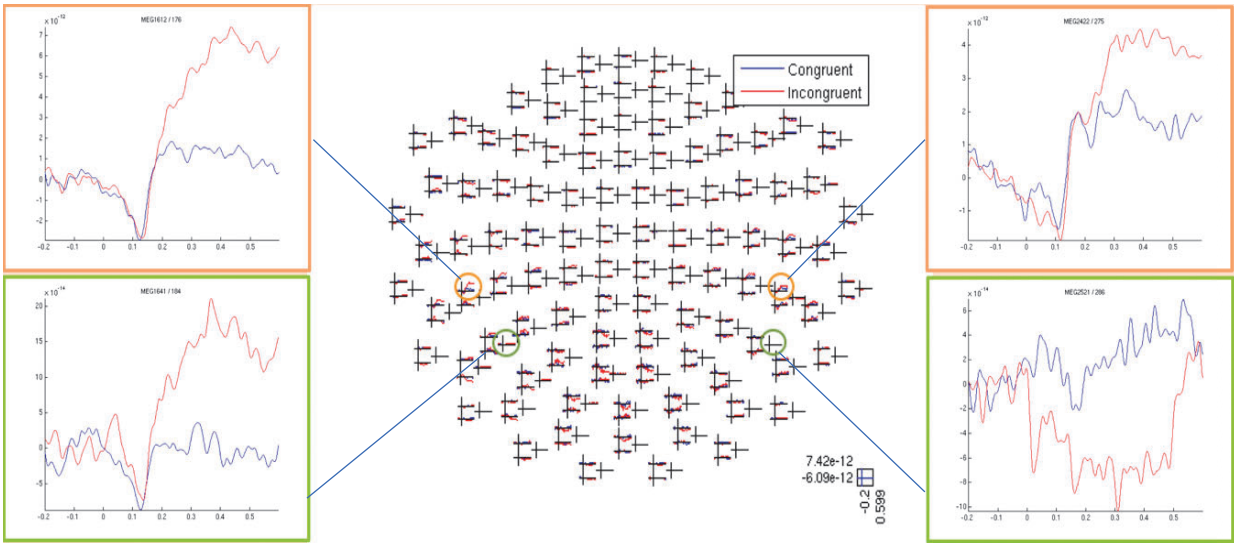

(a)

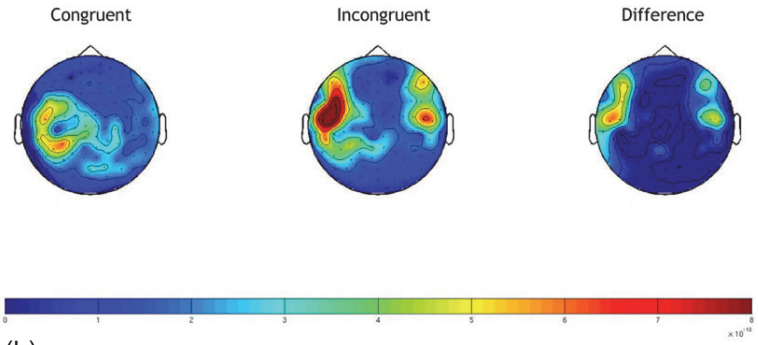

(b)

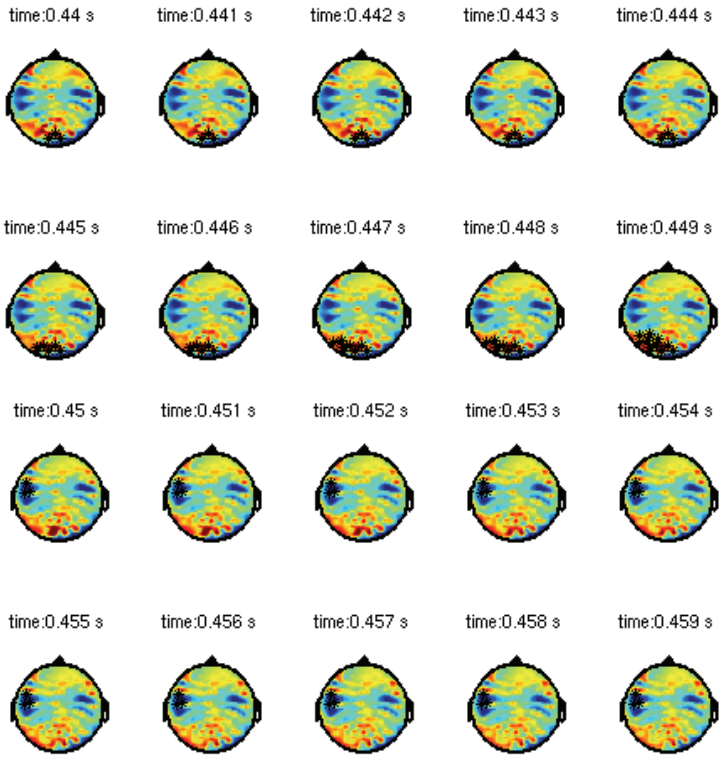

(c)

Figure 4.3: Scalp-time results:

a) Multiplot of the grand average ERFs for the congruent and incongruent conditions for all sensors, with insets for two representative couples of homologous gradiometers (see orange boxes) and magnetometers (see green boxes);

b) Single subject's topography of the ERFs of the two conditions and their difference, showing a strong dipolar pattern on the left hemisphere over temporal regions, in particular in the incongruent condition topoplot;

*c) Group topography of the significant channel-time clusters (marked with asterisks**) observed within the 0.3-0.531s time window; in this subset of topoplots, it is well visible the shift of the significant channel-time cluster from the occipito-temporal region to the left temporal lobe at the 0.455s time point.*

4.4 Language Laterality in the Aston Brain Centre *PCSK6* Cohort

After having validated the MEG N400m paradigm in a typical paediatric population, the same paradigm and acquisition protocol were used to assess receptive language dominance in the Aston Brain Centre *PCSK6*-genotyped cohort, with the primary aim of investigating the language component of the postulated hemispheric asymmetry endophenotype.

4.4.1 Participants and Data Acquisition

As part of the ChildBrain multimodal study, a total of 59 children who received diagnosis of dyslexia and their unaffected siblings/twins, all English native speakers and genotyped for *PCSK6* rs11855415, took part in the MEG study.

Subjects were first asked to sit comfortably under the MEG helmet without performing any particular task, apart from opening and closing their eyes when required, in order to record their brain activity while at rest. A subsample of 22 subjects was then assessed also for language lateralisation, taking part in the active experiment after the resting state recording was completed. Being language the specific focus of this study, resting state data will not be reported here.

Twenty-two children with age ranging between 5 and 17 years (mean 13.5 years), including 13 females and 9 males, 5 carriers and 17 non-carriers of the *PCSK6* rs11855415 minor allele, 11 dyslexics and 11 unaffected siblings/twins, were assessed for language dominance.

Handedness laterality measures were computed as described in Chapter 2 (paragraph 2.2.2). For this specific study, two dichotomous variables were considered: 1) handedness direction, grouping subjects into right-handers (RH, with LQ between 1 and 100) and left-handers (LH, with LQ between -100 and 0); 2) degree of handedness, independent from individual hand preference, grouping participants according to their consistent (LQ either 100 or -100) or inconsistent (all other LQs) handedness. Based on these criteria, all participants showed to be right-handed, 13 consistently and 9 inconsistently.

As described in detail in paragraph 4.2.2, each subject during the MEG experiment played the role of the alien-hunter, with the objective of catching aliens by pressing a button as soon as the word *alien/aliens* was heard within the spoken sentences. Two types of sentences, congruent (C) and incongruent (IC), ending respectively with a high-cloze probability word and a semantically anomalous word, were auditorily presented to modulate the N400m ERF.

4.4.2 MEG Data Pre-Processing

MaxFilter software (Elekta Neuromag Oy, version 2.2.10) with transformation to default head position and temporal extension of signal space separation (tSSS) (Taulu and Hari, 2009) was used, respectively, to decrease variance between-subjects due to asymmetric position of

the head inside the helmet, and to remove signal artefacts caused by movements. MaxFiltered data were then visually inspected, to identify channels with artifactual noise to be removed, and to make a comparison between default and original head position. A distance of 25mm was accepted as maximum difference between default and original head position's coordinates (Elekta Oy, 2010).

MEG data were then analysed in the MATLAB R2017a environment (The MathWorks® Inc., Natick, MA.) using Statistical Parametric Mapping (SPM12) software package, an open-source MATLAB toolbox for neurophysiological data analysis (http://www.fil.ion.ucl.ac.uk/spm/).

Signals were downsampled to 200 Hz sampling rate, and filtered between 0.1 and 40 Hz with a fifth-order Butterworth band-pass filter. Trials were segmented into 800ms epochs (ranging from -200 to 600 ms, relative to the target word's presentation), and then baseline-corrected (baseline from -200 to 0 ms). Remaining artefacts were detected and excluded by applying to all channels a simple thresholding of 80 microvolts relative to pre-stimulus baseline.

4.4.3 Sensor Space Analysis

Scalp-time analysis was performed to identify significant evoked effects that were phase-locked across trials at the subject level.

First, planar gradiometers were combined into one value for a scalar topographic representation, since they measure two orthogonal directions of the magnetic gradient at each location; the planar combination was done by taking the Root Mean Square (RMS) of the two gradiometers at each location. Data were then robustly averaged across the survived trials, for each condition and participant (Wager et al., 2005). Subsequently, trial-averaged data were contrasted over epochs, to obtain a differential ERF between the C and IC condition (see Figure 4.4 for ERF topoplots of both conditions and their difference, in one subject).

In order to create 3D (x, y, time) scalp-time images for each trial (Figure 4.5), a 2D (x, y) representation of the scalp was obtained, by projecting sensor locations from every trial onto a plane, and by interpolating linearly between them onto a 32×32pixel grid, tiled across each timepoint. This process was repeated for both magnetometers and combined gradiometers.

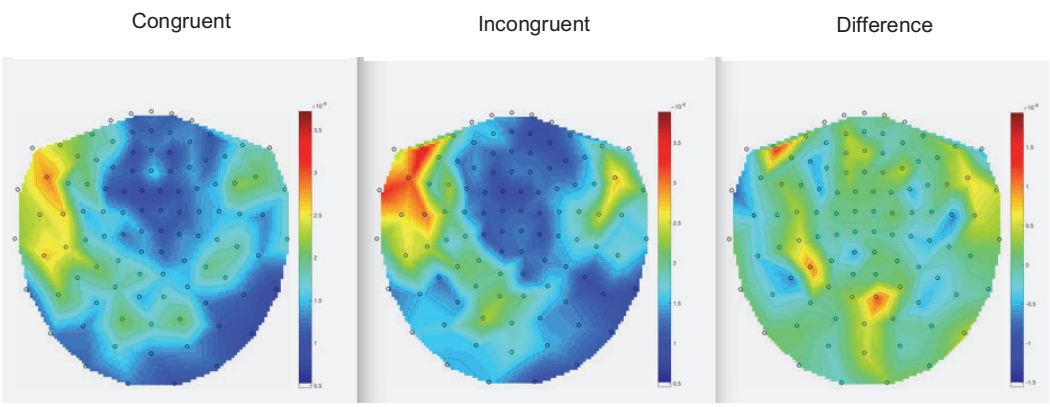

Figure 4.4: ERF individual topoplots (from subject n.226) of C, IC and IC-C difference at 400ms, showing a strong dipolar pattern over the left fronto-temporal regions.

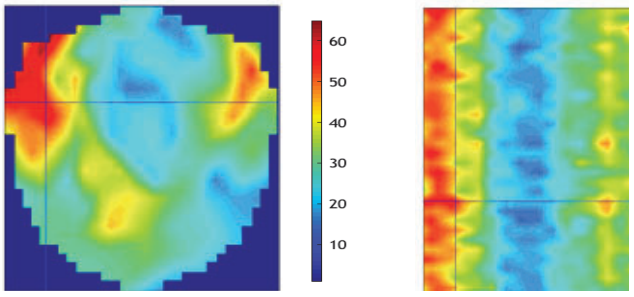

Figure 4.5: 3D Scalp-Time image (x, y, 400ms) for the 1st trial of the incongruent condition in subject n.226, showing a stronger dipolar pattern over the left fronto-temporal regions than the right homologous ones.

4.4.3.1 Scalp-Time Statistics

To identify locations in space and time in which a reliable difference between the C and IC conditions occurred in each subject, one 3D image per trial (per condition) was entered into a GLM using SPM statistical machinery. Ignoring temporal autocorrelation across trials, each trial was treated as an independent observation, so the GLM corresponded to a one-way, non-repeated-measures ANOVA within-subjects, with two levels. A simple F-contrast was defined to find where in space and time there were reliable differences between C and IC conditions. The GLM was run for each sensor-type, with 0.05 as threshold of the family-wise error (FWE) corrected *p*-value.In order to identify locations in time and space where the ERF amplitude in the two conditions differed reliably across subjects, each set of 60 3D images (per condition, per subject) was converted into one 4D (x, y, time, trials) NIfTI file, containing all the multiple 3D scalp-time images corresponding to non-rejected trials, per condition, per subject. The values of the exported images were normalised to reduce variance between-subjects.

The 44 (2 conditions x 22 subjects) 4D images were then entered into the group analysis, which was a repeated-measures ANOVA, to compare C and IC condition across subjects, as well as to perform subgroup comparisons (carriers vs non-carriers; subjects with consistent handedness vs those with inconsistent handedness; dyslexic vs unaffected siblings/twins). Subgroup-level ANOVAs aimed at disentangling the potential cross-influence among *PCSK6* rs11855415 genotype (henceforth *PCSK6* genotype), degree of handedness and affection status, on the N400m ERF and the underlying language processing.

Differently from the previous ANOVA across trials within-subjects, we corrected for the potential correlation (non-sphericity) of the error, induced by the repeated measurements derived from having two observations from each subject. Three contrasts were defined: a simple F-contrast to compare the two conditions, and two T-contrasts, with opposite signs on their weights, to look at the polarity of the difference. The GLMs were run using 0.05 (FWE-corrected) and 0.001(uncorrected) as *p*-value thresholds.

For illustration purposes, the space coordinates of the resulting significant clusters were mapped to the MNI template and then to Brodmann areas, by using the application mni2tal in BioImage Suite (Lacadie et al., 2008; http://sprout022.sprout.yale.edu/mni2tal/mni2tal.html).

4.4.3.2 Scalp-Time Results

None of the group comparisons reached the FWE-corrected significance threshold of 0.05. However, comparing C and IC conditions across subjects with F-contrast thresholded at $p<0.001$ uncorrected, two significant clusters were observed, in the right frontopolar cortex (BA10) and in regions possibly pointing towards the left dorsal posterior cingulate (BA31) (Table 4.1, Figures 4.6 and 4.7). Using T-contrasts to explore the polarity of the difference, this was positive in the IC condition in the left dorsal posterior cingulate (BA31).

Table 4.1 Brain areas with significant N400m activation (p<0.001 uncorrected) derived from the ANOVA between IC and C conditions, across all 22 subjects.

Region	F	df	*p*
R Frontopolar Cortex	12.05	2	0.000
L Dorsal Posterior Cingulate Gyrus	8.32	2	0.001

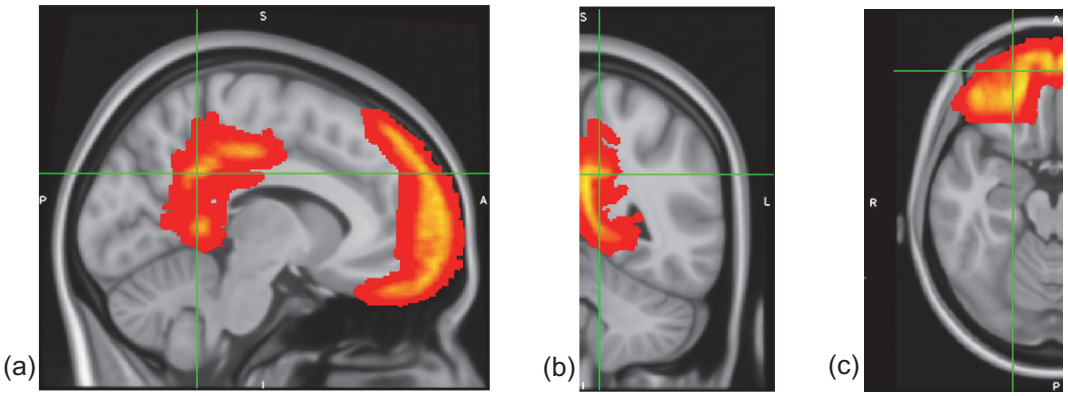

Figure 4.6: Sagittal (a), coronal (b) and axial (c) MNI template projections of the anatomical areas (right frontopolar and left posterior cingulate) with significant N400m activation (p<0.001 uncorrected), derived from the ANOVA between IC and C conditions across subjects.

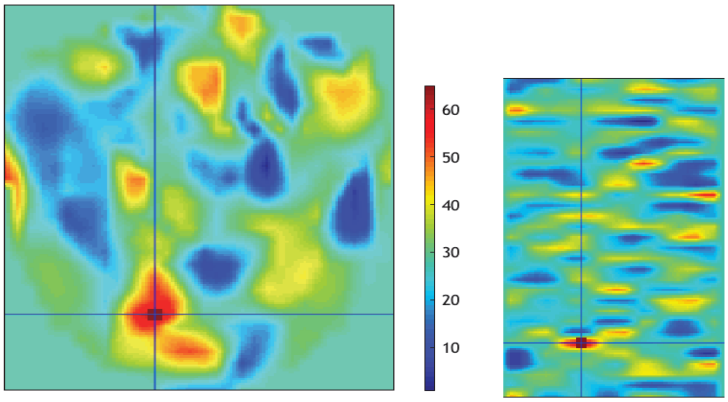

Figure 4.7: 3D Scalp-Time results (x, y, 400ms) of the ANOVA between C and IC conditions across subjects (p<0.001 uncorrected), showing significant activations in right frontal and left posterior regions.

The N400 effect was also evaluated at subgroup-level, to investigate whether there was a significant influence of *PCSK6* genotype, independently from dyslexia status and degree of handedness.

The F-contrast between carriers and non-carriers of the minor allele, thresholded at $p<0.001$ uncorrected, showed significant clusters in both right and left (right>left) plana temporale (BA41), and in the right cuneus (BA19) (Table 4.2, Figures 4.8 and 4.9). The T-contrast of greater N400 effect in carriers than in non-carriers showed significant clusters in the right and left planum temporale (BA41); while the T-contrast of greater N400 effect in non-carriers than in carriers showed significant clusters in the right cuneus (BA19).

Table 4.2: Brain areas with significant N400m activation (p<0.001 uncorrected) derived from the ANOVA between carriers and non-carriers.

Region	F	df	*p*
R Cuneus	12.27	2	0.000
R>L Plana Temporale	10.32	2	0.001

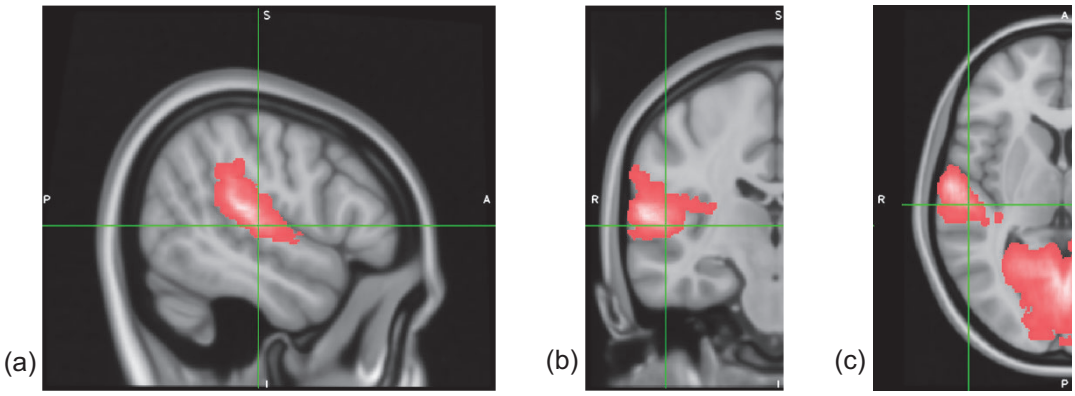

Figure 4.8: Sagittal (a), coronal (b) and axial (c) MNI template projections of the anatomical areas (right cuneus and right planum temporale) with significant N400m activation (p<0.001 uncorrected), derived from the ANOVA between carriers and non-carriers.

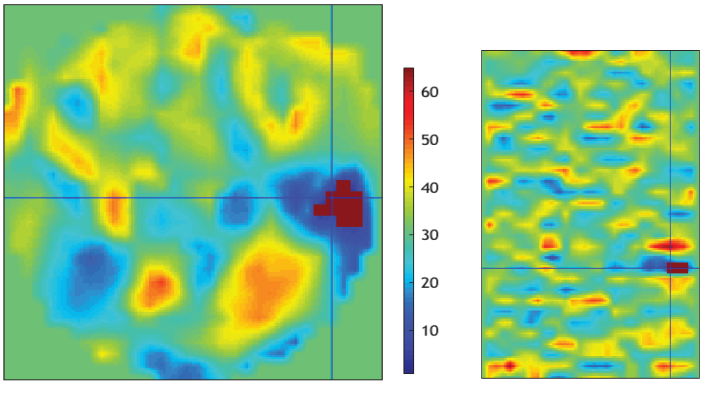

Figure 4.9: 3D Scalp-Time (x, y, 400ms) results of the ANOVA between carriers and non-carriers (p<0.001 uncorrected), showing significant activations in right occipital and posterior temporal regions.

The F-contrast between dyslexic and unaffected siblings/twins, thresholded at $p<0.001$ uncorrected, showed significant clusters in the right angular gyrus (BA39) and in both right and left (right>left) inferior frontal gyri (pars opercularis, BA45) (Table 4.3, Figures 4.10 and 4.11). The T-contrast of greater N400 effect in dyslexic than in non-dyslexic subjects showed significant clusters in the right prefrontal cortex (BA8, BA9), and possibly in the left ventral posterior cingulate (BA23); while the T-contrast of greater N400 effect in unaffected siblings/twins than in dyslexic subjects showed significant clusters in the left and right inferior frontal gyrus (pars opercularis, BA45) and right angular gyrus (BA39).

Table 4.3: Brain areas with significant N400m activation (p<0.001 uncorrected) derived from the ANOVA between dyslexic and unaffected siblings/twins.

Region	F	df	*p*
R Angular Gyrus	11.31	2	0.001
R>L Inferior Frontal Gyri (pars opercularis)	10.72	2	0.001

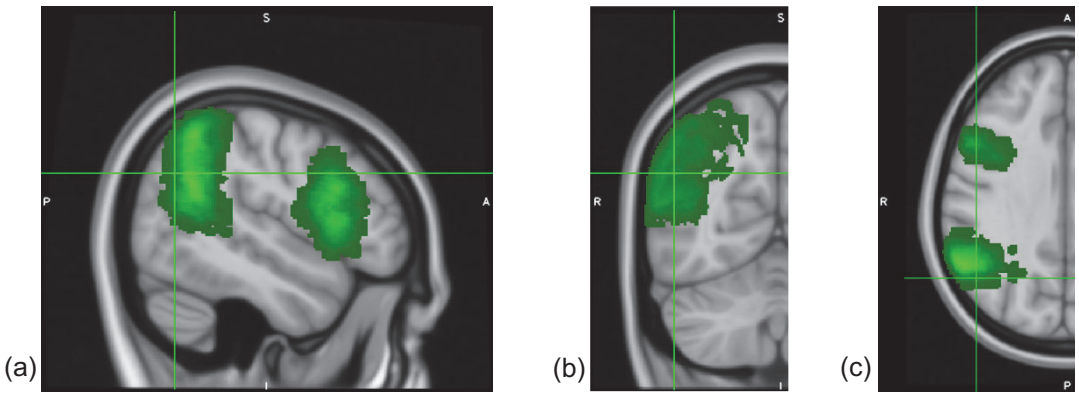

Figure 4.10: Sagittal (a), coronal (b) and axial (c)l MNI template projections of the anatomical areas (right angular gyrus and inferior frontal gyrus) with significant N400m activation (p<0.001 uncorrected), derived from the ANOVA between dyslexic and unaffected siblings/twins.

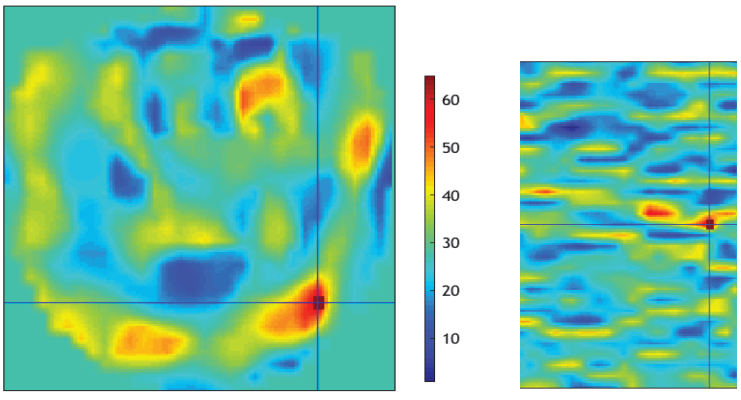

Figure 4.11: 3D Scalp-Time (x, y, 400ms) results of the ANOVA between dyslexic and unaffected siblings/twins (p<0.001 uncorrected), showing significant activations in right parietal and right frontal regions.

The F-contrast between consistent and inconsistent handedness subgroups, thresholded at $p<0.001$ uncorrected, showed significant clusters in the left frontal lobe, at the level of premotor (BA6) and motor (BA4) cortex (Table 4.4, Figures 4.12 and 4.13). The T-contrast of greater N400 effect in subjects with inconsistent handedness than in those with consistent handedness showed significant clusters in the left motor cortex (BA4) and in regions possibly pointing towards the right dorsal posterior cingulate (BA31); while the T-contrast of greater N400 effect in subjects with consistent handedness than in those with inconsistent handedness showed significant clusters in the left premotor cortex (BA6).

Table 4.4: Brain areas with significant N400m activation (p<0.001 uncorrected) derived from the ANOVA between consistent and inconsistent handedness.

Region	F	df	*p*
L Premotor Cortex	11.46	2	0.000
L Motor Cortex	11.03	2	0.001

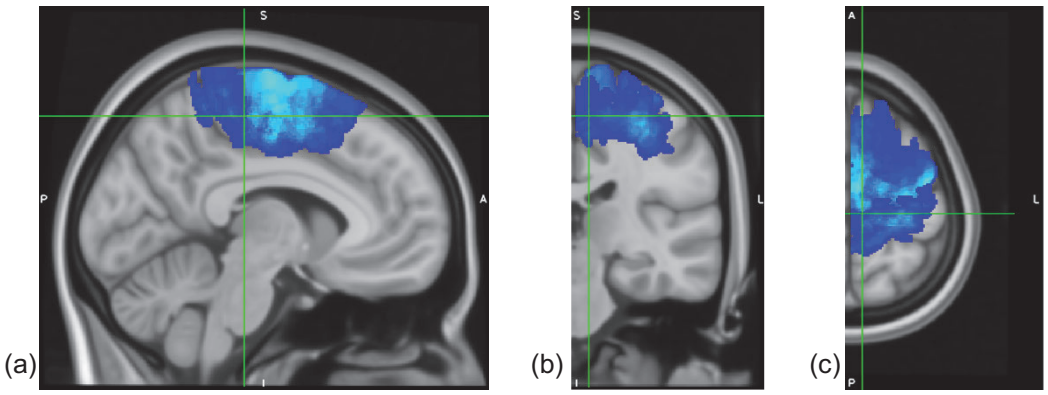

Figure 4.12: Sagittal (a), coronal (b) and axial (c) MNI template projections of the anatomical areas (left premotor and motor cortex) with significant N400m activation (p<0.001 uncorrected), derived from the ANOVA between consistent and inconsistent handedness.

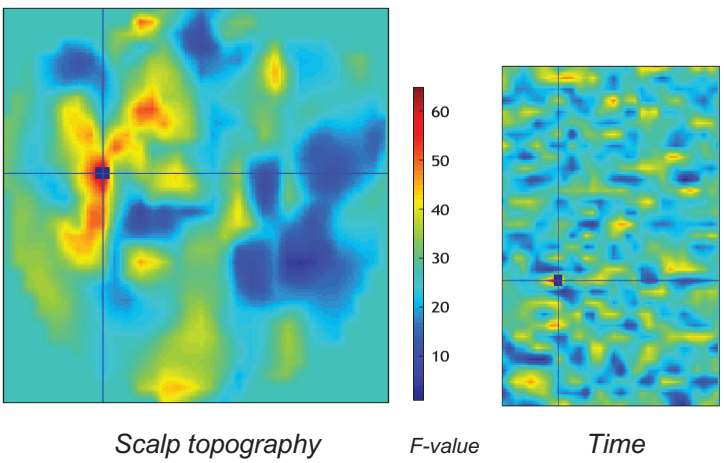

Figure 4.13: 3D Scalp-Time (x, y, 400ms) results of the ANOVA between consistent and inconsistent handedness (p<0.001 uncorrected), showing significant activations in left fronto-central regions.

4.4.4 Time-Frequency Analysis

Time-frequency analysis was performed to provide insights on oscillatory brain dynamics and language comprehension processes.

Morlet wavelets were used to decompose each trial into power and phase, across peristimulus time and frequency. A straight averaging of the power estimate across trials and across channels was performed, and a circular averaging of the phase estimate was run to produce a quantity called Phase-Locking Value (PLV).

For the baseline correction of the time-frequency power files, data were scaled with a log transform, since changes at high-frequency tend to be smaller than changes at lower frequencies. Trial-averaged data were then contrasted to create the image of the difference in power between IC and C conditions, for each subject (Figure 4.14).

(a)

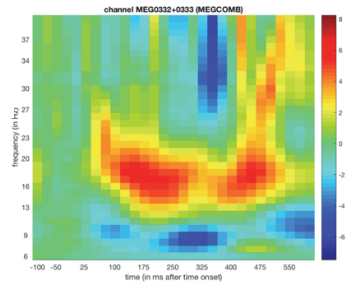

(b)

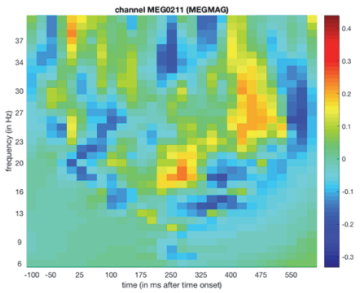

Figure 4.14: Time-Frequency Analysis:

a) Trial-averaged power for IC > C in channel MEG0332+0333 (left frontal) in subject n.226, showing an increase in power from 13 to 40 Hz between 350 and 500ms, that is most likely the evoked energy corresponding to the N400m in the left-fronto-temporal regions shown in Figure 4.5; additional power changes can be also seen, that might be not phase-locked, but induced.

b) Trial-averaged PLV for IC > C in channel MEG0211 (left temporal) in subject n.226, where IC condition increases phase-locking relative to C condition, between 400 and 500ms, suggesting a change in phase of ongoing beta oscillations, as well as their power.

4.4.4.1 Time-Frequency Statistics

One 2D power image per condition per subject was entered into a GLM, to perform a one-way repeated-measures ANOVA with two levels, in order to identify locations, in frequency and time, where a reliable difference between the IC and C conditions occurred across subjects.

To model the error correlation induced by repeated measurements, we allowed for dependencies, given the assumption of non-sphericity.

To make comparisons, the following contrasts were defined: a simple F-contrast to compare the IC and C conditions; two T-contrasts to look at the polarity of the IC-C difference; another F-contrast to compare the power N400m modulation within *PCSK6* (carriers vs non-carriers), handedness (consistence vs inconsistence) and affection status (dyslexic vs unaffected) subgroups. The GLMs were run using 0.05 (FWE-corrected) as *p*-value threshold.

4.4.4.2 Time-Frequency Results

Event-related power changes were particularly seen over the right frontal and left temporal regions, in the C condition, and in the occipital and frontal areas bilaterally, in the IC condition.

When comparing C and IC conditions across all subjects, with F-contrast thresholded at $p<0.05$ FWE-corrected, a significant increase in power was observed both at 7Hz 350ms, and at 40Hz 350-500ms. SPM for F-contrasts within all subgroups, thresholded at $p<0.05$ FWE-corrected, showed a significant change in power at 7Hz 375ms.

4.4.5 Source Reconstruction

To estimate the cortical sources giving rise to the MEG data, each individual structural MRI was co-registered to the individual MEG data, by using the fiducial points to create a head model defining cortex, skull and scalp meshes. The forward model was calculated based on the single-shell model for computing the lead field matrix (Nolte, 2003), and then inverted by using the Empirical Bayes Beamformer (EBB) (Belardinelli et al., 2012) in SPM (Figure 4.15).

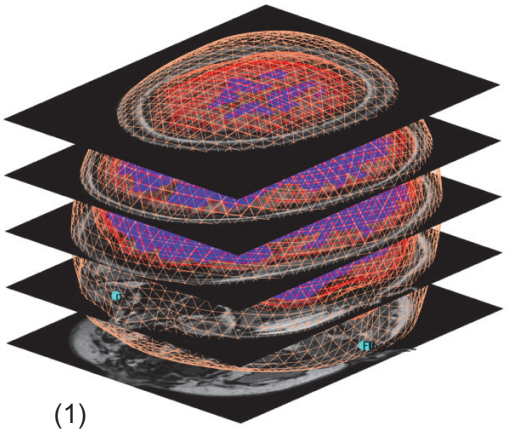

(1)

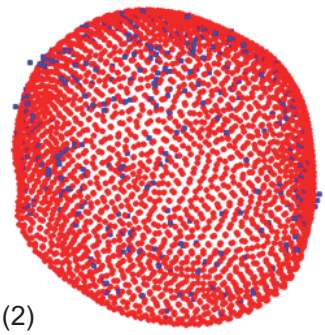

(2)

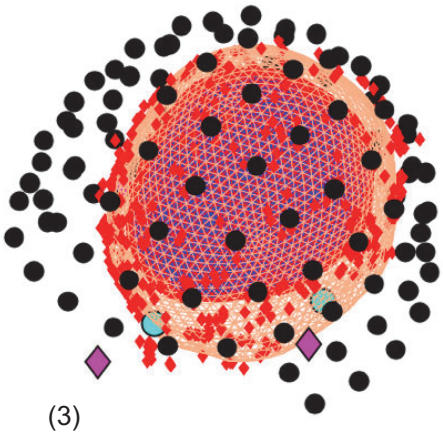

(3)

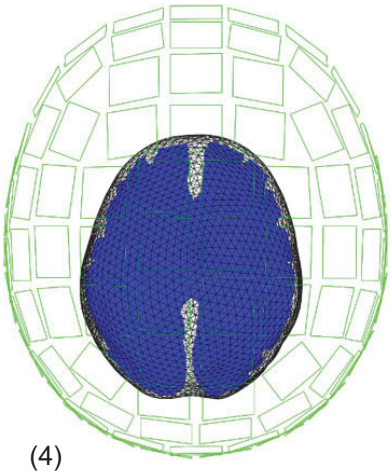

(4)

Figure 4.15: Co-registration and forward model steps in subject n.226:

1) *Creation of the cortical mesh (blue) based on the individual MRI (inner skull in red, scalp in orange, hardwired fiducials in light blue and MRI transverse slices in black and grey scale);*

2) *Co-registration with the MEG head shape points (blue), digitised with Polhemus;*

3) *Co-registration with the MEG sensor fiducials (light blue), sensor locations (black) and MRI fiducials (pink);*

4) *Creation of the forward model, using the single-shell model (mesh in blue, inner skull and scalp surfaces in black, MEG sensors in green).*

The EBB inverse solution is an alternative to many spatial priors, by having a single prior optimised using functional constraints (Belardinelli et al., 2012). Therefore, a single candidate source covariance was estimated by using beamformer priors, and then regularised in the Bayesian framework. This produced a Maximum Intensity Projection (MIP) of activity in source space, and a time series of activity for each condition; a peristimulus (PST) hanning taper to the channel time series was also applied, in order to down-weight the possible baseline noise at the beginning and end of the trial (see MIP estimated and PST for each inversion solution in Figure 4.17).

Based on the results of the group sensor-level and time-frequency analyses, the time window of interest was set at 350-500ms, and the frequency window at 6-40Hz. The source power was written both as a surface-based GIfTI mesh, using the default cortical smoothing size of 8 (Figure 4.16), and as a volumetric NIfTI image, involving interpolation; the latter was then used to compute the language laterality index, as described in the next paragraph 4.4.6.

As visible in Figure 4.17d, the EBB source reconstruction was much more focal and lateralised in comparison with the other inverse solution algorithms that were simulated on the data, including: 1) multiple spars priors (Greedy Search, GS in Figure 4.17a), corresponding to a sparse prior on the sources, with few ones active; 2) spatially COHerent sources (COH in Figure 4.17b), that is the spatial smoothness prior, allowing the mixture of two possible source covariance matrices (the minimum norm prior and a smooth source covariance matrix); 3) Independent Identically Distributed sources (IID in Figure 4.17c), that is the L2-minimum norm prior, assuming the prior probability of each active source as independent and identically distributed.

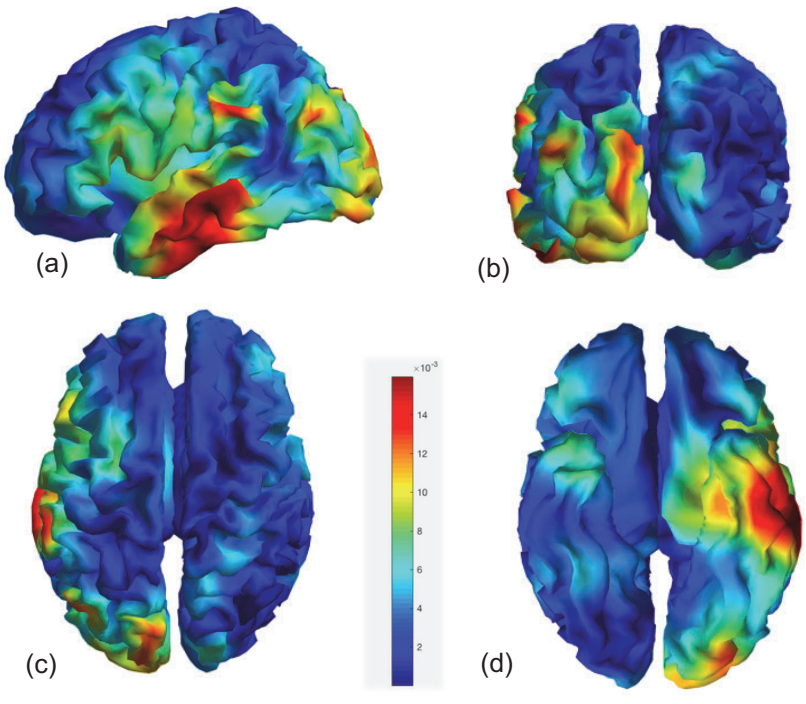

Figure 4.16: Power images of subject n.226, derived from EBB source reconstruction of IC condition at 400ms, on GIfTI mesh:

a) Left sagittal view, showing strong sources in the temporal lobe (inferior and middle temporal gyrus), inferior parietal lobule (supramarginal and angular gyrus) and occipital lobe (lingual gyrus);

b) Posterior view, showing strong source in the left occipital lobe (cuneate and lingual gyrus);

c) Top view, showing strong sources in the left cuneus and inferior parietal lobule;

d) Basal view, showing strong sources in the left lingual gyrus, inferior and middle temporal gyrus.

Figure 4.17: Comparison of inverse solutions for source reconstruction of IC condition in subject n.226.

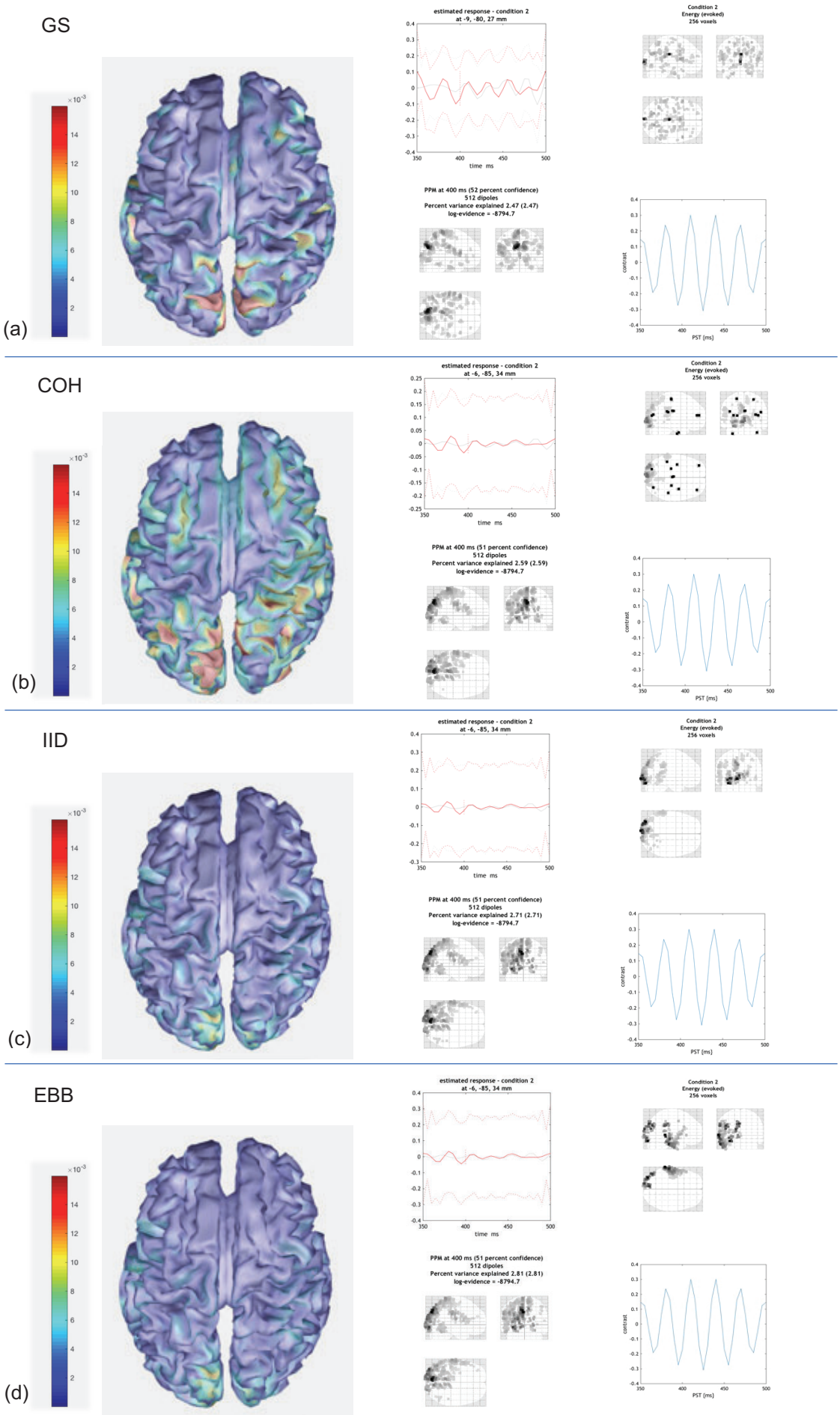

GS=Greedy Search multiple spars priors; COH=spatially COHerent sources; IID=Independent Identically Distributed sources; EBB=Empirical Bayes Beamformer; IC=incongruent.

4.4.5.1 Source Statistics

To identify the difference between the IC and C conditions in each subject, the source power GIfTI images were entered into a one-way, non-repeated-measures ANOVA with two levels. A simple F-contrast was defined to compare and identify reliable differences at the subject-level. The GLM was run using 0.05 (FWE-corrected) as *p*-value threshold.

Once obtained all the 44 (22 subjects × 2 conditions) GIfTI images for the power at 6-40Hz and 350-500ms, these were entered into the same repeated-measures ANOVA used for scalp-time and time-frequency group statistics. Simple F-contrasts were defined to compare C and IC conditions across all subjects, and to investigate subgroup potential differences (carriers vs non-carriers; consistent vs inconsistent handedness; dyslexic vs unaffected siblings/twins). The GLMs were run using 0.05 as *p*-value threshold.

4.4.5.2 Source Results

Group SPM for IC vs C power, at 6-40Hz and 350-500ms, across all 22 subjects, showed significant activation clusters in the left premotor cortex (BA6) as well as significant deeper sources in the left and right thalamus.

Same power sources were found at the subgroup-level; in addition, further significant activation clusters were observed in both right and left dorsal anterior cingulate gyri (BA32), and left prefrontal cortex (BA8), when comparing carriers with non-carriers, dyslexic with unaffected siblings/twins, consistent with inconsistent handedness subgroups (Figure 4.18).

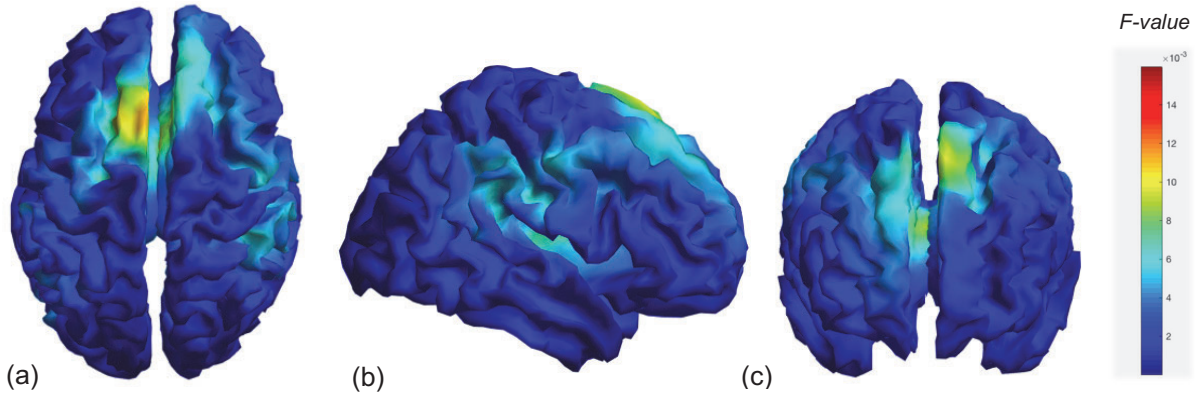

Figure 4.18: Power source images derived from subgroup analysis, comparing carriers with non-carriers:

a) Top view, showing significantly strong activations in the left premotor cortex and deep sources in both right and left anterior cingulate gyri;

b) Right sagittal view, showing mild activations in the superior frontal gyrus and inferior parietal lobule;

c) Frontal view, showing significantly strong activations in the left premotor cortex and deep sources in both right and left anterior cingulate gyri.

4.4.6 Language Laterality Analysis

To analyse receptive language dominance, a quantitative assessment of grey matter's activation asymmetry was conducted in each subject, by employing a bootstrap procedure on the source power NIfTI images, derived from the EBB source reconstruction. Such laterality analysis was performed in the LI-toolbox, implemented in SPM (Wilke and Lidzba, 2007). The midline (+/-5mm) was masked out, and five inclusive masks of the frontal, parietal, temporal, occipital, and cingulate cortices were selected for the analysis.

The lateralisation index (LI), related to the N400m power sources, was based on the following basic computation:

$$LI = (Left - Right) / (Left + Right)$$

Negative LI values indicate right hemispheric dominance, while positive values indicate left hemispheric dominance. From each regional LI, a laterality quotient (LQ) was also derived, by multiplying the LI by 100. The language LQ has a range between − 100 and 100, with negative values indicating rightward lateralisation, positive values indicating leftward lateralisation, and higher values showing a stronger asymmetry in the respective direction. A specific measure of degree of laterality was also determined, by taking the absolute value of LQ (ranging from 0 to 100), with higher values indicating stronger laterality. Additionally, a binary variable for direction of laterality was created, by categorising a negative LQ (from -100 to 0) as right hemispheric dominance, and a positive LQ (from 1 to 100) as left hemispheric dominance.

Following the approach of previous MEG studies (Raghavan et al., 2017; Tanaka et al., 2013), a ternary classification of language lateralisation was performed, using ±10 as threshold, and assuming values higher than 10 as indicating left hemispheric dominance (LD), lower than -10 as indicating right hemispheric dominance (RD), and between -10 and 10 as indicating symmetric bilateral language representation (BL).

These calculations resulted in four asymmetry measures as dependent variables: LQ, degree of laterality, direction of laterality and lateralisation.

4.4.6.1 Laterality Statistics

Statistical analyses were performed in SPSS® version 25 statistical software (IBM, Armonk, NY, USA). In each analysis, subjects were grouped according to the independent variable of interest, and matched by the other independent variables potentially affecting asymmetries, in order to disentangle any cross-influence on hemispheric dominance.

The three independent variables were: 1) *PCSK6* rs11855415 genotype (henceforth referred to as *PCSK6* genotype), grouping carriers vs non-carriers of the minor allele; 2) degree of handedness (determined as described in Chapter 2, paragraph 2.2.2), grouping consistent

vs inconsistent handedness; 3) affection status, grouping dyslexic vs unaffected siblings/twins. Therefore, to investigate the *PCSK6*-related endophenotype, carriers and non-carriers were matched by age, gender, affection status and degree of handedness; to look at the effect of degree of handedness, subjects with consistent and inconsistent handedness were matched by age, gender, affection status and genotype; to explore the effect of dyslexia status, dyslexic and unaffected subjects were matched by age, gender, degree of handedness and genotype.

The four dependent variables were analysed with different tests: LQ and degree of laterality, being interval-scaled variables, were tested parametrically using two-sample *t*-test; lateralisation and direction of laterality, being nominal variable, were tested non-parametrically using Mann-Whitney test.

Since five brain areas of interest (cingulate, frontal, temporal, parietal and occipital regions) were included in the analysis, Bonferroni correction resulted in a corrected significance threshold of p=0.05/5=0.01.

4.4.6.2 Laterality Results

As far as the power activation at 6-40Hz and 350-500ms is concerned, this was bilateral, mildly leftward lateralised at the level of cingulate, frontal, parietal and temporal regions, and strongly leftward lateralised in the occipital lobe (Figure 4.19), in all 22 subjects.

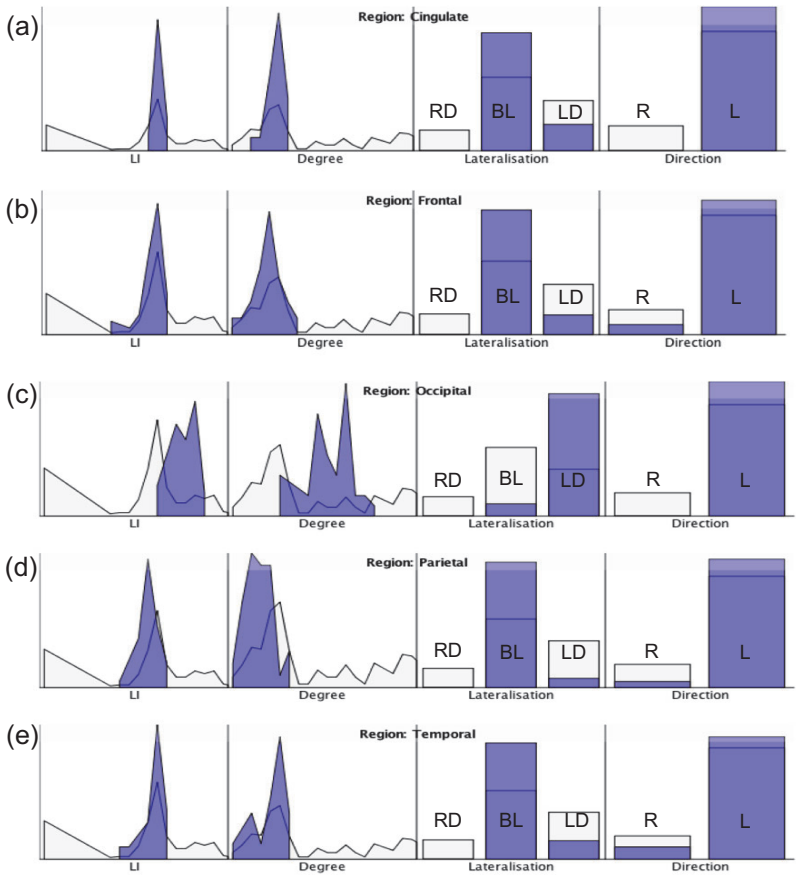

RD=right hemispheric dominance; BL=bilateral representation; LD=left hemispheric dominance; R=right; L=left; LI=laterality index.

Figure 4.19: LI, degree of laterality, direction of laterality, and lateralisation, in the cingulate, frontal, occipital, parietal and temporal regions, across all subjects:

a) Cingulate cortex showed a bilateral and mildly leftward activation;

b) Frontal cortex showed a bilateral and mildly leftward activation;

c) Occipital cortex showed a bilateral and strongly leftward lateralisation;

d) Parietal cortex showed a bilateral and mildly leftward activation;

e) Temporal cortex showed a bilateral and mildly leftward activation.

4.4.6.2.1 Laterality Quotient

None of the comparisons (carriers vs non-carriers; dyslexic vs unaffected siblings/twins; consistent vs inconsistent handedness) reached significance for neither the Bonferroni-corrected (0.01) nor the uncorrected (0.05) significance thresholds.

4.4.6.2.2 Degree of Laterality

None of the comparisons (carriers vs non-carriers; dyslexic vs unaffected siblings/twins; consistent vs inconsistent handedness) reached significance for the Bonferroni-corrected threshold (0.01). However, the uncorrected significance threshold (0.05) was reached by the effect of the affection status (dyslexic vs unaffected) on the low degree of frontal laterality (*p* 0.023) (Table 4.5).

*Table 4.5: Results of the t-tests with degree of laterality as dependent variable and affection status as independent variable. *Frontal region reached significance (<0.05).*

Region	t	df	*p*
Frontal	2.456	20	0.023*
Parietal	0.291	20	0.774
Temporal	0.728	20	0.475
Occipital	0.710	20	0.486
Cingulate	-0.826	20	0.418

4.4.6.2.3 Direction of Laterality

None of the comparisons (carriers vs non-carriers; dyslexic vs unaffected siblings/twins; consistent vs inconsistent handedness) reached significance for neither the Bonferroni-corrected (0.01) nor the uncorrected (0.05) significance thresholds.

4.4.6.2.4 Lateralisation

The Bonferroni-corrected significance threshold (0.01) was reached only by the effect of *PCSK6* genotype on the cingulate leftward lateralisation (*p* 0.007) (Table 4.6).

*Table 4.6: Results of the Mann-Whitney tests with lateralisation as dependent variable and PCSK6 genotype as independent variable. *Cingulate reached significance (<0.01).*

Region	Mann-Whitney U	N	*p*
Frontal	46.000	22	0.645
Parietal	40.000	22	0.588
Temporal	35.000	22	0.323
Occipital	36.500	22	0.346
Cingulate	65.500	22	0.007*

4.4.7 Discussion

4.4.7.1 The Relationship between N400m and Power Changes

Comparing the C and IC conditions across subjects, significant event-related power changes were observed in the theta frequency range (4-7Hz) at 7Hz, at 350ms, and in the gamma frequency range (25-100Hz) at 40Hz, at 350-500ms. In particular, a consistently smaller gamma power was observed for IC sentence endings than for C ones. Increased neuronal synchronisation in the theta band has been shown to be associated to retrieval of word-level information (Bastiaansen et al., 2005, 2008), while gamma band neuronal synchronisation around 40Hz has been observed in relation to sentence-level semantic processing (Bastiaansen and Hagoort, 2006; Varela et al., 2001).

In our participants, an increase in gamma power was particularly seen in the C condition, over the right frontal and left temporal regions, consistently with other studies (Hald et al., 2006; Urrutia et al., 2012), that reported increased gamma (~40 Hz) power during semantic unification operations, and gamma band event-related desynchronisation in association with semantic incongruency.

4.4.7.2 Modulation and Lateralisation of the N400m in the Cortico-Thalamic Network

For more than 150 years, since the time of Broca's (1865) and Wernicke's researches (1874), language functions were the focus of mainly cortico-centric studies, looking at the structural underpinnings of language processing within the cortex. However, in the last 30 years this view was progressively complemented by models looking also at subcortical regions as potential language-related structures (Crosson, 1985; Alexander et al., 1986; Nadeau and Crosson, 1997; Friederici and Kotz, 2003; Ullman, 2006; Wahl et al., 2008; Krugel et al., 2014).

According to the "selective engagement model" (Crosson, 1985), non-linguistic functions would pertain to the basal ganglia, and language abilities to cortico-thalamic networks, where thalamic nuclei would gate language-related information flow between the fronto-opercular and temporo-parietal areas and, on demand, coordinate their coupling for the integration of phonemic and semantic levels (Crosson, 1985; Nadeau and Crosson, 1997; cf. Johnson and Ojemann, 2000; Kraut et al., 2003; Wahl et al., 2008).

Our results particularly suit the Crosson's model of a cortico-thalamic network for syntactic and semantic language processing, since the N400 effect reflects the semantic retrieval of multiple cortical regions (Helenius et al., 1998; Halgren et al., 2002; Maess et al., 2006; Service et al., 2007; Vartiainen et al., 2009; Vistoli et al., 2011; Wang et al., 2012), as part of a more distributed semantic network. In this context, the thalamus may play a pivotal role in the task-dependent build-up of intercortical connectivity among cingulate, frontal and temporo-parietal cortices. The contribution to language organisation from each of these structures (Figures

4.20, 4.21 and 4.22) will be described in the ensuing sections, against the backdrop of our observations and the published literature.

4.4.7.2.1 Thalamus

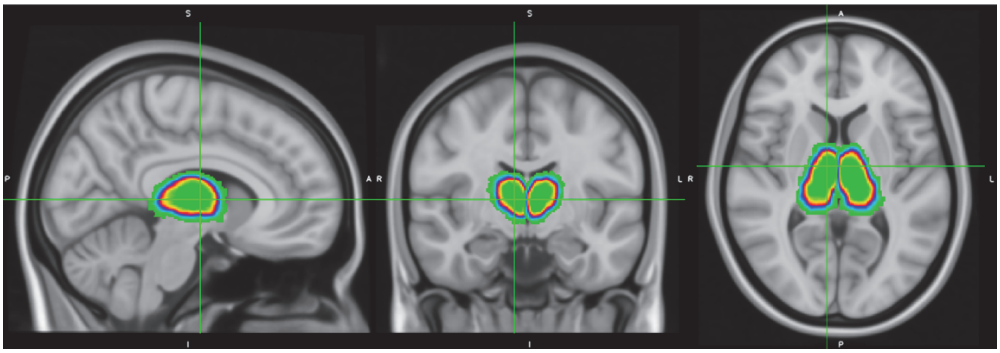

Figure 4.20: Sagittal, coronal and axial MNI template projections of left and right thalamus.

The Crosson's model of a cortico-thalamic language network has been further validated by several studies in the last two decades, particularly in the field of Deep Brain Stimulation (DBS) (Benabid et al., 2000; Krack et al., 2000; Schuurman et al., 2000; Wahl et al., 2008; Krugel et al., 2014).

Wahl et al. (2008) found that thalamic nuclei, but not basal ganglia, are engaged in the analysis of syntactic and semantic parameters of auditorily presented sentences. They used simultaneous scalp, basal and thalamic EEG recordings to map the cortico-basal organisation of language, by comparing depth-recorded and scalp-recorded ERPs (P600, N400, early left anterior negativity). Interestingly, depth-recorded ERPs were from both right and left ventral intermediate nuclei, even in case of strong lateralised scalp-recorded ERP. Similarly, our SPM for IC vs C power at 6-40Hz and 350-500ms across all 22 subjects, showed sources in both left and right thalami as well as in the left premotor cortex. These findings taken together make also plausible a thalamic centromedian origin with dense fronto-temporal connections, such as centromedian or pulvinar nuclei (Yingling and Skinner, 1977), relative to which even the more lateral recordings would be mostly symmetrical (Wahl et al., 2008).

A more recent DBS study (Krugel et al., 2014) also confirmed the thesis of a thalamic N400 modulation, with lack of subthalamic influence. In particular, a prolongation of lexical decision time alongside an attenuation of the N400 was observed in patients with ventral intermediate nucleus DBS, due to the disruption of the thalamic control over the cortical structures, that is crucial for word processing (Krugel et al., 2014).

Electrical stimulations performed in the context of thalamotomy showed that dysnomia and phonemic repetitions can be provoked by targeting anterior thalamic regions, while object anomia and lexical memory decline can be elicited by stimulating dorsal thalamic regions (Ojemann, 1975, 1976, 1983; Fedio and Van Buren, 1975; Hebb and Ojemann, 2012).

Functional imaging studies have also shown thalamic activations during speech-sound analysis and lexico-semantic tasks, alongside the involvement of temporal and frontal regions of the dominant hemisphere (Nadeau and Crosson, 1997; Slotnick et al., 2002; Kraut et al., 2002, 2003; Alain et al., 2005; Assaf et al., 2006; Von Kriegstein et al., 2008).

Finally, further insights on the language-related role of the thalamus come from clinical conditions, such as thalamic lesions of the centromedian complex, inferior peduncle (Yingling and Skinner, 1977; Nadeau and Crosson, 1997), ventral nuclei, mammillothalamic tract (Nishio et al., 2011), and infarctions of the left paramedian and tuberothalamic arteries, that can lead to thalamic aphasia, consisting in word finding difficulties, dysnomia and semantic paraphasia (Jonas, 1982; Nadeau and Crosson, 1997; Kuljic-Obradovic, 2003; Carrera and Bogousslavsky, 2006; De Witte et al., 2011).

4.4.7.2.2 Cingulate Cortex

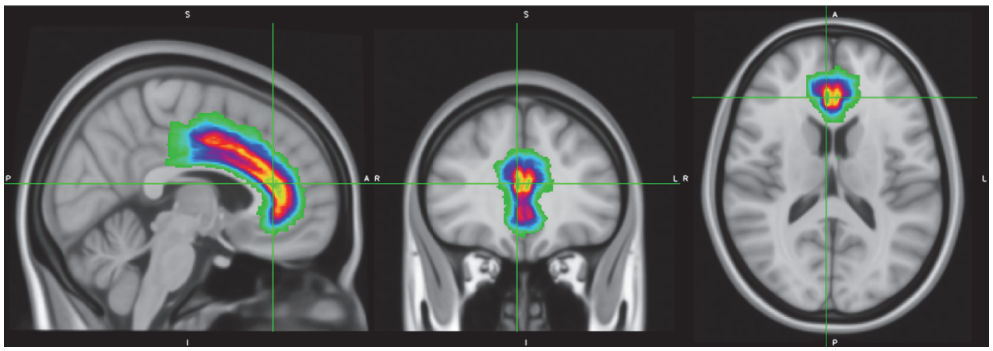

Figure 4.21: Sagittal, coronal and axial MNI template projections of the cingulate cortex.

In addition to the N400m thalamic sources, we also found significant source activations in the right and left dorsal anterior cingulate cortex (BA32) and left prefrontal cortex (BA8,9), when comparing carriers with non-carriers, dyslexic with unaffected siblings/twins, and consistent with inconsistent handedness subgroups.

It is interesting to notice that the engagement of the cingulate cortex during the language task was correctly hypothesised on the basis of the subject-, subgroup- and group-level scalp-time analyses, and confirmed by the source-level results.

When looking at the differential N400m ERF (IC>C) across all subjects, significant clusters were observed in the right frontopolar cortex (BA10) and in contralateral regions possibly pointing towards the dorsal posterior cingulate (BA31). Also, a greater N400 effect in dyslexic than in unaffected siblings/twins was observed in the right prefrontal cortex (BA8,9), and in contralateral regions possibly indicating the ventral posterior cingulate (BA23); while a greater N400 effect in subjects with inconsistent handedness than in those with consistent handedness was found in the left motor cortex (BA4), and contralaterally in regions pointing towards the right dorsal posterior cingulate (BA31).

The most interesting insights on the cingulate cortex come though from the laterality analysis, that considered the brain regional laterality indeces of the N400m power sources as dependent variables of *PCSK6* genotype, degree of handedness and affection status. This showed a significant effect of *PCSK6* genotype on the cingulate leftward lateralisation, while frontal degree of laterality was significantly associated with dyslexia status, independently from *PCSK6*. There might be a link between *PCSK6* and language organisation via the cingulate, representing one of the *PCSK6*-related functional endophenotypes independent from dyslexia.

The cingulate cortex receives inputs from both the thalamus and the neocortex, and, via the cingulum, projects to the entorhinal cortex. Based on fMRI evidence (Polli et al., 2005; Taylor et al., 2006), the dorsal part of the anterior cingulate cortex would play a role in conflict monitoring (Carter et al., 1998; Kiehl et al., 2000; Menon et al., 2001), while the rostral part in error detection (Falkenstein et al., 1991; Gehring et al., 1993). The posterior cingulate cortex is instead an important hub of the default mode network (Whitfield-Gabrieli and Ford, 2012) and semantic network (Binder et al., 2009), and its activity can indicate mediation of task demands, and a continued operation with the current cognitive set (Pearson et al., 2011). Both the anterior and posterior cingulate cortex have been reported to be linked to the N400 effect (Matsumoto et al., 2005; Kircher et al., 2009; Abel et al., 2012; Jacob et al., 2019). The anterior cingulate cortex is also the structure where the error-related negativity (ERN) ERP is known to be generated, according to dipole source modelling (Dehaene, Posner and Tucker, 1994), fMRI studies (Ito et al., 2003; Holroyd et al., 2004) and brain lesion research (Stemmer et al., 2004). The ERN is evoked by a mismatch between the actual and the intended response representations (Falkenstein et al., 1991, 2000; Gehring et al., 1993; Scheffers et al., 1996), in a comparable manner to the N400 ERP and other medial frontal negativities resulting from a mismatch process (Falkenstein et al., 1991).

4.4.7.2.3 Neocortex

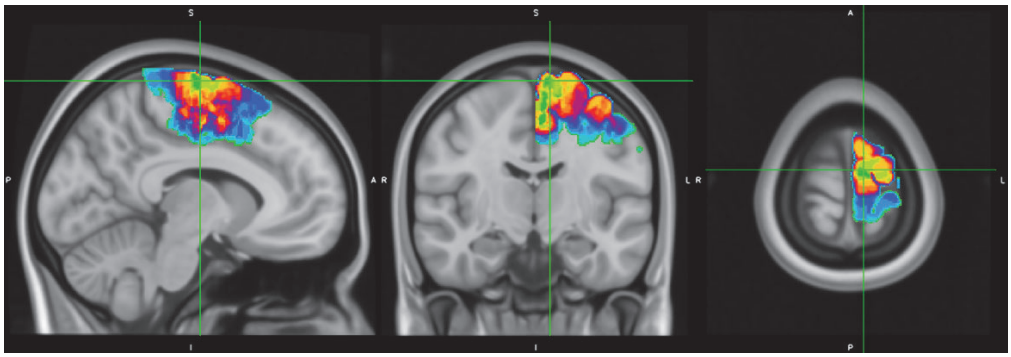

Figure 4.22: Sagittal, coronal and axial MNI template projections of the left premotor cortex.

The N400m ERF has been reported to be generated in bilateral, but left dominant, temporal regions (Helenius et al., 1998; Halgren et al., 2002; Vartiainen et al., 2009; Wang et al., 2012), with contributions from left prefrontal cortex (Halgren et al., 2002; Maess et al., 2006).

Our study also showed the bilateral cortical contribution to the N400m ERF from temporal and frontal lobes, alongside parietal and occipital activations, at the subject- and subgroup-level. In addition to what mentioned in the previous paragraph with regard to the subgroup-level N400m frontal and cingulate activations, a significantly greater N400 effect was also observed in the following regions: in the right and left planum temporale (BA41) in carriers than in non-carriers; in the right cuneus (BA19) in non-carriers than in carriers; in the right angular gyrus in unaffected siblings/twins than in dyslexic ones; in the left premotor cortex (BA6) in subjects with consistent handedness than in those with inconsistent handedness. However, at the neocortical level, source reconstruction showed only significant N400m frontal sources, in the left premotor cortex, at the subject-, subgroup- and group-level.

Consistently with our findings, Halgren et al. (2002) showed activations to semantic mismatch spreading to the left prefrontal areas, like inferior frontal gyrus and dorsolateral prefrontal cortex (Halgren et al., 2002); and fMRI studies (Rodd et al., 2005; Lauro et al., 2008; Boulenger et al., 2009) showed a similar fronto-temporal activation extending into anterior inferior frontal cortex. Interestingly, idiom-related activation in the middle frontal gyrus were observed to extend into frontocentral motor and premotor cortex (Boulenger et al., 2009), reflecting the motor cognition generated by abstract action-related language (Jeannerod, 2006; Boulenger et al., 2009). This might be also valid for some sentences of our child-friendly MEG paradigm (e.g. *the child went outside to play*), that might have elicited frontal activations also related to motor cognition.

According to the “functional neuroanatomic model for word semantic processing” (Lau et al., 2008): 1) matching lexico-semantic representations would be first stored and activated in the inferior and middle temporal gyrus; 2) the anterior temporal cortex and angular gyrus would integrate semantic information into context (Dronkers et al., 2004; Noppeney et al., 2008); 3) the inferior frontal gyrus would mediate controlled selection (with its posterior part) and retrieval (with its anterior part) of representations, based on top-down information (Friederici, 2002; Humphries et al., 2007; Mechelli et al., 2007). Therefore, each new word’s semantic representation would be integrated by the angular gyrus, and then selected and retrieved by the inferior frontal gyrus. Such model certainly helps the functional interpretation of the N400 effect observed in our subjects at the level of the inferior parietal and temporal cortex, as reflecting semantic integration, and of the inferior frontal cortex, as reflecting selection and retrieval processes.

Finally, our laterality analysis looking at the regional laterality indeces of the N400m power sources showed a significant independent effect of the dyslexia affection status on the low degree of laterality of the frontal lobes, in line with previous functional studies reporting a weaker language lateralisation in dyslexic individuals (Badcock et al., 2012; Park et al., 2012; Sun et al., 2010; Papanicolaou et al., 2003; Simos et al., 2000; Breier et al., 2003; Sarkari et al., 2002).

Chapter 5: Conclusions

5.1 Integrating Functional and Structural Endophenotypes

This thesis analysed the *PCSK6*-related extended endophenotype of functional and structural hemispheric asymmetries, by examining quantitatively the co-segregation of brain anatomy, physiology and neurocognitive laterality measures.

The main hypothesis was that atypical structural and functional hemispheric asymmetries may result from a disruption of the NODAL signalling pathway due to specific *PCSK6* genetic variants, and may become ultimately visible at the clinical level as developmental neurocognitive disorders, such as dyslexia.

Driven by previous GWAS' findings regarding the association of *PCSK6* rs11855415 with greater relative right handedness in dyslexia cohorts (Scerri et al., 2011; Brandler et al., 2013), we used the putative link between this genetic variant and developmental dyslexia as genotype – clinical phenotype association model, and we investigated the related structural and functional hemispheric asymmetries as its postulated extended endophenotype, via a multimodal integrated neuroimaging approach.

On the structural side, a significant difference at the level of the pars opercularis of the IFG, in terms of morphometry (density) but not of asymmetry, was revealed by the first MRI exploratory study on 14 participants, comparing carriers with non-carriers of *PCSK6* rs11855415 minor allele. Interestingly, carriers displayed a lower GM density in this structure than non-carriers, and also a significant positive correlation between the volume of the IFS rightward asymmetric cluster (asymmetry that was present in both carriers and non-carriers) and handedness LQ. The second MRI study, performed on the entire ABC cohort of 47 children, revealed instead the presence of a significant *PCSK6*-related asymmetry at the level of the pars opercularis of the IFG, which was more rightward lateralised in carriers than in non-carriers. In the ABC cohort, we also found a significant association between *PCSK6* and degree of asymmetry of the lateral orbitofrontal region, superior frontal gyrus, precentral gyrus, insula and amygdala, where carriers showed a lower degree of asymmetry than non-carriers, suggesting a potential influence of the *PCSK6* on the development of a less asymmetric frontal cortical and subcortical regions. Therefore, the fil rouge of the *PCSK6*-related structural findings observed across the MRI studies would link *PCSK6* rs11855415 to a specific rightward asymmetry of the pars opercularis of the IFG, within the context of a diminished degree of frontal asymmetries, where the right volume of the rightward asymmetry of the IFS would correlate positively to a higher degree of right-handedness in carriers.

On the functional side, in order to investigate the *PCSK6*-associated language asymmetries, our MEG study analysed the regional language laterality indeces derived from the N400m power sources, and showed a significant effect of *PCSK6* on the cingulate

lateralisation. Furthermore, carriers showed N400m bilateral thalamic and leftward cingulate sources, as well as left frontal source activations. These findings may therefore suggest a possible link between *PCSK6* and language lateralisation, via the cingulate cortex.

5.2 Testing Asymmetry Correlations

All the *PCSK6*-related associations found across the ChildBrain multimodal study, were further tested with a bivariate Pearson's correlation analysis of the asymmetry indices (derived from MEG, MRI and handedness) and neuropsychology scores, including both continuous and dichotomous categorical (*PCSK6* genotype and dyslexia status) variables.

The correlation analysis revealed the following associations between the *PCSK6* rs11855415 variant and: 1) the MEG-derived cingulate language lateralisation index (*p* 0.01, *r* 0.306); 2) the MRI-derived direction of asymmetry and LQ of the pars opercularis of the IFG (respectively, *p* 0.038, *r* 0.306 and *p* 0.007, *r* 0.390); 3) PegQ (*p* 0.027, -0.334) and degree of handedness (*p* 0.022, *r* -0.349). All significant correlations are included in Table 5.1.

The associations between *PCSK6* and the MRI- and MEG-derived laterality measures found in our studies were confirmed by significant positive correlations; the association of *PCSK6* with handedness (Scerri et al., 2011; Brandler et al., 2013) was also confirmed but, contrarily to what expected, by a significant negative correlation.

Table 5.1: Significant correlations across MRI/ MEG-derived asymmetry indeces, handedness, cognitive measures, PCSK6 genotype and dyslexia status, with respective r coefficient and p-value.

	SWE	Hand Deg	PegQ	Dys	*PCSK6*	PO LQ	PO Deg	PO Dir	Front LQ	Front Deg	Front Dir	Cing LQ	Cing Deg	Cing Lat
VIQ-PIQ									.623* .040		.712* .014			
SWE	-			-.58** .00						-.515* .029				
Hand Deg		-	-			.331* .028								
PegQ			-		-.334* .027	-.334* .027								
Dyslexia	.588* .000			-										
PCSK6			-.334* .027		-	.39** .007		.306* .038						.571* .011
PO IFG LQ		.331* .028			.39** .007	-	-	-						
PO IFG Deg						-	-	-						.541* .017
PO IFG Dir					.306* .038	-	-	-						.541* .017
Front LQ									-	-	-	.58** .009	.58** .009	
Front Deg	-.515* .029								-	-	-			
Front Dir									-	-	-	.495* .031	.495* .031	
Cing LQ									.58** .009		.495* .031	-	-	-
Cing Deg									.58** .009		.495 .031	-	-	-
Cing Lat					.571* .011		.541* .017					-	-	-

**Correlation significant at 0.05 (2-tailed, uncorrected). **Correlation significant at 0.01 (2-tailed, uncorrected). Cing=cingulate cortex; Deg=degree; Dir=direction; Dys=dyslexia; Front=frontal; Hand=handedness; IFG=inferior frontal gyrus; Lat=laterality; PO=pars opercularis; SWE=sight word efficiency; VIQ-PIQ=Verbal Intelligence Quotient - Performance Intelligence Quotient discrepancy.*

The bivariate Pearson's correlation revealed in fact the association of *PCSK6* rs11855415 with both a low degree of handedness and a low PegQ values, in contrast with what observed by Scerri et al. (2011) and Brandler et al. (2013) regarding the association of the same variant with increased relative right-hand skills (positive PegQ values) in dyslexic individuals. In dealing with these contrasting findings, it is relevant to recall the existence of another *PCSK6* variant, rs10523972, that was found to be associated to a lower degree of handedness (Arning et al., 2013), as well as to rightward asymmetries in the frontal and temporal lobes (Berretz et al., 2019), in healthy individuals. In light of this, it is plausible to advance the alternative hypothesis of a potential shared extended endophenotype, possibly consisting of rightward frontal asymmetries and low degree of handedness, between the *PCSK6* rs11855415 and rs10523972 variants, respectively in dyslexia-families and in the general population. A collaborative neuroimaging study would be therefore needed in order to investigate and compare the quantitative traits of functional and structural hemispheric asymmetries associated to both variants, and to look for those differential features, in particular in the temporal lobe (where we did not find any *PCSK6* rs11855415-related effect), that might make individuals possibly less prone to develop dyslexia in association to *PCSK6* rs10523972.

With regard to the other Pearson's correlations not directly related to *PCSK6*, they also confirmed the collateral findings of the multimodal study, highlighting the holistic nature of the functional-structural hemispheric asymmetries. In particular, degree of handedness was positively correlated with the MRI-derived LQ of the pars opercularis of the IFG and to the MEG-derived frontal degree of language laterality, corroborating the hypothesis that handedness lateralisation might be linked to language, via both structural and functional asymmetries of the frontal lobe. In addition, the MEG-derived cingulate language lateralisation index was positively correlated with the MRI-derived degree and direction (right) of asymmetry of the pars opercularis of the IFG; and the MEG-cingulate degree of language laterality and LQ were both positively correlated with the MEG-frontal LQ and left direction of laterality, confirming the cross-talking between cingulate and frontal regions within the cortico-thalamic semantic network, that we observed in the MEG study. Interestingly, the MEG-derived frontal degree of language asymmetry was negatively correlated with the sight word efficiency (SWE) standard score, while the MEG-derived frontal language direction and LQ were positively correlated with the VIQ-PIQ discrepancy (difference between verbal IQ and performance IQ), suggesting that MEG-derived language asymmetry measures can be reflected also by psychometric measures of hemispheric asymmetry.

Assembling the main findings of the MRI and MEG studies presented in this thesis, we can now construct the potential extended endophenotype for *PCSK6*-related hemispheric asymmetries in dyslexia families (Figure 5.1). The structural endophenotype would therefore consist of a low degree of asymmetry of the frontal lobes, with a rightward asymmetric cluster

at the level of the IFG pars opercularis. While the functional endophenotype would consist: on the receptive language side, of a fronto-cingulate-thalamic semantic network, originating from the thalami, passing through the cingulate gyri with leftward lateralisation, towards the left frontal cortex; on the handedness side, either of increased relative right-hand skills (Scerri et al., 2011; Brandler et al., 2013), possibly positively correlated with the right volume of the rightward asymmetric IFS (as observed in our first MRI study), or of a low degree of handedness and right-hand skills, as revealed by the Pearson's correlation.

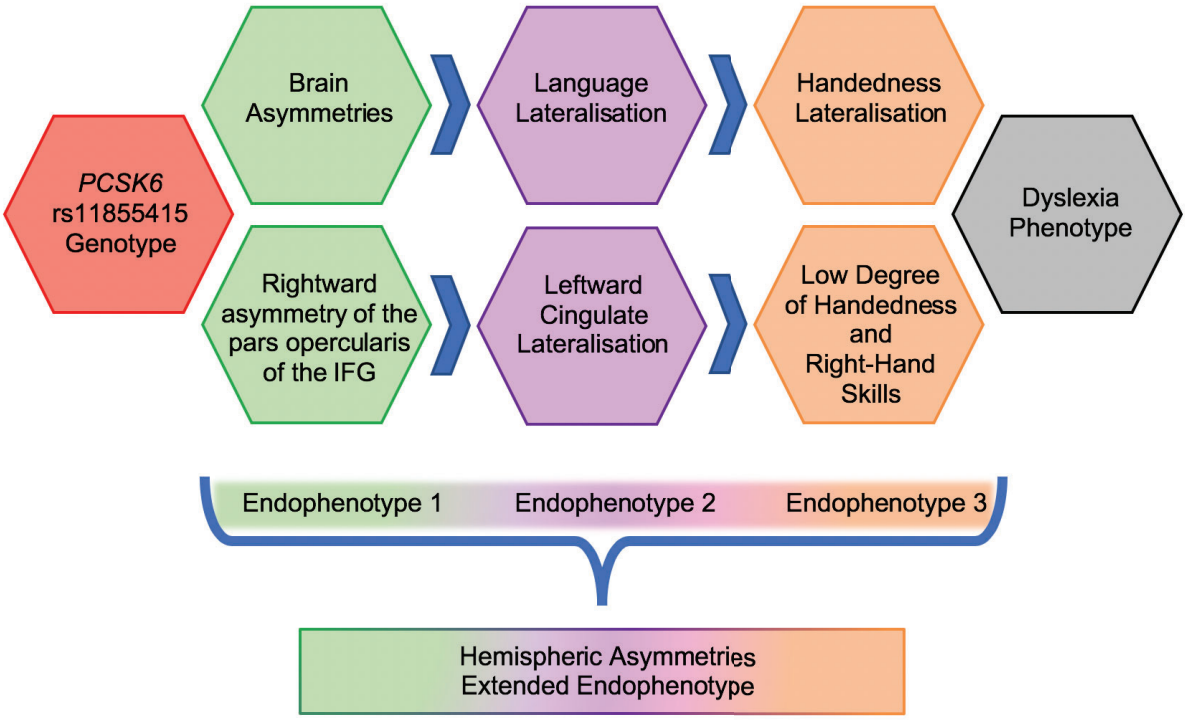

Figure 5.1 PCSK6-related hemispheric asymmetries extended endophenotype:

- *Endophenotype 1 is represented by a rightward asymmetry of the pars opercularis of the inferior frontal gyrus (IFG,) within the context of a general low degree of frontal asymmetries;*
- *Endophenotype 2 is represented by a fronto-cingulate-thalamic semantic network, originating from the thalami towards left frontal cortex, via cingulate leftward lateralisation.*
- *Endophenotype 3 is represented by a low degree of handedness and right-hand skills.*

The combination of the observed endophenotypes into a network-dimension, where the included traits are linked to each other by integrated functional-structural mechanisms, seems to satisfy the definition criteria of 'extended endophenotype', proposed by Prasad and Keshavan (2008). In our postulated *PCSK6* rs11855415-related extended endophenotype: (1) each trait was state-independent, and measured as quantitative endophenotype in dyslexic and unaffected siblings; (2) different levels of investigation and analysis (structural, physiological, cognitive and behavioural) have been involved; (3) the included

endophenotypes co-occurred within dyslexia families, in dyslexic children as well as in the unaffected siblings, and were correlated within the same individual; (4) the included functional and structural endophenotypes are putatively mechanistically related, given the still unclear nature of the link between brain structural and functional aymmetries. Furthermore, the state-independence of the *PCSK6* rs11855415-related findings in our dyslexia case-sibling population supports the hypothesis of the endophenotype against alternative models, such as pleiotropy, additive/interactive risk and neuroplasticity.

5.3 Future Directions

The choice of a family-based study helped to avoid possible spurious associations (Cardon and Palmer, 2003) and to increase the chances of including children displaying the genetic variant of interest. However, this study design might have resulted in subjects being overmatched on many variables, with a consequent loss of power and risk of false positive results (Witte et al., 1999). This issue has been partially prevented by building on findings from GWASs (Scerri et al., 2011; Brandler et al., 2013), and by matching subjects by any confounding variables that could potentially impact on asymmetries independently from the *PCSK6* rs11855415 variant. To ensure homogeneity of asymmetry variance, this was also assessed with Levene's test in each of the asymmetry analyses.

In order to reduce the replication uncertainty of our genotype-endophenotype associations, the introduction of an additional control group of unrelated unaffected children, and the increase of the sample size through a neuroimaging genetics collaborative network should be the priorities of future studies.

In conclusion, by deriving and integrating quantitative measures of grey matter asymmetries, language lateralisation and handedness dominance in a dyslexia family-based study, we constructed a prototypical *PCSK6* rs11855415-related extended endophenotype. Such model of functional and structural hemispheric asymmetry extended endophenotype will hopefully inform and help future studies in unveiling the pathway that goes from NODAL to neurocognitive disorders, passing through brains, minds and their atypical asymmetries.

References

Abel S., Dressel K., Weiller C., and Huber W. (2012). Enhancement and suppression in a lexical interference fMRI-paradigm. *Brain and Behavior*; 2: 109-127.

Aboitiz F., Scheibel A.B., Fisher R.S., and Zaidel E. (1992). Individual differences in brain asymmetries and fiber composition in the human corpus callosum. *Brain Research*; 598: 154-161.

Abou-Khalil B. (2007). An update on determination of language dominance in screening for epilepsy surgery: the Wada test and newer noninvasive alternatives. *Epilepsia*; 48(3): 442-55.

Abu-Rustum R.S., Ziade M.F., and Abu-Rustum S.E. (2013). Reference values for the right and left fetal choroid plexus at 11 to 13 weeks: an early sign of "developmental" laterality? *Journal of Ultrasound in Medicine*; 32: 1623-1629.

Achenbach T.M., McConaughy S.H., Ivanova M.Y., and Rescorla L.A. (2011). *Manual for the ASEBA Brief Problem Monitor™ (BPM).* Burlington, VT: University of Vermont, Research Center for Children, Youth, and Families.

Adler W.T., Platt M.P., Mehlhorn A.J., Haight J.L., Currier TA., Etchegaray M.A., Galaburda A., and Rosen G. (2013). Position of Neocortical Neurons Transfected at Different Gestational Ages with shRNA Targeted against Candidate Dyslexia Susceptibility Genes. *PloS ONE*; 8(5): e65179.

Alain C., Reinke K., McDonald K.L., Chau W., Tam F., Pacurar A., and Graham S. (2005). Left thalamo-cortical network implicated in successful speech separation and identification. *Neuroimage*; 26: 592-599.

Alexander G.E., DeLong M.R., and Strick P.L. (1986). Parallel organization of functionally segregated circuits linking basal ganglia and cortex. *Annual review of neuroscience*; *9*: 357-381.

Alhusaini S., Whelan C.D., Sisodiya, S.M., and Thompson P.M. (2016). Quantitative magnetic resonance imaging traits as endophenotypes for genetic mapping in epilepsy. *Neuroimage: Clinical*; 12: 526-534.

Almli C.R., Rivkin M.J., McKinstry R.C., and Brain Development Cooperative Group (2007). The NIH MRI study of normal brain development (Objective-2): newborns, infants, toddlers, and preschoolers. *Neuroimage;* 35(1): 308-25.

Amador-Arjona A., Elliott J., Miller A., Ginbey A., Pazour G.J., Enikolopov G., Roberts A.J., and Terskikh A.V. (2011). Primary cilia regulate proliferation of amplifying progenitors in adult

hippocampus: implications for learning and memory. *The Journal of Neuroscience*; 31: 9933-9944.

American Psychiatric Association (1994). *Diagnostic and Statistical Manual of Mental Disorders* (4th edition). Washington DC, APA.

American Psychiatric Association (2013) *Diagnostic and Statistical Manual of Mental Disorders* (5th edition). Washington DC, APA.

Amunts K. (2010). Structural indices of asymmetry. In K. Hughdahl and R. Westerhausen (Eds.), *The Two Halves of the Brain* (pp. 145-176). Cambridge MA: The MIT Press.

Anderson C.A., Pettersson F.H., Clarke G.M., Cardon L.R., Morris A.P., and Zondervan K.T. (2010). Data quality control in genetic case-control association studies. *Nature Protocols;* 5: 1564-1573.

Andersson J.L.R., Jenkinson M. and Smith S. (2007). Non-linear registration, aka Spatial normalisation. FMRIB technical report TR07JA2 from: www.fmrib.ox.ac.uk/analysis/techrep

Andescavage N.N., Du Plessis A., McCarter R., Serag A., Evangelou I., Vezina G., Robertson R., and Limperopoulos C. (2017). Complex trajectories of brain development in the healthy human fetus. *Cerebral Cortex*; 27: 5274-5283.

Ando J., Ono Y., and Wright M. J. (2001). Genetic structure of spatial and verbal working memory. *Behavior Genetics*; 31(6): 615-624.

Andrews W., Liapi A., Plachez C., Camurri L., Zhang J., Mori S., Murakami F., Parnavelas J.G., Sundaresan V., and Richards L.J. (2006). Robo1 regulates the development of major axon tracts and interneuron migration in the forebrain. *Development*; 133(11): 2243-2252.

Annett M. (1964). A model of the inheritance of handedness and cerebral dominance. *Nature;* 204: 59–60.

Annett M. (1970). A classification of hand preference by association analysis. *British Journal of Psychology*.; 61: 303-321.

Annett M. (1985). *Left, right, hand, brain: The right shifttheory*. London and Hillsdale, N.J.: Lawrence Erlbaum Associates.

Armstrong E., Schleicher A., Omran H., Curtis M., and Zilles K. (1995). The ontogeny of human gyrification. *Cerebral Cortex*; 5 (1):56-63.

Arning L., Ocklenburg S., Schulz S., Ness V., Gerding W.M., Hengstler J.G., Falkenstein M., Epplen J.T., Güntürkün O., and Beste C. (2013). PCSK6 VNTR Polymorphism Is Associated with Degree of Handedness but Not Direction of Handedness. *PLoS ONE;* 8(6): e67251.

Aron A.R., Robbins T.W., and Poldrack R.A. (2004). Inhibition and the right inferior frontal cortex. *Trends in Cognitive Sciences*; 8(4): 170-7.

Ashburner J., and Friston K.J. (2000). Voxel-based morphometry--the methods. *Neuroimage;* 11(6 Pt 1): 805-21.

Assaf M., Calhoun V.D., Kuzu C.H., Kraut M.A., Rivkin P.R., Hart J. Jr, and Pearlson G.D. (2006). Neural correlates of the object-recall process in semantic memory. *Psychiatric Research*; 147: 115-126.

Astrom R.L., Wadsworth S.J., and DeFries J.C. (2007). Etiology of the stability of reading difficulties: the longitudinal twin study of reading disabilities. *Twin Research and Human Genetics*; 10(03): 434-439.

Baala L., Briault S., Etchevers H.C., Laumonnier F., Natiq A., Amiel J., Boddaert N., Picard C., Sbiti A., Asermouh A., Attié-Bitach T., Encha-Razavi F., Munnich A., Sefiani A., and Lyonnet S. (2007). Homozygous silencing of T-box transcription factor EOMES leads to microcephaly with polymicrogyria and corpus callosum agenesis. *Nature Genetics;* 39: 454-6.

Baaré W F., Pol H.E.H., Boomsma D.I., Posthuma D., De Geus E.J., Schnack H.G., Van Haren N.E., Van Oel C.J., and Kahn R.S. (2001). Quantitative genetic modeling of variation in human brain morphology. *Cerebral Cortex*; 11(9): 816-824.

Babu D., and Roy S. (2013). Left–right asymmetry: cilia stir up new surprises in the node. *Open Biology*; 3: 130052.

Badcock N.A., Bishop D.V., Hardiman M.J., Barry J.G., and Watkins K.E. (2012). Co-localisation of abnormal brain structure and function in specific language impairment. *Brain and Language;* 120(3): 310-20.

Baddeley A. (1992). Working memory. *Science*; 255(5044): 556-559.

Bahi-Buisson N., Guttierrez-Delicado E., Soufflet C., Rio M., Daire V.C., Lacombe D., Héron D., Verloes A., Zuberi S., Burglen L., Afenjar A., Moutard M.L., Edery P., Novelli A., Bernardini L., Dulac O., Nabbout R., Plouin P., and Battaglia A. (2008). Spectrum of epilepsy in terminal 1p36 deletion syndrome. *Epilepsia*; 49: 509-15.

Bamforth F., Bamforth S., Poskitt K., Applegarth D., and Hall J. (1988). Abnormalities of corpus callosum in patients with inherited metabolic diseases. *The Lancet*; 2: 451.

Baranek C., Dittrich M., Parthasarathy S., Bonnon C.G., Britanova O., Lanshakov D., Boukhtouche F., Sommer J.E., Colmenares C., Tarabykin V., and Atanasoski S. (2012). Protooncogene Ski cooperates with the chromatin-remodeling factor Satb2 in specifying

callosal neurons. *Proceedings of the National Academy of Science of The United States of America*; 109: 3546-51.

Barkovich A.J., and Kjos B.O. (1988). Normal postnatal development of the corpus callosum as demonstrated by MR imaging. *AJNR American Journal of Neuroradiology*; 9: 487–91.

Barkovich A.J., Lyon G., and Evrard P. (1992). Formation, maturation, and disorders of white matter. *AJNR American Journal of Neuroradiology*; 13:447-61.

Barkovich A., Kuzniecky R., Jackson G., Guerrini R., and Dobyns W. (2005). A developmental and genetic classification for malformations of cortical development. *Neurology*; 65(12): 1873-1887.

Barkovich A.J., Guerrini R., Kuzniecky R.I., Jackson G.D., and Dobyns W.B. (2012). A developmental and genetic classification for malformations of cortical development: update 2012. *Brain*;135 (Pt 5):1348-69.

Barnea-Goraly N., Kwon H., Menon V., Eliez S., Lotspeich L., and Reiss A.L. (2004). White matter structure in autism: preliminary evidence from diffusion tensor imaging. *Biological Psychiatry;* 55(3): 323-326.

Barnea-Goraly N., Menon V., Eckert M., Tamm L., Bammer R., Karchemskiy A., Dant C.C., and Reiss A.L. (2005). White matter development during childhood and adolescence: a cross-sectional diffusion tensor imaging study. *Cerebral Cortex*; 15(12): 1848-1854.

Barr M.S., and Corballis M.C. (2002). The role of the anterior commissure in callosal agenesis. *Neuropsychology*; 16: 459-71.

Barrett S.E., and Rugg D.M. (1990). Event-related potentials and the semantic matching of pictures, *Brain and Cognition*; 14(2): 201-212.

Barth K.A., Miklosi A., Watkins J., Bianco I.H., Wilson S.W., and Andrew R.J. (2005). fsi zebrafish show concordant reversal of laterality of viscera, neuroanatomy, and a subset of behavioral responses. *Current Biology CB*; 15: 844-850.

Basile L. F. H., and Papanicolaou A. C. (1997). Source localization of the N400 response in a sentence-reading paradigm using evoked magnetic fields and magnetic resonance imaging. *Brain Research*; 762(1-2): 29-39.

Bastiaansen M.C.M., Van der Linden M., Ter Keurs M., Dijkstra T., and Hagoort P. (2005). Theta responses are involved in lexical-semantic retrieval during language processing. *Journal of Cognitive Neuroscience*; *17*(3): 530-541.

Bastiaansen M.C.M, and Hagoort P. (2006). Oscillatory neuronal dynamics during language comprehension. *Progress in Brain Research*; 159: 179-96.

Bastiaansen M.C.M., Oostenveld R., Jensen O., and Hagoort P. (2008). I see what you mean: Theta power increases are involved in the retrieval of lexical semantic information. *Brain and Language;* 106: 15-28.

Bates T.C., Luciano M., Castles A., Coltheart M., Wright M.J., and Martin N.G. (2007). Replication of reported linkages for dyslexia and spelling and suggestive evidence for novel regions on chromosomes 4 and 17. *European Journal of Human Genetics*; 15(2): 194-203.

Batouli S.A.H., Trollor J.N., Wen W., and Sachdev P.S. (2014). The heritability of volumes of brain structures and its relationship to age: A review of twin and family studies. *Ageing Research Reviews*; 13: 1-9.

Bayliss D.M., Jarrold C., Baddeley A.D., and Leigh E. (2005). Differential constraints on the working memory and reading abilities of individuals with learning difficulties and typically developing children. *Journal of Experimental Child Psychology*; 92(1): 76-99.

Beaton A.A. (1997). The relation of planum temporale asymmetry and morphology of the corpus callosum to handedness, gender, and dyslexia: a review of the evidence. *Brain and Language*; 60(2): 255-322.

Beaulieu C. (2002). The basis of anisotropic water diffusion in the nervous system–a technical review. *NMR in Biomedicine*; 15(7-8): 435-455.

Beaulieu C., Plewes C., Paulson L.A., Roy D., Snook L., Concha L., and Phillips L. (2005). Imaging brain connectivity in children with diverse reading ability. *Neuroimage*; 25(4): 1266-1271.

Belardinelli P., Ortiz E., Barnes G., Noppeney U., and Preissl H. (2012). Source Reconstruction Accuracy of MEG and EEG Bayesian Inversion Approaches. *PLoS ONE;* 7(12): e51985.

Benabid A.L., Koudsié A., Benazzouz A., Fraix V., Ashraf A., Le Bas J.F., Chabardes S., and Pollak P. (2000). Subthalamic stimulation for Parkinson's disease. *Archives of Medical Research*; 31(3): 282-9.

Benadiba C., Magnani D., Niquille M., Morlé L., Valloton D., Nawabi H., Ait-Lounis A., Otsmane B., Reith W., Theil T., Hornung J.P., Lebrand C., and Durand B. (2012). The ciliogenic transcription factor RFX3 regulates early midline distribution of guidepost neurons required for corpus callosum development. *PLoS Genetics*; 8: e1002606.

Benes F.M. (1989). Myelination of cortical-hippocampal relays during late adolescence. *Schizophrenia Bulletin*; 15(4): 585.

Berretz G., Arning L., Gerding W.M., Friedrich P., Fraenz C., Schlüter C., Epplen, J.T., Güntürkün O., Beste C., Genç E., and Ocklenburg S. (2019). Structural Asymmetry in the

Frontal and Temporal Lobes Is Associated with PCSK6 VNTR Polymorphism. *Molecular Neurobiology;* 56(11): 7765-7773.

Bertoncini J., Morais J., Bijeljac-Babic R., McAdams S., Peretz I., and Mehler J. (1989). Dichotic perception and laterality in neonates. *Brain and Language;* 37: 591-605.

Binder J.R., Desai R.H., Graves W.W., and Conant L.L. (2009). Where is the semantic system? A critical review and meta-analysis of 120 functional neuroimaging studies. *Cerebral Cortex*; 19(12): 2767-2796.

Binder J.R., and Desai R.H. (2011). The neurobiology of semantic memory. *Trends in Cognitive Sciences*; 15: 527-536.

Bishop D.V.M. (2013). Cerebral asymmetry and language development: cause, correlate, or consequence? *Science;* 340: 1230531.

Blanchet M.H., Le Good J.A., Oorschot V., Baflast S., Minchiotti G., Klumperman J., and Constam D.B. (2008). Cripto localizes Nodal at the limiting membrane of early endosomes. *Science Signaling;* 1(45): ra13.

Blanchet M.H., Le Good J.A., Mesnard D., Oorschot V., Baflast S., Minchiotti G., Klumperman J., and Constam D.B. (2008). Cripto recruits Furin and PACE4 and controls Nodal trafficking during proteolytic maturation. *The EMBO Journal;* 27: 2580-2591.

Blokland G.A.M., McMahon K.L., Hoffman J., Zhu G., Meredith M., Martin N.G., Thompson P.M., De Zubicaray G.I., and Wright M.J. (2008). Quantifying the heritability of task-related brain activation and performance during the N-back working memory task: a twin fMRI study. *Biological Psychology*; 79: 70-79.

Bloom J.S., and Hynd G.W. (2005). The role of the corpus callosum in interhemispheric transfer of information: excitation or inhibition? *Neuropsychology Review;* 15: 59-71.

Boon M., Jorissen M., Proesmans M., and De Boeck K. (2013). Primary ciliary dyskinesia, an orphan disease. *European Journal of Pediatrics*; 172: 151-162.

Boulenger V., Hauk O., and Pulvermüller F. (2009). Grasping ideas with the motor system: semantic somatotopy in idiom comprehension. *Cerebral Cortex*; 19(8): 1905-1914.

Bourgeois J.-P., and Rakic P. (1993). Changes of synaptic density in the primary visual cortex of the macaque monkey from fetal to adult stage. *The Journal of Neuroscience*; 13(7): 2801-2820.

Brandler W.M., Morris A.P., Evans D.M., Scerri T.S., Kemp J.P., Timpson N.J., St Pourcain B., Smith G.D., Ring S.M., Stein J., Monaco A.P., Talcott J.B., Fisher S.E., Webber C., and

Paracchini S. (2013). Common variants in left/right asymmetry genes and pathways are associated with relative hand skill. *PLoS Genetics*; 9: e1003751.

Brandler W.M., and Paracchini S. (2014). The genetic relationship between handedness and neurodevelopmental disorders. *Trends in Molecular Medicine*; 20(2): 83-90.

Breier J.I., Simos P.G., Fletcher J.M., Castillo E.M., Zhang W., and Papanicolaou A.C. (2003). Abnormal activation of temporoparietal language areas during phonetic analysis in children with dyslexia. *Neuropsychology*; 17: 610-621.

Broca P. (1865). Sur le siege de la faculte du langage articule. *Bulletin de la Societe d'anthropologie*; 6: 337-93.

Brown W.S., and Paul L.K. (2000). Cognitive and psychosocial deficits in agenesis of the corpus callosum with normal intelligence. *Cognitive Neuropsychiatry;* 5: 135-157.

Bullmore E.T., Suckling J., Overmeyer S., Rabe-Hesketh S., Taylor E., and Brammer M.J. (1999). Global, voxel, and cluster tests, by theory and permutation, for a difference between two groups of structural MR images of the brain. *IEEE Transactions on Medical Imaging*; 18(1): 32-42.

Cardon L.R., and Palmer L.J. (2003). Population stratification and spurious allelic association. *Lancet*; 361(9357): 598-604.

Carrera E., and Bogousslavsky J. (2006). The thalamus and behavior: effects of anatomically distinct strokes. *Neurology*; 66: 1817-1823.

Carrion-Castillo A., Franke B., and Fisher S.E. (2013). Molecular genetics of dyslexia: an overview. *Dyslexia*; 19(4): 214-240.

Carter C.S., Braver T.S., Barch D.M., Botvinick M.M., Noll D., and Cohen J.D. (1998). Anterior cingulate cortex, error detection, and the on-line monitoring of performance. *Science*; 280: 747-749.

Casey B.J., Cohen J.D., Jezzard P., Turner R., Noll D.C., Trainor R.J., Giedd J., Kaysen D., Hertz-Pannier L., and Rapoport J.L. (1995). Activation of prefrontal cortex in children during a nonspatial working memory task with functional MRI. *Neuroimage*; 2(3): 221229.

Chance S.A. (2014). The cortical microstructural basis of lateralized cognition: a review. *Frontiers in Psychology*; 5: 820.

Chandrasekar G., Vesterlund L., Hultenby K., Tapia-Paez I., and Kere J. (2013). The Zebrafish Orthologue of the Dyslexia Candidate Gene DYX1C1 Is Essential for Cilia Growth and Function. *PloS ONE*; 8(5): e63123.

Chapman N.H., Igo R.P., Thomson J.B., Matsushita M., Brkanac Z., Holzman T., Berninger V.W., Wijsman E.M., and Raskind W.H. (2004). Linkage analyses of four regions previously implicated in dyslexia: confirmation of a locus on chromosome 15q. *American Journal of Medical Genetics Part B: Neuropsychiatric Genetics*; 131(1): 67-75.

Chew S., Balasubramanian R., Chan W., Kang P.B., Andrews C., and Webb B.O. (2013). A novel syndrome caused by the E410K amino acid substitution in the neuronal β-tubulin isotype 3. *Brain*; 136: 522-35.

Chi J.G., Dooling E.C., and Gilles F.H. (1977a). Gyral development of the human brain. *Annals of Neurology*; 1: 86-93.

Chi J.G., Dooling E.C., and Gilles F.H. (1977b). Left-right asymmetries of the temporal speech areas of the human fetus. *Archives of Neurology;* 34: 346-348.

Chiang M.-C., Barysheva M., Shattuck D.W., Lee A.D., Madsen S.K., Avedissian C., Klunder A.D., Toga A.W., McMahon K.L., de Zubicaray G.I., Wright M.J., Srivastava A., Balov N., and Thompson P.M. (2009). Genetics of brain fiber architecture and intellectual performance. *The Journal of Neuroscience*; 29(7): 2212-2224.

Chiarello C., Lombardino L.J., Kacinik N.A., Otto R., Leonard C.M. (2006). Neuroanatomical and behavioral asymmetry in an adult compensated dyslexic. *Brain and Language*; 98: 169-181.

Chiarello C., Vazquez D., Felton A., and Leonard C.M. (2013). Structural asymmetry of anterior insula: behavioral correlates and individual differences. *Brain and Language*; 126: 109-122.

Christ A., Christa A., Kur E., Lioubinski O., Bachmann S., Willnow T.E., and Hammes A. (2012). LRP2 is an auxiliary SHH receptor required to condition the forebrain ventral midline for inductive signals. *Developmental Cell*; 22: 268-78.

Christopoulos G.I., Tobler P.N., Bossaerts P., Dolan R.J., and Schultz W. (2009). Neural Correlates of Value, Risk, and Risk Aversion Contributing to Decision Making under Risk. *The Journal of Neuroscience*; 29(40): 12574-12583.

Clarke J.M., and Zaidel E. (1994). Anatomical-behavioral relationships: corpus callosum morphometry and hemispheric specialization. *Behavioural Brain Research*; 64: 185-202.

Concha M.L., Burdine R.D., Russell C., Schier A.F., and Wilson S.W. (2000). A nodal signaling pathway regulates the laterality of neuroanatomical asymmetries in the zebrafish forebrain. *Neuron;* 28: 399-409.

Constam D.B., and Robertson E.J. (2000). SPC4/PACE4 regulates a TGFbeta signaling network during axis formation. *Genes & Development*; 14(9): 1146-55.

Cook N.D. (1984). Homotopic callosal inhibition. *Brain and Language*; 23: 116-125.

Cope N., Harold D., Hill G., Moskvina V., Stevenson J., Holmans P., Owen M.J., O'Donovan M.C., and Williams J. (2005). Strong Evidence That KIAA0319 on Chromosome 6p Is a Susceptibility Gene for Developmental Dyslexia. *The American Journal of Human Genetics*; 76(4): 581-591.

Coquelle F.M., Levy T., Bergmann S., Wolf S.G., Bar-El D., Sapir T., Brody Y., Orr I., Barkai N., Eichele G., and Reiner O. (2006). Common and divergent roles for members of the mouse DCX superfamily. *Cell Cycle;* 5: 976-983.

Corballis M.C. (2013). Early signs of brain asymmetry. *Trends in Cognitive Sciences*; 17: 554-555.

Coryell J.F., and Michel G.F. (1978). How supine postural preferences of infants can contribute toward the development of handedness. *Infant Behavior and Development*; 1: 245-257.

Coughlin E.M., Christensen E., Kunz P.L., Krishnamoorthy K.S., Walker V., Dennis N.R., Chalmers R.A., Elpeleg O.N., Whelan D., Pollitt R.J., Ramesh V., Mandell R., and Shih V.E. (1998). Molecular analysis and prenatal diagnosis of human fumarase deficiency. *Molecular Genetics and Metabolism*; 63: 254-62.

Coulson S., and Williams R.F. (2005). Hemispheric asymmetries and joke comprehension. *Neuropsychologia*; 43(1): 128-41.

Coulson S., and Wu Y.C. (2005). Right hemisphere activation of joke-related information: an event-related brain potential study. *Journal of Cognitive Neuroscience*; 17(3): 494-506.

Coulson S., Federmeier K.D., Van Petten C., and Kutas M.J. (2005). Right hemisphere sensitivity to word- and sentence-level context: evidence from event-related brain potentials. *Journal of Experimental Psychology. Learning, Memory and Cognition*; 31(1): 129-47.

Crosson B. (1985). Subcortical functions in language: A working model. *Brain and Language*; 25: 257-292.

Currier T.A., Etchegaray M.A., Haight J.L., Galaburda A.M., and Rosen G.D. (2011). The effects of embryonic knockdown of the candidate dyslexia susceptibility gene homologue Dyx1c1 on the distribution of GABAergic neurons in the cerebral cortex. *Neuroscience*; 172: 535-546.

Dale A.M., Liu A.K., Fischl B.R., Buckner R.L., Belliveau J.W., Lewine, J.D., and Halgren E. (2000). Dynamic statistical parametric mapping: Combining fMRI and MEG for high-resolution imaging of cortical activity. *Neuron*; 26: 55-67.

Dalby M., Elbro C., and Stødkilde-Jørgensen H. (1998). Temporal lobe asymmetry and dyslexia: an in vivo study using MRI. *Brain and Language;* 62: 51-69.

Dastot-Le Moal F., Wilson M., Mowat D., Collot N., Niel F., and Goossens M. (2007). ZFHX1B mutations in patients with Mowat-Wilson syndrome. *Human Mutation*; 28: 313-21.

David A.S., Wacharasindhu A., and Lishman W.A. (1993). Severe psychiatric disturbance and abnormalities of the corpus callosum: review and case series. *Journal of Neurology, Neurosurgery & Psychiatry;* 56: 85-93.

Davis E.E., and Katsanis N. (2012). The ciliopathies: a transitional model into systems biology of human genetic disease. *Current Opinion in Genetics & Development*; 22(3): 290-303.

Davy A., Bush J.O., and Soriano P. (2006). Inhibition of gap junction communication at ectopic Eph/ephrin boundaries underlies craniofrontonasal syndrome. *PLoS Biology*; 4: e315.

De Kovel C.G.F., Lisgo S.N., Fisher S.E., and Francks C. (2018). Subtle left-right asymmetry of gene expression profiles in embryonic and foetal human brains. *Scientific Reports;* 8: 12606.

DeFries J.C., Fulker D.W., and LaBuda M.C. (1987). Evidence for a genetic aetiology in reading disability of twins. *Nature*; 329(6139): 537-539.

De Witte L., Brouns R., Kavadias D., Engelborghs S., De Deyn P.P., and Marien P. (2011). Cognitive, affective and behavioural disturbances following vascular thalamic lesions: a review. *Cortex*; 47: 273-319.

Degreef G., Lantos G., Bogerts B., Ashtari M., and Lieberman J. (1992). Abnormalities of the septum pellucidum on MR scans in first-episode schizophrenia patients. *AJNR American Journal of Neuroradiology*; 13(3): 835-840.

Dehaene S., Posner M.I., and Tucker D.M. (1994). Localization of a Neural System for Error Detection and Compensation. *Psychological Science*; 5(5): 303-305.

Démonet J.-F., Taylor M.J., and Chaix Y. (2004). Developmental dyslexia. *The Lancet*; 363(9419): 1451-1460.

Den Braber A., Bohlken M., Brouwer R., Van ‘t Ent D., Kanai R., Kahn R.S., De Geus E.J., Hulshoff Pol H.E., and Boomsma D.I. (2013). Heritability of subcortical brain measures: a perspective for future genome-wide association studies. *Neuroimage*; 83: 98-102.

Deutsch G.K., Dougherty R.F., Bammer R., Siok W.T., Gabrieli J.D., and Wandell B. (2005). Children's reading performance is correlated with white matter structure measured by diffusion tensor imaging. *Cortex*; 41(3): 354-363.

Dos Santos Sequeira S., Woerner W., Walter C., Kreuder F., Lueken U., Westerhausen R., Wittling R.A., Schweiger E., and Wittling W. (2006). Handedness, dichotic-listening ear advantage, and gender effects on planum temporale asymmetry – a volumetric investigation using structural magnetic resonance imaging. *Neuropsychologia;* 44: 622-636.

Douaud G., Smith S., Jenkinson M., Behrens T., Johansen-Berg H., Vickers J., James S., Voets N., Watkins K., Matthews P.M., and James A. (2007). Anatomically related grey and white matter abnormalities in adolescent-onset schizophrenia. *Brain;* 130: 2375-2386.

Dronkers N.F., Wilkins D.P., Van Valin R.D., Redfern B.B., and Jaeger J.J. (2004). Lesion analysis of the brain areas involved in language comprehension. *Cognition*: 92(1–2): 145-177.

Duara R., Kusch A., Gross-Glenn K., Barker W.W., Jallad B., Pascal S., Loewenstein D.A., Sheldon J., Rabin M., Levin B., and Lubs H. (1991). Neuroanatomic differences between dyslexic and normal readers on magnetic resonance imaging scans. *Archives of Neurology*; 48: 410-416.

Dubois J., Dehaene-Lambertz G., Kulikova S., Poupon C., Hüppi P.S., and Hertz-Pannier L. (2014). The early development of brain white matter: A review of imaging studies in fetuses, newborns and infants. *Neuroscience*; 276(C): 48-71.

Dumontheil I., Roggeman C., Ziermans T., Peyrard-Janvid M., Matsson H., Kere J., and Klingberg T. (2011). Influence of the COMT Genotype on Working Memory and Brain Activity Changes During Development. *Biological Psychiatry*; 70(3): 222-229.

Dunsirn S., Smyser C., Liao S., Inder T., and Pineda R. (2016). Defining the nature and implications of head turn preference in the preterm infant. *Early Human Development*; 96: 53-60.

Eckert M.A., and Leonard C.M. (2000). Structural imaging in dyslexia: The planum temporale. *Mental Retardation and Developmental Disabilities Research Review*; 6: 198-206.

Eglinton E., and Annett M. (1994). Handedness and dyslexia: a meta-analysis. *Perceptual and Motor Skills*; 79(3 Pt 2): 1611-1616.

Eicher J.D., and Gruen J.R. (2013). Imaging-genetics in dyslexia: Connecting risk genetic variants to brain neuroimaging and ultimately to reading impairments. *Molecular Genetics and Metabolism*; 110(3): 201-212.

Eicher J.D., Powers N.R., Miller L.L., Mueller K.L., Mascheretti S., Marino C., Willcutt E.G., DeFries J.C., Olson R.K., Smith S.D., Pennington B.F., Tomblin J.B., Ring S.M., and Gruen J.R. (2014). Characterization of the DYX2 locus on chromosome 6p22 with reading disability, language impairment, and IQ. *Human Genetics*; 113 (7): 869-81.

Elekta Oy (2010). *Elekta Neuromag MaxFilter™ User's Guide Software version 2.2 October 2010.* Helsinki, Finland.

Entus A.K. (1980). Hemispheric asymmetry in processing of dichotically presented speech and nonspeech stimuli by infants. In S.J. Segalowitz and F.A. Gruber (Eds.), *Language development and neurological theory* (pp. 63-73). New York: Academic Press.

Evans A.C., and Brain Development Cooperative Group (2006). The NIH MRI study of normal brain development. *Neuroimage;* 30: 184-202.

Fahimeh D. (2014). *White matter connections: developmental neuroimaging studies of the associations between genes, brain and behavior*. PhD Thesis.

Falkenstein M., Hohnsbein J., Hoormann J., and Blanke L. (1991). Effects of crossmodal divided attention on late ERP components: II. Error processing in choice reaction tasks. *Electroencephalography & Clinical Neurophysiology*; 78(6): 447-455.

Falkenstein M., Hoormann J., Christ S., and Hohnsbein J. (2000). ERP components on reaction errors and their functional significance: a tutorial. *Biological Psychology*: 51(2-3): 87-107.

Federmeier K.D., and Kutas M. (1999). Right words and left words: Electrophysiological evidence for hemispheric differences in meaning processing. *Cognitive Brain Research*; 8: 373-392.

Federmeier K.D., Wlotko E.W., and Meyer A.M. (2008). What's "right" in language comprehension: ERPs reveal right hemisphere language capabilities. *Language and Linguistics Compass*; 2(1): 1-17.

Fedio P., and Van Buren J.M. (1975). Memory and perceptual deficits during electrical stimulation in the left and right thalamus and parietal subcortex. *Brain and Language*; 2: 78-100.

Fischer M.S., Ryan S.B., and Dobyns W.B. (1992). Mechanisms of interhemispheric transfer and patterns of cognitive function in acallosal patients of normal intelligence. *Archives of Neurology;* 49: 271-277.

Fisher S.E., and DeFries J.C. (2002). Developmental dyslexia: genetic dissection of a complex cognitive trait. *Nature Reviews: Neuroscience*; 3(10): 767-780.

Fletcher J.M., Lyon G.R., Fuchs L.S., and Barnes M.A. (2007). *Learning disabilities: From identification to intervention.* New York: Guilford Press.

Fonov V., Evans A., McKinstry R., Almli C., and Collins D. (2009). Unbiased nonlinear average age-appropriate brain templates from birth to adulthood. *Neuroimage;* 47 Suppl.1: S102.

Friederici A.D. (2002). Towards a neural basis of auditory sentence processing. *Trends in Cognitive Sciences*; 6(2): 78-84.

Friederici A.D., and Kotz S.A. (2003). The brain basis of syntactic processes: functional imaging and lesion studies. *Neuroimage;* 20 Suppl. 1: S8-17.

Frith C.D., Friston K., Herold S., Silbersweig D., Fletcher P., Cahill C., Dolan R.J., Frackowiak R.S., and Liddle P.F. (1995). Regional brain activity in chronic schizophrenic patients during the performance of a verbal fluency task. *The British Journal of Psychiatry*; 167(3): 343-349.

Gabel L.A., Gibson C.J., Gruen J.R., and LoTurco J.J. (2010). Progress towards a cellular neurobiology of reading disability. *Neurobiology of Disease*; 38(2): 173180.

Galaburda A., and Kemper T. (1979). Cytoarchitectonic abnormalities in developmental dyslexia: a case study. *Annals of Neurology;* 6:94-700.

Galaburda A.M., Sherman G.F., Rosen G.D., Aboitiz F., and Geschwind N. (1985). Developmental dyslexia: four consecutive patients with cortical anomalies. *Annals of Neurology*; 2: 222-33.

Galaburda A.M. (1989). Ordinary and extraordinary brain development: Anatomical variation in developmental dyslexia. *Annals of Dyslexia;* 39: 65-80.

Galaburda A.M., Rosen G.D., and Sherman G.F. (1990). Individual variability in cortical organization: its relationship to brain laterality and implications to function. *Neuropsychologia;* 28: 529–546.

Gathercole S.E., Pickering S.J., Ambridge B., and Wearing H. (2004). The structure of working memory from 4 to 15 years of age. *Developmental Psychology*; 40(2): 177.

Gathercole S.E., Alloway T.P., Willis C., and Adams A.-M. (2006). Working memory in children with reading disabilities. *Journal of Experimental Child Psychology*; 93(3): 265-281.

Gauger L.M., Lombardino L.J., and Leonard C.M. (1997). Brain morphology in children with specific language impairment. *Journal of Speech and Hearing Research*; 40(6): 1272-1284.

Gehring W.J., Goss B., Coles M.G.H., Meyer D.E., and Donchin E. (1993). A Neural System for Error Detection and Compensation. *Psychological Science*; 4(6): 385-390.

Gershon E., and Goldin L. (1986). Clinical methods in psychiatric genetics. I. Robustness of genetic marker investigative strategies. *Acta Psychiatrica Scandinavica*; 74(2): 113-118.

Gervain J., Macagno F., Cogoi S., Peña M., and Mehler J. (2008). The neonate brain detects speech structure. *Proceedings of the National Academy of Sciences of the United Stated of America*; 105: 14222-14227.

Giedd J.N., Blumenthal J., Jeffries N.O., Castellanos F.X., Liu H., Zijdenbos A., Paus T., Evans A.C., and Rapoport J.L. (1999). Brain development during childhood and adolescence: a longitudinal MRI study. *Nature Neuroscience*; 2(10): 861-863.

Giorgio A., Watkins K., Douaud G., James A., James S., De Stefano N., Matthews P.M., Smith S.M., and Johansen-Berg H. (2008). Changes in white matter microstructure during adolescence. *Neuroimage*; 39(1): 52-61.

Glahn D.C., Thompson P.M., and Blangero J. (2007). Neuroimaging endophenotypes: strategies for finding genes influencing brain structure and function. *Human Brain Mapping*; 28(6): 488-501.

Glahn D.C., and Blangero J. (2011). Why endophenotype development requires families. *Chinese Science Bulletin*; 56: 3382-3384.

Glahn D.C., Knowles E.E., McKay D.R., Sprooten E., Raventós H., Blangero J., Gottesman I., and Almasy L. (2014). Arguments for the Sake of Endophenotypes: Examining Common Misconceptions About the Use of Endophenotypes In Psychiatric Genetics. *American Journal of Medical Genetics. Part B, Neuropsychiatric Genetics: the official publication of the International Society of Psychiatric Genetics*; 0(2): 122-130.

Goddings A.-L., Mills K., Clasen L., Giedd J., Viner R., and Blakemore S.-J. (2014). Longitudinal MRI to assess effect of puberty on subcortical brain development: an observational study. *The Lancet*; 383: S52.

Goetz S.C., and Anderson K.V. (2010). The primary cilium: a signalling centre during vertebrate development. *Nature Reviews: Genetics*; 11: 331-344.

Gogtay N., Giedd J.N., Lusk L., Hayashi K.M., Greenstein D., Vaituzis A.C., Nugent T.F. 3rd, Herman D.H., Clasen L.S., Toga A.W., Rapoport J.L., and Thompson P.M. (2004). Dynamic mapping of human cortical development during childhood through early adulthood. *Proceedings of the National Academy of Sciences of the United States of America*; 101(21): 8174-8179.

Goldman A.L., Pezawas L., Mattay V.S., Fischl B., Verchinski B.A., Zoltick B., Weinberger D.R., and Meyer-Lindenberg A. (2008). Heritability of brain morphology related to schizophrenia: a large-scale automated magnetic resonance imaging segmentation study. *Biological Psychiatry*; 63: 475-483.

Good C.D., Johnsrude I.S., Ashburner J., Henson R.N., Friston K.J., and Frackowiak R.S. (2001). A voxel-based morphometric study of ageing in 465 normal adult human brains. *Neuroimage;* 14: 21-36.

Gottesman I.I., and Gould T.D. (2003). The endophenotype concept in psychiatry: etymology and strategic intentions. *The American Journal of Psychiatry*; 160(4): 636-45.

Gould T., and Gottesman I. (2006). Psychiatric endophenotypes and the development of valid animal models. *Genes, Brain, and Behavior*; 5(2): 113-119.

Greve D.N., Van der Haegen L., Cai Q., Stufflebeam S., Sabuncu M.R., Fischl B., and Brysbaert M. (2013). A surface-based analysis of language lateralization and cortical asymmetry. *Journal of Cognitive Neuroscience*; 25: 1477-1492.

Grey S.E., and Van Hell J.G. (2017). Foreign-accented speaker identity affects neural correlates of language comprehension. *Journal of Neurolinguistics*; 42: 93-108.

Grigorenko E.L., Wood F.B., Meyer M.S., and Pauls D.L. (2000). Chromosome 6p influences on different dyslexia-related cognitive processes: further confirmation. *The American Journal of Human Genetics*; 66(2): 715-723.

Güntürkün O., and Ocklenburg S. (2017). Ontogenesis of lateralization. *Neuron;* 94: 249–263.

Haag A., Moeller N., Knake S., Hermsen A., Oertel W.H., Rosenow F., and Hamer H.M. (2010). Language lateralization in children using functional transcranial Doppler sonography. *Developmental Medicine and Child Neurology;* 52: 331-336.

Habib M. (2000). The neurological basis of developmental dyslexia: an overview and working hypothesis. *Brain*; 123(12): 2373-99.

Habib M., and Giraud K. (2013). Dyslexia. *Handbook of Clinical Neurology;* 111: 229-235.

Hagoort P., Baggio G., and Willems R.M. (2009). Semantic unification. In M.S. Gazzaniga (Ed.), *The cognitive neurosciences*, 4th ed. (pp. 819-836). Cambridge, MA: MIT Press.

Hahne A., and Friederici A.D. (2002). Differential task effects on semantic and syntactic processes as revealed by ERPs. *Brain Research: Cognitive Brain Research;* 13(3): 339-56.

Hald L.A., Bastiaansen M.C.M., and Hagoort P. (2006). EEG theta and gamma responses to semantic violations in online sentence processing, *Brain and Language;* 96: 90-105.

Halgren E., Dhond R.P., Christensen N., Van Petten C., Marinkovic K., Lewine J.D., Dale A.M., and Simos P.G. (2002). N400-like magnetoencephalography responses modulated by semantic context, word frequency, and lexical class in sentences. *Neuroimage;* 17(3): 1101-16.

Hämäläinen M., Hari R., Ilmoniemi R.J., Knuutila J., and Lounasmaa O.V. (1993). Magnetoencephalography theory, instrumentation, and applications to noninvasive studies of the working human brain. *Reviews of Modern Physics;* 65(2): 413-497.

Hardan A.Y., Pabalan M., Gupta N., Bansal R., Melhem N.M., Fedorov S., Keshavan M.S., and Minshew N.J. (2009). Corpus callosum volume in children with autism. *Psychiatry Research;* 174(1): 57-61.

Haslam R.H.A., Dalby J.T., Johns R.D., and Rademaker A.W. (1981). Cerebral asymmetry in developmental dyslexia. *Archives of Neurology*; 38(11): 679-682.

Hebb A.O., and Ojemann G.A. (2013). The thalamus and language revisited. *Brain and Language*; 126 (1): 99-10.

Helenius P., Salmelin R., Service E., and Connolly J.F. (1998). Distinct time courses of word and context comprehension in the left temporal cortex. *Brain;* 121: 1133-1142.

Helenius P., Salmelin R., Service E., Connolly J.F., Leinonen S., and Lyytinen H. (2002). Cortical Activation during Spoken-Word Segmentation in Nonreading-Impaired and Dyslexic Adults. *The Journal of Neuroscience*; 22(7): 2936-2944.

Hepper P.G., Shahidullah S., and White R. (1990). Origins of fetal handedness. *Nature;* 347: 431.

Hepper P.G., Shahidullah S., and White R. (1991). Handedness in the human fetus. *Neuropsychologia;* 29: 1107-1111.

Hepper P.G., McCartney G.R., and Shannon E.A. (1998). Lateralised behaviour in first trimester human foetuses. *Neuropsychologia;* 36: 531-534.

Hepper P.G., Wells D.L., and Lynch C. (2005). Prenatal thumb sucking is related to postnatal handedness. *Neuropsychologia;* 43: 313-315.

Hering-Hanit R., Achiron R., Lipitz S., and Achiron A. (2001). Asymmetry of fetal cerebral hemispheres: in utero ultrasound study. *Archives of Disease in Childhood: Fetal and Neonatal Edition*; 85: F194-F196.

Hervé P.Y., Zago L., Petit L., Mazoyer B., and Tzourio-Mazoyer N. (2013). Revisiting human hemispheric specialization with neuroimaging. *Trends in Cognitive Sciences*; 17(2): 69-80.

Hier D.B., LeMay M., Rosenberger P.B., and Perlo V.P. (1978). Developmental dyslexia: evidence for a sub- group with a reversal of cerebral asymmetry. *Archives of Neurology;* 35(2): 90-92.

Higginbotham H., Eom T.Y., Mariani L.E., Bachleda A., Hirt J., Gukassyan V., Cusack C.L., Lai C., Caspary T., and Anton E.S. (2012). ARL13B in primary cilia regulates the migration and placement of interneurons in the developing cerebral cortex. *Developmental Cell;* 23(5): 925-938.

Hildebrandt F., Benzing T., and Katsanis N. (2011). Ciliopathies. *The New England Journal of Medicine;* 364: 1533-1543.

Hines M., Chiu L., McAdams L.A., Bentler P.M., and Lipcamon J. (1992). Cognition and the corpus callosum: verbal fluency, visuospatial ability, and language lateralization related to midsagittal surface areas of callosal subregions. *Behavioral Neuroscience;* 106: 3-14.

Hoenig K., Sim E-J., Bochev V., Herrnberger B., and Kiefer M. (2008). Conceptual flexibility in the human brain: dynamic recruitment of semantic maps from visual, motor, and motion-related areas. *Journal of Cognitive Neuroscience*; 20: 1799-1814.

Holcomb P.J., and Neville H.J. (1990). Auditory and Visual Semantic Priming in Lexical Decision: A Comparison Using Event-related Brain Potentials. *Language and Cognitive Processes*; 5(4): 281-312.

Holroyd C.B., Nieuwenhuis S., Yeung N., Nystrom L., Mars R.B., Coles M.G., and Cohen J.D. (2004). Dorsal anterior cingulate cortex shows fMRI response to internal and external error signals. *Nature Neuroscience;* 7(5): 497-8.

Humphries C., Binder J.R., Medler D.A., and Liebenthal E. (2007). Time course of semantic processes during sentence comprehension: an fMRI study, *Neuroimage;* 36(3): 924-932.

Hutchins G.M., and Moore G.W. (1988). Growth and asymmetry of the human liver during the embryonic period. *Pediatric Pathology*; 8: 17-24.

Huttenlocher P.R., and Dabholkar A.S. (1997). Regional differences in synaptogenesis in human cerebral cortex. *The Journal of Comparative Neurology;* 387(2): 167-178.

Hynd G.W., Semrud-Clikeman M., Lorys A.R., Novey E.S., and Eliopulos D. (1990). Brain morphology in developmental dyslexia and attention deficit disorder/hyperactivity. *Archives of Neurology*; 47: 919-926.

Ihara A., Hirata M., Fujimaki N., Goto T., Umekawa Y., Fujita N., Terazono Y., Matani A., Wei Q., Yoshimine T., Yorifuji S., and Murata T. (2010). Neuroimaging study on brain asymmetries in situs inversus totalis. *Journal of the Neurological Sciences;* 288(1-2): 72-78.

Illingworth S., and Bishop D.M. (2009). Atypical cerebral lateralisation in adults with compensated developmental dyslexia demonstrated using functional transcranial Doppler ultrasound; *Brain and Language*; 111(1): 61-65.

Imamura T., Yamadori A., Shiga Y., Sahara M., and Abiko H. (1994). Is disturbed transfer of learning in callosal agenesis due to a disconnection syndrome? *Behavioral Neurology;* 7: 43-48.

International Dyslexia Association (2002). Definition of Dyslexia, adopted by the IDA Board of Directors. https://dyslexiaida.org/definition-of-dyslexia/

Ito S., Stuphorn V., Brown J.W., and Schall J.D. (2003). Performance monitoring by the anterior cingulate cortex during saccade countermanding. *Science*; 302: 120-122.

Ivliev A.E., AC't Hoen P., van Roon-Mom W.M., Peters D.J., and Sergeeva M.G. (2012). Exploring the transcriptome of ciliated cells using in silico dissection of human tissues. *PloS ONE*; 7(4): e35618.

Jacob M.S., Ford J.M., Roach B.J., Calhoun V.D., and Mathalon D.H. (2019). Aberrant activity in conceptual networks underlies N400 deficits and unusual thoughts in schizophrenia. *Neuroimage: Clinical*; 24: 1-8.

Jamadar S., Powers N., Meda S., Gelernter J., Gruen J., and Pearlson G. (2011). Genetic influences of cortical gray matter in language-related regions in healthy controls and schizophrenia. *Schizophrenia Research*; 129(2): 141-148.

Jäncke L., and Steinmetz H. (1994). Interhemispheric transfer time and corpus callosum size. *Neuroreport;* 5: 2385-2388.

Jeannerod M. (2006). *Motor cognition: what action tells the self*. New York: Oxford University Press.

Jenkinson M., and Smith S. (2001). A global optimisation method for robust affine registration of brain images. *Medical Image Analysis*; 5: 143-56.

Jenkinson M., Bannister P., Brady M., and Smith S. (2002). Improved optimization for the robust and accurate linear registration and motion correction of brain images. *Neuroimage;* 17(2): 825-41.

Jernigan T.L., Hesselink J.R., Sowell E., and Tallal P.A. (1991). Cerebral structure on magnetic resonance imaging in language- and learning-impaired children. *Archives of Neurology*; 48: 539-545.

John B., and Lewis K.R. (1996). Chromosome variability and geographic distribution in insects. *Science*; 152(3723): 711-721.

Johnson M.D., and Ojemann G.A. (2000). The role of the human thalamus in language and memory: evidence from electrophysiological studies. *Brain and Cognition*; 42(2): 218-30.

Johnson J.M., Castle J., Garrett-Engele P., Kan Z., Loerch P.M., Armour C.D., Santos R., Schadt E.E., Stoughton R., and Shoemaker D.D. (2003). Genome-wide survey of human alternative pre-mRNA splicing with exon junction microarrays. *Science;* 302: 2141-2144.

Jonas S. (1982). The thalamus and aphasia, including transcortical aphasia: a review. *Journal of Communication Disorders*; *15*(1): 31-41.

Karlebach G., and Francks C. (2015). Lateralization of gene expression in human language cortex. *Cortex;* 67: 30-36.

Kasprian G., Langs G., Brugger P.C., Bittner M., Weber M., Arantes M., and Prayer D. (2011). The prenatal origin of hemispheric asymmetry: an in utero neuroimaging study. *Cerebral Cortex;* 21(5): 1076-1083.

Kathiriya I.S., and Srivastava D. (2000). Left-right asymmetry and cardiac looping: implications for cardiac development and congenital heart disease. *American Journal of Medical Genetics*; 97: 271-279.

Kaufman A.S. (1990). *Assessing adolescent and adult intelligence.* Allyn & Bacon.

Kennedy D.N., Haselgrove C., Hodge S.M., Rane P.S., Makris N., and Frazier J.A. (2012). CANDIShare: a resource for pediatric neuroimaging data. *Neuroinformatics*; 10(3): 319-22.

Kere J. (2014). The molecular genetics and neurobiology of developmental dyslexia as model of a complex phenotype*. Biochemical and Biophysical Research Communications*; 452: 236-243.

Kiehl K.A., Liddle P.F., and Hopfinger J.B. (2000). Error processing and the rostral anterior cingulate: An event-related fMRI study. *Psychophysiology*; 37: 216-223.

Kircher T., Sass K., Sachs O., and Krach S. (2009). Priming words with pictures: neural correlates of semantic associations in a cross-modal priming task using fMRI. *Human Brain Mapping*; 4116-4128

Kivilevitch Z., Achiron R., and Zalel Y. (2010). Fetal brain asymmetry: in utero sonographic study of normal fetuses. *American Journal of Obstetrics and Gynecology*; 202: 359.e1-359.e8.

Klein A., and Tourville J. (2012). 101 Labeled Brain Images and a Consistent Human Cortical Labeling Protocol. *Frontiers in Neuroscience*; 6: 171.

Klingberg T., Hedehus M., Temple E., Salz T., Gabrieli J.D., Moseley M.E., and Poldrack R.A. (2000). Microstructure of temporo-parietal white matter as a basis for reading ability: evidence from diffusion tensor magnetic resonance imaging. *Neuron*; 25(2): 493-500.

Klingberg T., Forssberg H., and Westerberg H. (2002). Increased brain activity in frontal and parietal cortex underlies the development of visuospatial working memory capacity during childhood. *Journal of Cognitive Neuroscience*; 14(1): 110.

Knecht S., Deppe M., Ebner A., Henningsen H., Huber T., Jokeit H., and Ringelstein E.B. (1998). Non-invasive determination of language lateralization by functional transcranial Doppler sonography: a comparison with the Wada test. *Stroke*; 29(1): 82-6.

Knecht S., Dräger B., Deppe M., Bobe L., Lohmann H., Flöel A., Ringelstein E.-B., and Henningsen H. (2000). Handedness and hemispheric language dominance in healthy humans. *Brain*; 123 (12): 2512-2518.

Kolb B., and Gibb R. (2011). Brain plasticity and behaviour in the developing brain. *Journal of the Canadian Academy of Child and Adolescent Psychiatry*; 20(4): 265.

Konishi Y., Mikawa H., and Suzuki J. (1986). Asymmetrical head-turning of preterm infants: Some effects on later postural and functional lateralities. *Developmental Medicine and Child Neurology*; 28: 450-457.

Koten J.W.Jr., Wood G., Hagoort P., Goebel R., Propping P., Willmes K., and Boomsma D.I. (2009). Genetic contribution to variation in cognitive function: an FMRI study in twins. *Science*; 323: 1737-1740.

Krack P., Poepping M., Weinert D., Schrader B., and Deuschl G. (2000). Thalamic, pallidal, or subthalamic surgery for Parkinson's disease? *Journal of Neurology*; 247: 122-134.

Kramer A.F., and Donchin E. (1987). Brain potentials as indices of orthographic and phonological interaction during word matching. *Journal of Experimental Psychology: Learning, Memory, and Cognition*; 13(1): 76-86.

Kraut M.A., Kremen S., Moo L.R., Segal J.B., Calhoun V., and Hart J.Jr. (2002). Object activation in semantic memory from visual multimodal feature input. *Journal of Cognitive Neuroscience*; *14*(1): 37-47.

Kraut M.A., Calhoun V., Pitcock J.A., Cusick C., and Hart J.Jr. (2003). Neural hybrid model of semantic object memory: implications from event-related timing using fMRI. *Journal of the International Neuropsychological Society: JINS*; *9*(7): 1031-1040.

Kronbichler M., Wimmer H., Staffen W., Hutzler F., Mair A., and Ladurner G. (2008). Developmental dyslexia: gray matter abnormalities in the occipitotemporal cortex. *Human Brain Mapping*; 29(5): 613-625.

Krugel L.K., Ehlen F., Tiedt H.O., Kühn A.A., and Klostermann F. (2014). Differential impact of thalamic versus subthalamic deep brain stimulation on lexical processing. *Neuropsychologia*; 63: 175-84.

Kuljic-Obradovic D.C. (2003). Subcortical aphasia: three different language disorder syndromes? *European Journal of Neurology*; 10: 445-448.

Kumamoto N., Gu Y., Wang J., Janoschka S., Takemaru K., Levine J., and Ge S. (2012). A role for primary cilia in glutamatergic synaptic integration of adult-born neurons. *Nature Neuroscience;* 15(3): 399-405.

Kurth F., Gaser C., and Luders E. (2015). A 12-step user guide for analyzing voxel-wise gray matter asymmetries in statistical parametric mapping (SPM). *Nature Protocols*; 10(2): 293-304.

Kushch A., Gross-Glenn K., Jallad B., Lubs H., Rabin M., Feldman E., and Duara R. (1993). Temporal lobe surface area measurements on MRI in normal and dyslexic readers. *Neuropsychologia;* 31(8): 811-821.

Kutas M., and Hillyard S.A. (1980). Reading senseless sentences: brain potentials reflect semantic incongruity. *Science;* 207(4427): 203-5.

Kutas M., and Hillyard S.A. (1982). The lateral distribution of event-related potentials during sentence processing. *Neuropsychologia*; 20: 579-590.

Kutas M., and Federmeier K.D. (2011). Thirty years and counting: finding meaning in the N400 component of the event-related brain potential (ERP). *Annual Review of Psychology*; 62: 621-47.

Kwon H., Kuriki S., Kim J. M., Lee Y. H., Kim K., and Nam K. (2005). Meg study on neural activities associated with syntactic and semantic violations in spoken korean sentences. *Neuroscience Research*; 51: 349-357.

Lacadie C.M., Fulbright R.K., Rajeevan N., Constable R.T., and Papademetris X. (2008). More accurate Talairach coordinates for neuroimaging using non-linear registration. *NeuroImage*; *42*(2): 717-725.

LaMantia A., and Rakic P. (1990). Axon overproduction and elimination in the corpus callosum of the developing rhesus monkey. *The Journal of Neuroscience*; 10(7): 2156-2175.

Larsen J.P., Høien T., Lundberg I., and Ødegaard H. (1990). MRI evaluation of the size and symmetry of the planum temporale in adolescents with developmental dyslexia. *Brain and Language*; 39(2): 289-301.

Lau E.F., Phillips C., and Poeppel D. (2008). A cortical network for semantics: (de)constructing the N400. *Nature Reviews: Neuroscience*; 9(12): 920-33.

Lauro L.J., Tettamanti M., Cappa S.F., and Papagno C. (2008). Idiom comprehension: A prefrontal task? *Cerebral Cortex*; 18: 162-170.

Lebel C., Walker L., Leemans A., Phillips L., and Beaulieu C. (2008). Microstructural maturation of the human brain from childhood to adulthood. *Neuroimage*; 40(3): 1044-1055.

Lebel C., and Beaulieu C. (2011). Longitudinal development of human brain wiring continues from childhood into adulthood. *The Journal of Neuroscience*; 31(30): 10937-10947.

Lebel C., Gee M., Camicioli R., Wieler M., Martin W., and Beaulieu C. (2012). Diffusion tensor imaging of white matter tract evolution over the lifespan. *Neuroimage*; 60(1): 340-352.

Leboyer M., Bellivier F., Nosten-Bertrand M., Jouvent R., Pauls D., and Mallet J. (1998). Psychiatric genetics: search for phenotypes. *Trends in Neurosciences*; 21(3): 102-105.

Lenox R.H., Gould T.D., and Manji H.K. (2002). Endophenotypes in bipolar disorder. *American Journal of Medical Genetics*; 114(4): 391-406.

Lenroot R.K., Gogtay N., Greenstein D.K., Wells E.M., Wallace G.L., Clasen L.S., Blumenthal J.D., Lerch J., Zijdenbos A.P., Evans A.C., Thompson P.M., and Giedd J.N. (2007). Sexual dimorphism of brain developmental trajectories during childhood and adolescence. *Neuroimage*; 36(4): 1065-1073.

Lenzenweger M.F. (2013). Endophenotype, Intermediate Phenotype, Biomarker: Definitions, Concept Comparisons, Clarifications. *Depression and Anxiety*; 30: 185-189.

Leonard C.M., Voeller K.K.S., Lombardino L.J., Morris M.K., Hynd G.W., Alexander A.W. Andersen H.G., Garofalakis M., Honeyman J.C., Mao J., Agee O.F., and Staab E.V. (1993). Anomalous cerebral structure in dyslexia revealed with MRI. *Archives of Neurology;* 50: 461-469.

Leonard C.M., and Eckert M.A. (2008). Asymmetry and dyslexia. *Developmental Neuropsychology*; 33: 663-681.

Levy J., and Trevarthen C. (1977). Perceptual, semantic, and phonetic aspects of elementary language processes in split-brain patients*. Brain;* 100: 105-118.

Lewis S.W., Reveley M.A., David A.S., and Ron M.A. (1988). Agenesis of the corpus callosum and schizophrenia: a case report. *Psychological Medicine;* 18: 341-347.

López-Bendito G., Flames N., Ma L., Fouquet C., Di Meglio T., Chedotal A., Tessier-Lavigne M., and Marín O. (2007). Robo1 and Robo2 cooperate to control the guidance of major axonal tracts in the mammalian forebrain*. The Journal of Neuroscience*; 27(13): 3395-3407.

Luciana M., and Nelson C.A. (1998). The functional emergence of prefrontally-guided working memory systems in four-to eight-year-old children. *Neuropsychologia*; 36(3): 273-293.

Luders E., Toga A.W., and Thompson P.M. (2014). Why size matters: differences in brain volume account for apparent sex differences in callosal anatomy: the sexual dimorphism of the corpus callosum. *Neuroimage*; 84: 820-4.

Lyon G.R. (2003). Reading disabilities: Why do some children have difficulty learning to read? What can be done about it. *Perspectives*; 29(2): 17-19.

Maess B., Herrmann C.S., Hahne A., Nakamura A., and Friederici A.D. (2006). Localizing the distributed language network responsible for the N400 measured by MEG during auditory sentence processing. *Brain Research;* 1096(1): 163-172.

Mahmoudzadeh M., Dehaene-Lambertz G., Fournier M., Kongolo G., Goudjil S., Dubois J., Grebe R., and Wallois F. (2013). Syllabic discrimination in premature human infants prior to complete formation of cortical layers. *Proceedings of the National Academy of Sciences of the United States of America;* 110: 4846-4851.

Maris E., and Oostenveld R. (2007). Nonparametric statistical testing of EEG- and MEG-data. *Journal of Neuroscience Methods*; 164(1): 177-90.

Marshall W.F., and Nonaka S. (2006). Cilia: tuning in to the cell's antenna. *Current Biology*; 16(15): R604-R614.

Massinen S., Tammimies K., Tapia-Páez I., Matsson H., Hokkanen M.-E., Söderberg O., Landegren U., Castrén E., Gustafsson J.A., Treuter E., and Kere J. (2009). Functional interaction of *DYX1C1* with estrogen receptors suggests involvement of hormonal pathways in dyslexia. *Human Molecular Genetics*; 18(15): 2802-2812.

Massinen S., Hokkanen M.-E., Matsson H., Tammimies K., Tapia-Páez I., Dahlström-Heuser V., Kuja-Panula J., Burghoorn J., Jeppsson K.E., Swoboda P., Peyrard-Janvid M., Toftgård R., Castrén E., and Kere J. (2011). Increased expression of the dyslexia candidate gene DCDC2 affects length and signaling of primary cilia in neurons. *PloS ONE*; 6(6): e20580.

Matsumoto A., Iidaka T., Haneda K., Okada T., and Sadato N. (2005). Linking semantic priming effect in functional MRI and event-related potentials, *Neuroimage*; 24: 624-634.

Matthews S.C., Simmons A.N., Strigo I., Jang K., Stein M.B., and Paulus M.P. (2007). Heritability of anterior cingulate response to conflict: an fMRI study in female twins. *Neuroimage*; 38: 223-227.

McCandliss B.D., Cohen L., and Dehaene S. (2003). The visual word form area: expertise for reading in the fusiform gyrus. *Trends in Cognitive Sciences*; 7(7): 293-299.

McCartney G., and Hepper P. (1999). Development of lateralized behaviour in the human fetus from 12 to 27 weeks' gestation. *Developmental Medicine and Child Neurology*; 41: 83-86.

McGrath L.M., Smith S.D., and Pennington B.F. (2006). Breakthroughs in the search for dyslexia candidate genes. *Trends in Molecular Medicine*; 12(7): 333-341.

McManus I.C. (1985). Handedness, language dominance and aphasia: a genetic model. *Psychological Medicine: Monograph Supplement*; 8: 1-40.

Mechelli A., Josephs O., Lambon Ralph M.A., McClelland J.L., and Price C.J. (2007). Dissociating stimulus-driven semantic and phonological effect during reading and naming. *Human Brain Mapping*; *28*(3): 205-217.

Meda S.A., Gelernter J., Gruen J.R., Calhoun V.D., Meng H., Cope N.A., and Pearlson G.D. (2008). Polymorphism of DCDC2 reveals differences in cortical morphology of healthy individuals - a preliminary voxel based morphometry study. *Brain Imaging and Behaviour*; 2(1): 21-26.

Meng H., Smith S.D., Hager K., Held M., Liu J., Olson R.K., Pennington B.F., DeFries J.C., Gelernter J., O'Reilly-Pol T., Somlo S., Skudlarski P., Shaywitz S.E., Shaywitz B.A., Marchione K., Wang Y., Paramasivam M., LoTurco J.J., Page G.P., and Gruen J.R. (2005). DCDC2 is associated with reading disability and modulates neuronal development in the brain. *Proceedings of the National Academy of Sciences of the United States of America*; 102(47): 17053-17058.

Meno C., Takeuchi J., Sakuma R., Koshiba-Takeuchi K., Ohishi S., Saijoh Y., Miyazaki J., ten Dijke P., Ogura T., and Hamada H. (2001). Diffusion of nodal signaling activity in the absence of the feedback inhibitor Lefty2. *Developmental Cell;* 1(1): 127-138.

Menon V., Adleman N.E., White C.D., Glover G.H., and Reiss A.L. (2001). Error-related brain activation during a Go/NoGo response inhibition task. *Human Brain Mapping*; 12(3): 131-43.

Meyer-Lindenberg A., and Weinberger D.R. (2006). Intermediate phenotypes and genetic mechanisms of psychiatric disorders. *Nature Reviews: Neuroscience*; 7(10): 818-27.

Michel G.F. (1981). Right-handedness: a consequence of infant supine head-orientation preference? *Science;* 212: 685-687.

Minagawa-Kawai Y., Cristià A., and Dupoux E. (2011). Cerebral lateralization and early speech acquisition: a developmental scenario. *Developmental Cognitive Neuroscience*; 1: 217–232.

Modat M., Ridgway G.R., Taylor Z.A., Lehmann M., Barnes J., Hawkes D.J., Fox N.C., and Ourselin S. (2010). Fast free-form deformation using graphics processing units. *Computer Methods and Programs in Biomedicine*; 98(3): 278-284.

Moffat S.D., Hampson E., and Lee D.H. (1998). Morphology of the planum temporale and corpus callosum in left handers with evidence of left and right hemisphere speech representation. *Brain;* 121: 2369-2379.

Muntané G., Santpere G., Verendeev A., Seeley W.W., Jacobs B., Hopkins W.D., Navarro A., and Sherwood C.C. (2017). Interhemispheric gene expression differences in the cerebral cortex of humans and macaque monkeys. *Brain Structure & Function*; 222(7): 3241-3254.

Nadeau S.E., and Crosson B. (1997). Subcortical aphasia. *Brain and Language*; 58(3): 355-402, 418-23.

Nagy Z., Westerberg H., and Klingberg T. (2004). Maturation of white matter is associated with the development of cognitive functions during childhood. *Journal of Cognitive Neuroscience*; 16(7): 1227-1233.

Neville H.J., Mills D.L., and Lawson D.S. (1992). Fractionating language: different neural subsystems with different sensitive periods. *Cerebral Cortex*; 2(3): 244-58.

Nichols T.E., and Holmes A.P. (2002). Nonparametric permutation tests for functional neuroimaging: a primer with examples. *Human Brain Mapping*; 15: 1-25.

Niogi S.N., and McCandliss B.D. (2006). Left lateralized white matter microstructure accounts for individual differences in reading ability and disability. *Neuropsychologia*; 44(11): 2178-2188.

Nishio Y., Hashimoto M., Ishii K., and Mori E. (2011). Neuroanatomy of a neurobehavioral disturbance in the left anterior thalamic infarction, *The Journal of Neurology, Neurosurgery, and Psychiatry*; 82: 1195-1200.

Nobre A.C., Allison T., and McCarthy G. (1994). Word recognition in the human inferior temporal lobe. *Nature;* 372: 260-263

Nolte G. (2003). The magnetic lead field theorem in the quasi-static approximation and its use for magnetoencephalography forward calculation in realistic volume conductors. *Physics in Medicine and Biology*; 48(22): 3637-52.

Noonan K.A., Jefferies E., Visser M., and Ralph M.A.L. (2013). Going beyond inferior prefrontal involvement in semantic control: evidence for the additional contribution of dorsal angular gyrus and posterior middle temporal cortex. *Journal of Cognitive Neuroscience*; 25(11): 1824-1850.

Nopola-Hemmi J., Taipale M., Haltia T., Lehesjoki A.-E., Voutilainen A., and Kere J. (2000). Two translocations of chromosome 15q associated with dyslexia. *Journal of Medical Genetics*; 37(10): 771-775.

Noppeney U., Josephs O., Hocking J., Price C.J., and Friston K.J. (2008). The effect of prior visual information on recognition of speech and sounds. *Cerebral Cortex;* 18: 598-609.

Nowicka A., and Tacikowski P. (2011). Transcallosal transfer of information and functional asymmetry of the human brain. *Laterality;* 16: 35-74.

Ocklenburg S., and Güntürkün O. (2009). Head-turning asymmetries during kissing and their association with lateral preference. *Laterality;* 14: 79-85.

Ocklenburg S., Westerhausen R., Hirnstein M., and Hugdahl K. (2013). Auditory hallucinations and reduced language lateralization in schizophrenia: a meta-analysis of dichotic listening studies. *Journal of the International Neuropsychological Society: JINS;* 19: 410-418.

Ocklenburg S., Friedrich P., Güntürkün O., and Genç E. (2016). Intrahemispheric white matter asymmetries: the missing link between brain structure and functional lateralization? *Reviews in the Neurosciences*; 27: 465-480.

Ocklenburg S., Schmitz J., Moinfar Z., Moser D., Klose R., Lor S., Kunz G., Tegenthoff M., Faustmann P., Francks C., Epplen J.T, Kumsta R., and Güntürkün O. (2017). Epigenetic regulation of lateralized fetal spinal gene expression underlies hemispheric asymmetries. *eLife*; 6: e22784.

Oldfield R.C. (1971). The assessment and analysis of handedness: the Edinburgh inventory. *Neuropsychologia;* 9: 97-113.

Olesen P.J., Nagy Z., Westerberg H., and Klingberg T. (2003). Combined analysis of DTI and fMRI data reveals a joint maturation of white and grey matter in a fronto-parietal network. *Cognitive Brain Research*; 18(1): 48-57.

Olichney J.M., Van Petten C., Paller K.A., Salmon D.P., Iragui V.J., and Kutas M. (2000). Word repetition in amnesia. Electrophysiological measures of impaired and spared memory. *Brain*; 123: 1948-1963.

Ojemann G.A. (1975). Language and the thalamus: object naming and recall during and after thalamic stimulation. *Brain and Language*; 2: 101-120.

Ojemann G.A. (1976). Subcortical language mechanisms. In H. Whitaker and H.A. Whitaker (Eds.), *Studies in neurolinguistics* (Vol. 1: pp. 103-138). New York: Academic Press.

Ojemann G.A. (1983). Brain organization for language from the perspective of electrical-stimulation mapping. *Behavioral and Brain Sciences*; 6: 189-206.

Oostenveld R., Fries P., Maris E., and Schoffelen J-M. (2011). FieldTrip: Open Source Software for Advanced Analysis of MEG, EEG, and Invasive Electrophysiological Data. *Computational Intelligence and Neuroscience*; 2011:156869.

Orton S.T. (1925). “Word-blindness” in school children. *Archives of Neurology and Psychiatry*; 14: 581-615.

Osbun N., Li J., O'Driscoll M.C., Strominger Z., Wakahiro M., Rider E., Bukshpun P., Boland E., Spurrell C.H., Schackwitz W., Pennacchio L.A., Dobyns W.B., Black G.C., and Sherr E.H. (2011). Genetic and functional analyses identify DISC1 as a novel callosal agenesis candidate gene. *American Journal of Medical Genetics: Part A*; 155A(8): 1865-76.

Østby Y., Tamnes C.K., Fjell A.M., and Walhovd K. B. (2011). Morphometry and connectivity of the fronto-parietal verbal working memory network in development. *Neuropsychologia*; 49(14): 3854-3862.

Ourselin S., Roche A., Prima S., and Ayache N. (2000). Block Matching: A General Framework to Improve Robustness of Rigid Registration of Medical Images. In S.L Delp, A.M. DiGioia, B. Jaramaz (Eds.), *Medical Image Computing and Computer-Assisted Intervention 2000 (*LNCS 1935: pp. 557-566). Springer-Verlag Berlin Heidelberg.

Pal D.K., and Strug L.J. (2014). The genetics of common epilepsies: common or distinct? *Lancet Neurology*; 13: 859–860.

Panizzon M.S., Fennema-Notestine C., Eyler L.T., Jernigan T.L., Prom-Wormley E., Neale M., Jacobson K., Lyons M.J., Grant M.D., Franz C.E., Xian H., Tsuang M., Fischl B., Seidman L., Dale A., and Kremen W.S. (2009). Distinct genetic influences on cortical surface area and cortical thickness. *Cerebral Cortex*; 19(11): 2728-35.

Papanicolaou A.C., Simos P.G., Breier J.I., Fletcher J.M., Foorman B.R., Francis D., Castillo E.M., and Davis R.N. (2003). Brain mechanisms for reading in children with and without dyslexia: a review of studies of normal development and plasticity. *Developmental Neuropsychology*; 24(2-3): 593-612.

Paracchini S., Thomas A., Castro S., Lai C., Paramasivam M., Wang Y., Keating B.J., Taylor J.M., Hacking D.F., Scerri T., Francks C., Richardson A.J., Wade-Martins R., Stein J.F., Knight J.C., Copp A.J., LoTurco J., and Monaco A.P. (2006). The chromosome 6p22 haplotype associated with dyslexia reduces the expression of *KIAA0319*, a novel gene involved in neuronal migration. *Human Molecular Genetics*; 15(10): 1659-1666.

Parma V., Brasselet R., Zoia S., Bulgheroni M., and Castiello U. (2017). The origin of human handedness and its role in pre-birth motor control. *Scientific Reports*; 7: 16804.

Park H.R., Badzakova-Trajkov G., and Waldie K.E. (2012). Brain activity in bilingual developmental dyslexia: an fMRI study. *Neurocase*; 18(4): 286-297.

Pasteur L. (1883). La dissymétrie moléculaire. Conference of the Société chimique de Paris, reported in *Oeuvres Complètes* (Vol. 1: pp. 369-380). Paris: Masson, 1922.

Patterson K., and Besner D. (1984). Is the right hemisphere literate? *Cognitive Neuropsychology*; 1(4): 315-341.

Paul L.K., Van Lancker-Sidtis D., Schieffer B., Dietrich R., and Brown W.S. (2003). Communicative deficits in agenesis of the corpus callosum: nonliteral language and affective prosody. *Brain and Language;* 85: 313-324.

Paulesu E., Démonet J.-F., Fazio F., McCrory E., Chanoine V., Brunswick N., Cappa S.F., Cossu G., Habib M., Frith C.D., and Frith U. (2001). Dyslexia: cultural diversity and biological unity. *Science*; 291(5511): 2165-2167.

Paus T., Zijdenbos A., Worsley K., Collins D.L., Blumenthal J., Giedd J.N., Rapoport J.L., and Evans A.C. (1999). Structural maturation of neural pathways in children and adolescents: in vivo study. *Science*; 283(5409): 1908-1911.

Paus T. (2010). Growth of white matter in the adolescent brain: myelin or axon? *Brain and Cognition*; 72(1): 26-35.

Pearson J.M., Heilbronner S.R., Barack D.L., Hayden B.Y., and Platt M.L. (2011). Posterior cingulate cortex: adapting behavior to a changing world. *Trends in Cognitive Sciences*; 15(4):143-51.

Peña M., Maki A., Kovacić D., Dehaene-Lambertz G., Koizumi H., Bouquet F., and Mehler J. (2003). Sounds and silence: an optical topography study of language recognition at birth. *Proceedings of the National Academy of Sciences of the United States of America;* 100: 11702-11705.

Peper J.S., Brouwer R.M., Boomsma D.I., Kahn R.S., and Hulshoff Pol H.E. (2007). Genetic influences on human brain structure: a review of brain imaging studies in twins. *Human Brain Mapping*; 28: 464-473.

Peschansky V.J., Burbridge T.J., Volz A.J., Fiondella C., Wissner-Gross Z., Galaburda A.M., LoTurco J.J., and Rosen G.D. (2010). The effect of variation in expression of the candidate dyslexia susceptibility gene homolog Kiaa0319 on neuronal migration and dendritic morphology in the rat. *Cerebral Cortex*; 20(4): 884897.

Petretto D.R., and Masala C. (2017). Dyslexia and Specific Learning Disorders: New International Diagnostic Criteria. *Journal of Childhood & Developmental Disorders;* 3(4): 19.

Pfefferbaum A., Mathalon D.H., Sullivan E.V., Rawles J.M., Zipursky R.B., and Lim K.O. (1994). A quantitative magnetic resonance imaging study of changes in brain morphology from infancy to late adulthood. *Archives of Neurology*; 51(9): 874-887.

Pfefferbaum A., Sullivan E.V., and Carmelli D. (2001). Genetic regulation of regional microstructure of the corpus callosum in late life. *Neuroreport;* 12(8): 16771681.

Phan T.V., Sima D.M., Beelen C., Vanderauwera J., Smeets D., and Vandermosten M. (2018). Evaluation of methods for volumetric analysis of pediatric brain data: The childmetrix pipeline versus adult-based approaches. *Neuroimage: Clinical*; 19: 734-744.

Piedra M.E., Icardo J.M., Albajar M., Rodriguez-Rey J.C., and Ros M.A. (1998). Pitx2 participates in the late phase of the pathway controlling left-right asymmetry. *Cell*; 94: 319-324.

Plante E. (1991). MRI findings in the parents and siblings of specifically language-impaired boys. *Brain and Language*; 41(1): 67-80.

Pol H.E.H., Schnack H.G., Posthuma D., Mandl R.C., Baaré W.F., Van Oel C., Van Haren N.E., Collins D.L., Evans A.C., Amunts K., Bürgel U., Zilles K., De Geus E., Boomsma D.I., and Kahn R.S. (2006). Genetic contributions to human brain morphology and intelligence. *The Journal of Neuroscience*; 26(40): 10235-10242.

Polk T.A., Park J., Smith M.R., and Park D.C. (2007). Nature versus nurture in ventral visual cortex: a functional magnetic resonance imaging study of twins. *The Journal of Neuroscience*; 27: 13921-13925.

Polli F.E., Barton J.J.S., Cain MS., Thakkar C.N., Rauch S.L., and Manoach D.S. (2005). Rostral and dorsal anterior cingulate cortex make dissociable contributions during antisaccade error commission. *Proceedings of the National Academy of Sciences*; 102 (43): 15700-15705.

Posthuma D., De Geus E., Neale M., Pol H.H., Baare W., Kahn R., and Boomsma D. (2000). Multivariate genetic analysis of brain structure in an extended twin design. *Behavior Genetics*; 30(4): 311-319.

Postle B.R., Zarahn E., and D'Esposito M. (2000). Using event-related fMRI to assess delay-period activity during performance of spatial and nonspatial working memory tasks. *Brain Research Protocols*; 5(1): 57-66.

Prasad K.M., and Keshavan M. (2008). Structural Cerebral Variations as Useful Endophenotypes in Schizophrenia: Do They Help Construct "Extended Endophenotypes"? *Schizophrenia Bulletin*; 34(4): 774-90.

Price C.J., Moore C., Humphreys G., and Wise R. (1997). Segregating semantic from phonological processes during reading. *Journal of Cognitive Neuroscience*; 9(6): 727-733.

Raghavan M., Li Z., Carlson C., Anderson C.T., Stout J., Sabsevitz D.S., Swanson S.J., and Binder J.R. (2017). MEG language lateralization in partial epilepsy using dSPM of auditory event-related fields. *Epilepsy & Behavior: E&B*; *73*: 247-255.

Rankin C.T., Bunton T., Lawler A.M., and Lee S.J. (2000). Regulation of left-right patterning in mice by growth/differentiation factor-1. *Nature Genetics*; 24: 262–265.

Rasmussen T., and Milner B. (1975). Clinical and Surgical Studies of the Cerebral Speech Area in Man. In K.J. Zülch, O.D. Creutzfeldt, G.C. Galbraith (Eds.), *Cerebral Localization* (pp. 238-257). Springer Verlag; New York.

Reissmann E., Jörnvall H., Blokzijl A., Andersson O., Chang C., Minchiotti G., Persico M.G., Ibáñez C.F., and Brivanlou A.H. (2001). The orphan receptor ALK7 and the Activin receptor ALK4 mediate signaling by Nodal proteins during vertebrate development. *Genes & Development*; 15: 2010-2022.

Richlan F., Kronbichler M., and Wimmer H. (2011). Meta-analyzing brain dysfunctions in dyslexic children and adults. *Neuroimage*; 56(3): 1735-1742.

Ringo J.L., Doty R.W., Demeter S., and Simard P.Y. (1994). Time is of the essence: a conjecture that hemispheric specialization arises from interhemispheric conduction delay. *Cerebral Cortex;* 4: 331-343.

Rodd J.M., Davis M.H., and Johnsrude I.S. (2005). The Neural Mechanisms of Speech Comprehension: fMRI studies of Semantic Ambiguity. *Cerebral Cortex*; 15 (8): 1261-1269.

Rodel M., Dudley J.G., and Bourdeau M. (1983). Hemispheric differences for semantically and phonologically primed nouns: A tachistoscopic study in normal. *Perception & Psychophysics*; 34 (6): 523-531.

Rorden C., Karnath H.O., and Bonilha L. (2007). Improving lesion-symptom mapping. *Journal of Cognitive Neuroscience*; 19: 1081-1088.

Rueckert D., Sonoda L.I., Hayes C., Hill D.L., Leach M.O., and Hawkes D.J. (1999). Nonrigid registration using free-form deformations: application to breast MR images. *IEEE Transactions on Medical Imaging*; 18(8): 712-21.

Rugg M.D. (1984). Event-related potentials and the phonological processing of words and non-words. *Neuropsychologia*; 22(4): 435-443.

Rumsey J.M., Dorwart R., Vermess M., Denckla M.B., Kruesi M.J., and Rapoport J.L. (1986). Magnetic resonance imaging of brain anat- omy in severe developmental dyslexia. *Archives of Neurology*; 43(10):1045-1046.

Rumsey J.M., Donohue B.C., Brady D.R., Nace K., Giedd J.N., Andreason P. (1997). A magnetic resonance imaging study of planum temporale asymmetry in men with developmental dyslexia. *Archives of Neurology*; 54(12): 1481-1489.

Saran J. (1982). The thalamus and aphasia, including transcortical aphasia: a review. The *Journal of Communication Disorders*; 15: 31-41.

Slotnick S.D., Moo L.R., Kraut M.A., Lesser R.P., and Hart J.Jr. (2002). Interactions between thalamic and cortical rhythms during semantic memory recall in human. *Proceedings of the National Academy of Sciences of the United States of America*; 99: 6440-6443.

Sacco S., Moutard M-L., and Fagard J. (2006). Agenesis of the corpus callosum and the establishment of handedness. *Developmental Psychobiology*; 48: 472-481.

Sakuma R., Ohnishi Yi Y., Meno C., Fujii H., Juan H., Takeuchi J., Ogura T., Li E., Miyazono K., and Hamada H. (2002). Inhibition of Nodal signalling by Lefty mediated through interaction with common receptors and efficient diffusion. *Genes to Cells;* 7(4): 401-412.

Salmelin R., Service E., Kiesila P., Uutela K., and Salonen O. (1996). Impaired visual word processing in dyslexia revealed with magnetoencephalography. *Annals of Neurology*; 40: 157-162.

Sarkari S., Simos P.G., Fletcher J.M., Castillo E.M., Breier J.I., and Papanicolaou A.C. (2002). Contributions of magnetic source imaging to the understanding of dyslexia. *Seminars in Pediatric Neurology*; 9: 229-238.

Scerri T.S., Brandler W.M., Paracchini S., Morris A.P., Ring S.M., Richardson A.J., Talcott J.B., Stein J., and Monaco A.P. (2011). PCSK6 is associated with handedness in individuals with dyslexia. *Human Molecular Genetics;* 20(3): 608-614.

Scheffers M.K., Coles M.G.H., Bernstein P., Gehring W. J., and Donchin E. (1996). Event-related potentials and error-related processing: An analysis of incorrect responses to go and no-go stimuli. *Psychophysiology*; 33: 42-53.

Schmithorst V.J., Wilke M., Dardzinski B.J., and Holland S.K. (2002). Correlation of white matter diffusivity and anisotropy with age during childhood and adolescence: a cross-sectional diffusion-tensor MR imaging study. *Radiology*; 222(1): 212.

Schmitt J.E., Eyler L.T., Giedd J.N., Kremen W.S., Kendler K.S., and Neale M.C. (2007). Review of twin and family studies on neuroanatomic phenotypes and typical neurodevelopment. *Twin Research and Human Genetics*; 10(05): 683694.

Schmitz J., Lor S., Klose R., Güntürkün O., and Ocklenburg, S. (2017). The functional genetics of handedness and language lateralization: insights from gene ontology, pathway and disease association analyses. *Frontiers in Psychology*; 8: 1144.

Schmitz J., Güntürkün O., and Ocklenburg S. (2019). Building an Asymmetrical Brain: The Molecular Perspective. *Frontiers in Psychology*; 10: 982.

Schulte-Körne G., Ziegler A., Deimel W., Schumacher J., Plume E., Bachmann C., Kleensang A., Propping P., Nöthen M.M., Warnke A., Remschmidt H., and König I.R. (2007).

Interrelationship and familiality of dyslexia related quantitative measures. *Annals of Human Genetics*; 71(2): 160-175.

Schulte-Körne G. (2014). Specific learning disabilities from DSM-IV to DSM-5. *Zeitschrift für Kinder- und Jugendpsychiatrie und Psychotherapie;* 42: 369-372.

Schultz R.T., Cho N.K., Staib L.H., Kier L.E., Fletcher J.M., and Shaywitz S.E. (1994). Brain morphology in normal and dyslexic children. The influence of sex and age. *Annals of Neurol*ogy; 35(6): 732-742.

Schumacher J., Anthoni H., Dahdouh F., König I.R., Hillmer A.M., Kluck N., Manthey M., Plume E., Warnke A., Remschmidt H., Hülsmann J., Cichon S., Lindgren C.M., Propping P., Zucchelli M., Ziegler A., Peyrard-Janvid M., Schulte-Körne G., Nöthen M.M., and Kere J. (2006). Strong genetic evidence of DCDC2 as a susceptibility gene for dyslexia. *The American Journal of Human Genetics;* 78(1): 52-62.

Schuurman P.R., Bosch D.A., Bossuyt P.M., Bonsel G.J., van Someren E.J., De Bie R.M., Merkus M.P., and Speelman J.D. (2000). A comparison of continuous thalamic stimulation and thalamotomy for suppression of severe tremor. *The New England Journal of Medicine*; 342(7): 461-8.

Service E., Helenius P., Maury S., and Salmelin R. (2007). Localization of syntactic and semantic brain responses using magnetoencephalography. *Journal of Cognitive Neuroscience;* 19: 1193-1205.

Shapleske J., Rossell S.L., Woodruff P.W., and David A.S. (1999). The planum temporale: a systematic, quantitative review of its structural, functional and clinical significance. *Brain Research Reviews*.; 29(1): 26-49.

Shaw P., Kabani N.J., Lerch J.P., Eckstrand K., Lenroot R., Gogtay N., Greenstein D., Clasen L., Evans A., Rapoport J.L., Giedd J.N., and Wise S.P. (2008). Neurodevelopmental trajectories of the human cerebral cortex. *The Journal of Neuroscience;* 28(14): 3586-3594.

Shaywitz S.E., Shaywitz B.A., Fletcher J.M., and Escobar M.D. (1990). Prevalence of reading disability in boys and girls. *JAMA: the journal of the American Medical Association*; 264(8): 998-1002.

Shaywitz S.E., Escobar M.D., Shaywitz B.A., Fletcher J.M., and Makuch R. (1992). Evidence that dyslexia may represent the lower tail of a normal distribution of reading ability. *The New England Journal of Medicine*; 326(3): 145150.

Shaywitz B.A., Shaywltz S.E., Pugh K.R., Constable R.T., Skudlarski P., Fulbright R.K., Bronen R.A., Fletcher J.M., Shankweiler D.P., Katz L., and Gore J.C. (1995). Sex differences in the functional organization of the brain for language. *Nature*; 373(6515): 607-9.

Shaywitz B.A., Shaywitz S.E., Pugh K.R., Mencl W.E., Fulbright R.K., Skudlarski P., Constable R.T., Marchione K.E., Fletcher J.M., Lyon G.R., and Gore J.C. (2002). Disruption of posterior brain systems for reading in children with developmental dyslexia. *Biological Psychiatry*; 52(2): 101-110.

Shaywitz B.A., Shaywitz S.E., Blachman B.A., Pugh K.R., Fulbright R.K., Skudlarski P., Mencl W.E., Constable R.T., Holahan J.M., Marchione K.E., Fletcher J.M., Lyon G.R., and Gore J.C. (2004). Development of left occipitotemporal systems for skilled reading in children after a phonologicallybased intervention. *Biological Psychiatry*; 55(9): 926-933.

Shen Y., Dies K.A., Holm I.A., Bridgemohan C., Sobeih M.M., Caronna E.B., Miller K.J., Frazier J.A., Silverstein I., Picker J., Weissman L., Raffalli P., Jeste S., Demmer L.A., Peters H.K., Brewster S.J., Kowalczyk S.J., Rosen-Sheidley B., McGowan C., Duda A.W. 3rd, Lincoln S.A., Lowe K.R., Schonwald A., Robbins M., Hisama F., Wolff R., Becker R., Nasir R., Urion D.K., Milunsky J.M., Rappaport L., Gusella J.F., Walsh C.A., Wu B.L., Miller D.T., and Autism Consortium Clinical Genetics/DNA Diagnostics Collaboration (2010). Clinical genetic testing for patients with autsim spectrum disorders. *Pediatrics;* 125: e727-735.

Sherr E.H. (2003). The ARX story (epilepsy, mental retardation, autism and cerebral malformations): one gene leads to many phenotypes. *Current Opinion in Pediatrics;* 15: 567-571.

Silani G., Frith U., Demonet J.-F., Fazio F., Perani D., Price C., Frith C.D., and Paulesu E. (2005). Brain abnormalities underlying altered activation in dyslexia: a voxel based morphometry study. *Brain*; 128(10): 2453-2461.

Silva-Pereyra J., Rivera-Gaxiola M., Aubert E., Bosch J., Galan L., and Salazar A. (2003). N400 during lexical decision tasks: a current source localization study. *Clinical Neurophysiology;* 114(12): 2469-2486.

Simos P.G., Basile L.F.H., and Papanicolaou A.C. (1997). Source localization of the N400 response in a sentence-reading paradigm using evoked magnetic fields and magnetic resonance imaging. *Brain Research;* 762(1-2): 29-39.

Simos P.G., Breier J.I., Fletcher J.M., Bergman E., and Papanicolaou A.C. (2000). Cerebral mechanisms involved in word reading in dyslexic children: a magnetic source imaging approach. *Cerebral Cortex*; 10: 809-816.

Smith S.M. (2002). Fast robust automated brain extraction. *Human Brain Mapping*; 17: 143-55.

Smith S.M., Jenkinson M., Woolrich M.W., Beckmann C.F., Behrens T.E., Johansen-Berg H., Bannister P.R., De Luca M., Drobnjak I., Flitney D.E., Niazy R.K., Saunders J., Vickers J.,

Zhang Y., De Stefano N., Brady J.M., and Matthews P.M. (2004). Advances in functional and structural MR image analysis and implementation as FSL. *Neuroimage*; 23 Suppl. 1: S208-219.

Smith S.M., and Nichols T.E. (2009). Threshold-free cluster enhancement: addressing problems of smoothing, threshold dependence and localisation in cluster inference. *Neuroimage*; 44(1): 83-98.

Sowell E.R., Thompson P.M., Leonard C.M., Welcome S.E., Kan E., and Toga A.W. (2004). Longitudinal mapping of cortical thickness and brain growth in normal children. *The Journal of Neuroscience*; 24(38): 8223-8231.

Squeglia L.M., Jacobus J., Sorg S.F., Jernigan T.L., and Tapert S.F. (2013). Early Adolescent Cortical Thinning Is Related to Better Neuropsychological Performance. *Journal of the International Neuropsychological Society: JINS*; 19(09): 962-970.

Steding G. (2009). *The anatomy of the human embryo: a scanning electron-microscope atlas* (pp. 1-13). Basel: Karger.

Steinmetz H., Volkmann J., Jäncke L., and Freund H.J. (1991). Anatomical left-right asymmetry of language-related temporal cortex is different in left- and right-handers. *Annals of Neurology;* 29: 315-319.

Ströckens F., Güntürkün O., and Ocklenburg S. (2013). Limb preferences in non-human vertebrates. *Laterality;* 18: 536-575.

Sun T., Patoine C., Abu-Khalil A., Visvader J., Sum E., Cherry T.J., Orkin S.H., Geschwind D.H., and Walsh C.A. (2005). Early asymmetry of gene transcription in embryonic human left and right cerebral cortex. *Science;* 308: 1794-1798.

Sun Y.F., Lee J.S., and Kirby R. (2010). Brain imaging findings in dyslexia. *Pediatrics and Neonatology*; 51(2): 89-96.

Swanson H.L., and Beebe-Frankenberger M. (2004). The Relationship Between Working Memory and Mathematical Problem Solving in Children at Risk and Not at Risk for Serious Math Difficulties. *Journal of Educational Psychology*; 96(3): 471.

Swayze V.W.I.I., Andreasen N.C., Ehrhardt J.C., Yuh W.T., Alliger R.J., and Cohen G.A. (1990). Developmental abnormalities of the corpus callosum in schizophrenia. *Archives of Neurology;* 47: 805-808.

Szalkowski C.E., Fiondella C.G., Galaburda A.M., Rosen G.D., LoTurco J.J., and Fitch R.H. (2012). Neocortical disruption and behavioral impairments in rats following in utero RNAi of

candidate dyslexia risk gene Kiaa0319. *International Journal of Developmental Neuroscience*; 30(4): 293-302.

Tabin C.J., and Vogan K.J. (2003). A two-cilia model for vertebrate left–right axis specification. *Genes & Development;* 17: 1-6

Taipale M., Kaminen N., Nopola-Hemmi J., Haltia T., Myllyluoma B., Lyytinen H., Muller K., Kaaranen M., Lindsberg P.J., Hannula-Jouppi K., and Kere J. (2003). A candidate gene for developmental dyslexia encodes a nuclear tetratricopeptide repeat domain protein dynamically regulated in brain. *Proceedings of the National Academy of Sciences of the United States of America*; 100(20): 1155311558.

Takao D., Nemoto T., Abe T., Kiyonari H., Kajiura-Kobayashi H., Shiratori H., and Nonaka S. (2013). Asymmetric distribution of dynamic calcium signals in the node of mouse embryo during left–right axis formation. *Developmental Biology;* 376(1): 23-30.

Tamnes C.K., Østby Y., Walhovd K.B., Westlye L.T., Due-Tønnessen P., and Fjell, A.M. (2010). Neuroanatomical correlates of executive functions in children and adolescents: a magnetic resonance imaging (MRI) study of cortical thickness. *Neuropsychologia*; 48(9): 2496-2508.

Tamnes C.K., Walhovd K.B., Grydeland H., Holland D., Østby Y., Dale A.M., and Fjell A.M. (2013). Longitudinal working memory development is related to structural maturation of frontal and parietal cortices. *Journal of Cognitive Neuroscience*; 25(10): 1611-1623.

Tanaka N., Liu H., Reinsberger C., Madsen J.R., Bourgeois B.F., Dworetzky B.A., Hämäläinen M.S., and Stufflebeam S.M. (2013). Language lateralization represented by spatiotemporal mapping of magnetoencephalography. *AJNR. American journal of neuroradiology*: *34*(3): 558-563.

Taulu S., and Hari R. (2009). Removal of magnetoencephalographic artifacts with temporal signal-space separation: demonstration with single-trial auditory-evoked responses. *Human Brain Mapping*; 30(5): 1524-1534.

Taylor S.F., Martis B., Fitzgerald K.D., Welsh R.C., Abelson J.L., Liberzon I., Himle J.A., and Gehring W.J. (2006). Medial frontal cortex activity and loss-related responses to errors. *Journal of Neuroscience*; 26(15): 4063-4070.

The FIL Methods Group, Wellcome Centre for Human Neuroimaging UCL Queen Square Institute of Neurology (2014). *SPM12 Manual*. London, United Kingdom.

Thomas K.M., King S.W., Franzen P.L., Welsh T.F., Berkowitz A.L., Noll D.C., Birmaher V., and Casey B.J. (1999). A developmental functional MRI study of spatial working memory. *Neuroimage*; 10(3): 327-338.

Thomas J.L., Spassky N., Perez Villegas E.M., Olivier C., Cobos I., Goujet-Zalc C., Martinez S., and Zalc B. (2000). Spatiotemporal development of oligodendrocytes in the embryonic brain. *Journal of Neuroscience Research*; 59(4): 471-476.

Thompson P.M. et al., Alzheimer's Disease Neuroimaging Initiative, EPIGEN Consortium, IMAGEN Consortium, Saguenay Youth Study (SYS) Group (2014). The ENIGMA Consortium: large-scale collaborative analyses of neuroimaging and genetic data. *Brain Imaging and Behavior*; 8(2):153-82.

Tibbo P., Nopoulos P., Arndt S., and Andreasen N.C. (1998). Corpus callosum shape and size in male patients with schizophrenia. *Biological Psychiatry;* 44: 405-412.

Trulioff A., Ermakov A.I., and Malashichev Y. (2017). Primary Cilia as a Possible Link between Left-Right Asymmetry and Neurodevelopmental Diseases. *Genes (Basel);* 8(2): 48.

Turken U., and Dronkers N.F. (2011). The neural architecture of the language comprehension network: converging evidence from lesion and connectivity analyses. *Frontiers in Systems Neuroscience*; 5: 1.

Ullman M.T. (2006). Is Broca's area part of a basal ganglia thalamocortical circuit? *Cortex;* 42(4): 480-5.

Unni D.K., Piper M., Moldrich R.X., Gobius I., Liu S., Fothergill T., Donahoo A.L., Baisden J.M., Cooper H.M., and Richards L.J. (2012). Multiple Slits regulate the development of midline glial populations and the corpus callosum. *Developmental Biology*; 365(1): 36-49.

Urrutia M., de Vega M., and Bastiaansen M. (2012). Understanding counterfactuals in discourse modulates ERP and oscillatory γ rhythms in the EEG. *Brain Research*; 1455: 40-55.

Van den Brink D., Brown C.M., and Hagoort P. (2001). Electrophysiological evidence for early contextual influences during spoken-word recognition: N200 versus N400 effects. *Journal of Cognitive Neuroscience*; 13(7): 967-985.

Van der Knaap L.J., and Van der Ham I.J. (2011). How does the corpus callosum mediate interhemispheric transfer? A review. *Behavioural Brain Research*; 223: 211-221.

Van Essen D.C., Drury H.A., Joshi S., and Miller M.I. (1998). Functional and structural mapping of human cerebral cortex: solutions are in the surfaces. *Proceedings of the National Academy of Sciences of the United States of America*; 95(3): 788-95.

Van Essen D.C., Lewis J.W., Drury H.A., Hadjikhani N., Tootell R.B., Bakircioglu M., and Miller M.I. (2001). Mapping visual cortex in monkeys and humans using surface-based atlases. *Vision Research*; 41(10-11): 1359-78.

Van Leeuwen M., Van den Berg S.M., Peper J.S., Pol H.E.H., and Boomsma D.I. (2009). Genetic covariance structure of reading, intelligence and memory in children. *Behavior Genetics*; 39(3): 245-254.

Van Petten C., and Rheinfelder H. (1995). Conceptual relationships between spoken words and environmental sounds: event-related brain potential measures. *Neuropsychologia*; 33(4): 485-508.

Van Petten C., and Luka B.J. (2006). Neural localization of semantic context effects in electromagnetic and hemodynamic studies. *Brain and Language*; 97(3): 279-93.

Van Reeuwijk J., Arts H.H., and Roepman R. (2011). Scrutinizing ciliopathies by unraveling ciliary interaction networks. *Human Molecular Genetics*; 20: R149-R157.

Varela F., Lachaux J., Rodriguez E., and Martinerie J. (2001). The brainweb: phase synchronization and large-scale integration. *Nature Reviews. Neuroscience*; 2(4): 229-39.

Vartiainen J., Parviainen T., and Salmelin R. (2009). Spatiotemporal convergence of semantic processing in reading and speech perception. *The Journal of Neuroscience;* 29: 9271-9280.

Vestergaard M., Madsen K.S., Baaré W.F., Skimminge A., Ejersbo L.R., Ramsøy T.Z., Gerlach C., Åkeson P., Paulson O.B., and Jernigan T.L. (2011). White matter microstructure in superior longitudinal fasciculus associated with spatial working memory performance in children. *Journal of Cognitive Neuroscience*; 23(9): 2135-2146.

Vinckenbosch E., Robichon F., and Eliez S. (2005). Gray matter alteration in dyslexia: converging evidence from volumetric and voxel-by-voxel MRI analyses. *Neuropsychologia*; 43(3): 324-31.

Vistoli D., Passerieux C., Houze B., Hardy-Bayle M.C., and Brunet-Gouet E. (2011). Neural basis of semantic priming in schizophrenia during a lexical decision task: a magneto-encephalography study. *Schizophrenia Research*; 130: 114-122.

Von Kriegstein K., Patterson R.D., and Griffiths T.D. (2008). Task-dependent modulation of medial geniculate body is behaviorally relevant for speech recognition. *Current Biology*; 18: 1855-1859.

Von Plessen K., Lundervold A., Duta N., Heiervang E., Klauschen F., Smievoll A.I., Ersland L., and Hugdahl K. (2002). Less developed corpus callosum in dyslexic subjects--a structural MRI study. *Neuropsychologia*; 40(7):1035-44.

Vortkamp A., Gessler M., and Grzeschik K.H. (1991). GLI3 zinc-finger gene interrupted by translocations in Greig syndrome families. *Nature;* 352(6335): 539-540.

Wager T.D., Keller M.C., Lacey S.C., and Jonides J. (2005). Increased sensitivity in neuroimaging analyses using robust regression. *Neuroimage*; *26*(1): 99-113.

Wahl M., Marzinzik F., Friederici A.D., Hahne A., Kupsch A., Schneider G.H., Saddy D., Curio G., and Klostermann F. (2008). The human thalamus processes syntactic and semantic language violations. *Neuron*; 59(5): 695-707.

Wang L., Jensen O., van den Brink D., Weder N., Schoffelen J., Magyari L., Hagoort P., and Bastiaansen M. (2012). Beta oscillations relate to the N400 m during language comprehension. *Human Brain Mapping*; 33(12): 2898-2912.

Watanabe K., Hamada S., Bianco C., Mancino M., Nagaoka T., Gonzales M., Bailly V., Strizzi L., and Salomon D.S. (2007). Requirement of glycosylphosphatidylinositol anchor of Cripto-1 for trans activity as a Nodal co-receptor. *The Journal of Biological Chemistry*; 282(49): 35772-35786.

Wechsler D. (1981). The psychometric tradition: Developing the Wechsler Adult Intelligence Scale. *Contemporary Educational Psychology; 6*(2): 82-85.

Wedeen V.J., Hagmann P., Tseng W.Y.I., Reese T.G., and Weisskoff R.M. (2005). Mapping complex tissue architecture with diffusion spectrum magnetic resonance imaging. *Magnetic Resonance in Medicine*; 54(6): 1377-1386.

Weinberger D.R., Luchins D.J., Morihisa J., and Wyatt R.J. (1982). Asymmetrical volumes of the right and left frontal and occipital regions of the human brain. *Annals of Neurology;* 11: 97-100.

Weiss L.A., Shen Y., Korn J.M., Arking D.E., Miller D.T., Fossdal R., Saemundsen E., Stefansson H., Ferreira M.A., Green T., Platt O.S., Ruderfer D.M., Walsh C.A., Altshuler D., Chakravarti A., Tanzi R.E., Stefansson K., Santangelo S.L., Gusella J.F., Sklar P., Wu B.L., Daly M.J., and Autism Consortium (2008). Association between microdeletion and microduplication at 16p11.2 and autism. *The New England Journal of Medicine;* 358(7): 667-675.

Wernicke C. (1874). *Der Aphasische symptomencomplex*. Breslau: Cohn and Weigert.

Westerhausen R., and Hugdahl K. (2008). The corpus callosum in dichotic listening studies of hemispheric asymmetry: a review of clinical and experimental evidence. *Neuroscience and Biobehavioral Reviews;* 32: 1044-1054.

Whitfield-Gabrieli S., and Ford J.M. (2012). Default mode network activity and connectivity in psychopathology. *Annual Review of Clinical Psychology*; 8: 49-76.

Wierenga L.M., Langen M., Oranje B., and Durston S. (2014). Unique developmental trajectories of cortical thickness and surface area. *Neuroimage*; 87: 120-126.

Wilke M., and Lidzba K. (2007). LI-tool: a new toolbox to assess lateralization in functional MR-data. *Journal of Neuroscience Methods*; 163(1): 128-36.

Willaredt M.A., Hasenpusch-Theil K., Gardner H.A., Kitanovic I., Hirschfeld-Warneken V.C., Gojak C.P., Gorgas K., Bradford C.L., Spatz J., Wölfl S., Theil T., and Tucker K.L. (2008). A crucial role for primary cilia in cortical morphogenesis. *The Journal of Neuroscience;* 28(48): 12887-12900.

Winkler A.M., Kochunov P., Blangero J., Almasy L., Zilles K., Fox P.T., Duggirala R., and Glahn D.C. (2010). Cortical Thickness or Grey Matter Volume? The importance of selecting the phenotype for imaging genetics studies. *Neuroimage*; 53(3): 1135-46.

Witelson S.F. (1985). The brain connection: the corpus callosum is larger in left-handers. *Science*; 229: 665-668.

Witte J.S., Gauderman W.J., and Thomas D.C. (1999). Asymptotic bias and efficiency in case-control studies of candidate genes and gene-environment interactions: basic family designs. *American Journal of Epidemiology*; 149(8): 693-705.

Wolf R.C., Höse A., Frasch K., Walter H., and Vasic N. (2008). Volumetric abnormalities associated with cognitive deficits in patients with schizophrenia. *European Psychiatry;* 23: 541-548.

World Health Organization (1992). *International statistical classification of diseases and related health problems: 10th revision (ICD-10)*. Geneva, Switzerland, WHO.

Wrana J.L., Attisano L., Wieser R., Ventura F., and Massagué J. (1994). Mechanism of activation of the TGF-b receptor. *Nature;* 370(6488): 341-347.

Wright I.C., McGuire P.K., Poline J.B., Travere J.M., Murray R.M., Frith C.D., Frackowiak R.S., and Friston K.J. (1995). A voxel-based method for the statistical analysis of gray and white matter density applied to schizophrenia. *Neuroimage*; 2(4): 244-52.

Wright I.C., Sham P., Murray R.M., Weinberger D.R., and Bullmore E.T. (2002). Genetic contributions to regional variability in human brain structure: methods and preliminary results. *Neuroimage*; 17(1): 256-271.

Yakovlev P.I., and Lecours A.-R. (1967). The myelogenetic cycles of regional maturation of the brain. *Regional development of the brain in early life*; 3-70.

Yamashita H., ten Dijke P., Franzén P., Miyazono K., and Heldin C.H. (1994). Formation of hetero-oligomeric complexes of type I and type II receptors for transforming growth factor-b. *The Journal of Biological Chemistry*; 269(31): 20172-20178.

Yazgan M.Y., Wexler B.E., Kinsbourne M., Peterson B., and Leckman J.F. (1995). Functional significance of individual variations in callosal area. *Neuropsychologia;* 33: 769-779.

Yeo C., and Whitman M. (2001). Nodal signals to Smads through Cripto-dependent and Cripto-independent mechanisms. *Molecular Cell;* 7: 949-957.

Yingling C.D., and Skinner J.E. (1977). Gating of thalamic input to the cerebral cortex by reticularis thalami. *Progress in Clinical Neurophysiology; 1:* 70-96.

Zaghloul N.A., and Katsanis N. (2010). Functional modules, mutational load and human genetic disease. *Trends in Genetics: TIG;* 26: 168-176.

Zatorre R.J., Fields R.D., and Johansen-Berg H. (2012). Plasticity in gray and white: neuroimaging changes in brain structure during learning. *Nature Neuroscience*; 15(4): 528-536.

Zhang Y., Brady M., and Smith S. (2001). Segmentation of brain MR images through a hidden Markov random field model and the expectation-maximization algorithm. *IEEE Transactions on Medical Imaging;* 20: 45-57.

Zhong S., He Y., Shu H., and Gong G. (2017). Developmental Changes in Topological Asymmetry Between Hemispheric Brain White Matter Networks from Adolescence to Young Adulthood. *Cerebral Cortex*; 27(4): 2560-2570.

Zhou X., Sasaki H., Lowe L., Hogan B. L., and Kuehn M.R. (1993). Nodal is a novel TGF-beta-like gene expressed in the mouse node during gastrulation. *Nature;* 361: 543-547.

Ziermans T., Dumontheil I., Roggeman C., Peyrard-Janvid M., Matsson H., Kere J., and Klingberg T. (2012). Working memory brain activity and capacity link MAOA polymorphism to aggressive behavior during development. *Translational Psychiatry*; 2(2): e85.

Zilles K. (1990). Cortex. In G. Paxinos (Ed.), *The Human Nervous System* (pp. 757-802). San Diego: Academic Press Inc.